

NUCLEAR STRUCTURE STUDIES IN HARTREE-FOCK REPRESENTATION

by

Indira Kakkar

POST GRADUATE OFFICE

This thesis has been approved
for the award of the Degree of
Doctor of Philosophy (Ph.D.)
in accordance with the
regulations of the Indian
Institute of Technology Kanpur

Date: 5/3/70



DEPARTMENT OF PHYSICS

INDIAN INSTITUTE OF TECHNOLOGY KANPUR

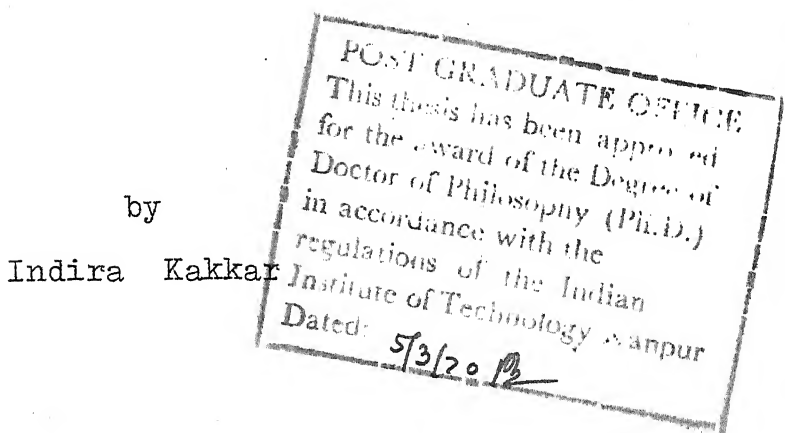
December 1969

PHY - 1969 - D - KA K - NUC

NUCLEAR STRUCTURE STUDIES IN HARTREE-FOCK REPRESENTATION

A Thesis Submitted
In Partial Fulfilment of the Requirements
for the Degree of

DOCTOR OF PHILOSOPHY



to the

22821

DEPARTMENT OF PHYSICS
INDIAN INSTITUTE OF TECHNOLOGY KANPUR

December 1969

DEDICATED TO THE LOVING MEMORY OF MY LATE FATHER
WHO DURING HIS LIFETIME INSPIRED ME TO TAKE
PHYSICS AS CAREER BUT IS NO MORE NOW TO SEE
HIS DESIRE ASSUMING A SHAPE.

Certified that the work presented in this
thesis is the original work of Miss Indira Kakkar
carried out under my supervision.

Waghmare
Y. R. Waghmare
Assistant Professor of
Physics

Department of Physics
Indian Institute of Technology
Kanpur, India

ACKNOWLEDGEMENTS

Expressing gratitude to one's supervisor has unfortunately become an act which is ritualistically performed with the result that there is no way left for a research scholar who genuinely and profoundly feels how much she owes to her supervisor except to fall back upon some of the cliches and phrases. I, therefore, really do not know how to say that I owe everything that is of value in my dissertation to Prof. Y.R. Waghmare for his unfailing eagerness to get involved in my problems at all stages, for his giving me new insight by initiating discussions and for his extending me moral and intellectual support.

I am very much thankful to Prof. J. Mahanty for his interest in this work and to Drs. G.K. Mehta and R.M. Singru for their useful discussions and valuable suggestions during the course of this work.

I would like to express my appreciation for the helpful co-operation of the staff of Computer Centre of this institute. I am thankful to Dr. J.P. Svenne for providing me the computer programs.

I wish to thank my colleagues who have been helpful to me in many respects.

Thanks are due to the Council of Scientific and Industrial Research, New Delhi, India, for financial assistance.

Finally, it is a pleasure to thank Shri Rameshwar Lal for undertaking the typing of this thesis with patience and interest.

INDIRA KAKKAR

Department of Physics
Indian Institute of Technology
Kanpur

TABLE OF CONTENTS

	<i>Page</i>
LIST OF TABLES	i
LIST OF FIGURES	vi
PREFACE	x
 CHAPTER I INTRODUCTION	1
I.1 Independent Particle Model	1
I.2 Hartree-Fock Method	5
I.3 Brueckner Theory	10
I.4 Problems for Present Work	15
 CHAPTER II NUCLEON-NUCLEON INTERACTIONS	20
II.1 Realistic Potentials	20
II.1a Local Potentials	22
II.1b Non-local Potentials	25
II.1c Velocity-Dependent Potentials	26
II.2 Effective Potentials	27
II.3 Potential Matrix Elements Obtained Directly from Phase Shifts	36
II.4 Summary	47
 CHAPTER III HARTREE-FOCK THEORY FOR FINITE NUCLEI	50
III.1 Hartree and Hartree-Fock Equations	50
III.2 Different Ways of Doing HF	54
III.2a Coordinate-Space Representation	54
III.2b Oscillator Representation	55

		Page
III.3	Calculation of the Matrix Elements in Oscillator Basis	59
III.3a	One-Body Matrix Elements	59
III.3b	Two-Body Matrix Elements	59
III.3c	Matrix Elements of HF Single Particle Potential	63
III.4	Iterative Solutions of HF Equations	66
III.5	Coulomb and Centre-of-Mass Corrections	68
III.5a	Coulomb Correction	69
III.5b	Centre-of-Mass Motion	71
III.6	Hartree-Fock Density Distribution and R.M.S. Radii	73
III.6a	Density	73
III.6b	R.M.S. Radius	74
III.7	HF Potential	75
III.8	Choice of Nuclei for Spherical HF Calculations	77
III.9	Single Oscillator Approximation Limit to HF Solutions	78
III.10	Validity of the HF Approximation	81
CHAPTER IV	APPLICATIONS OF HARTREE-FOCK THEORY AND DISCUSSION	84
IV.1	Details of the Calculations	84
IV.2	Effective Yale Interaction Results	86
IV.2a	Binding Energy, Single Particle Energies and Root-Mean-Square Radius	86

	Page
IV.2b Hartree-Fock Wave Functions and Density	102
IV.2c Hartree-Fock Potential	115
IV.3 Sussex Interaction Results	131
IV.4 Discussion	147
IV.5 Results for Single Oscillator Configuration Approximation	165
 CHAPTER V CONFIGURATION MIXING CALCULATIONS WITH HARTREE-FOCK WAVE FUNCTIONS	174
V.1 Details of the Calculations	174
V.2 Results and Discussion	181
 APPENDIX A	xiii
APPENDIX B	xv
APPENDIX C	xvii
 REFERENCES	xx

LIST OF TABLES

Number		Page
IV.1	Calculated HF properties with effective Yale interaction for the nuclei ^4He , ^8Be , ^{12}C and ^{16}O .	89
IV.2	Effect of coulomb and centre-of-mass corrections on total ground state energy of ^4He , ^8Be , ^{12}C and ^{16}O obtained with effective Yale interaction, $b = 2.09\text{F}$.	92
IV.3	Effect of coulomb and centre-of-mass corrections on HF single particle energies of ^4He , ^8Be , ^{12}C and ^{16}O obtained with effective Yale interaction, $b = 2.09\text{F}$.	94
IV.4	Effect of coulomb and centre-of-mass corrections on charge and mass radius of ^4He , ^8Be , ^{12}C and ^{16}O obtained with effective Yale interaction, $b = 2.09\text{F}$.	95
IV.5	HF single particle energies of ^{10}Be , ^{18}O and ^{16}O for effective Yale interaction obtained without coulomb and centre-of-mass corrections.	97
IV.6	Comparison of single particle neutron energies obtained directly with eigenvalues of ^{16}O obtained with effective Yale interaction.	100
IV.7	Particle-hole states in ^{16}O obtained with effective Yale interaction.	101
IV.8	Expansion coefficients for ^4He obtained with effective Yale interaction, $b = 1.76\text{F}$.	103

Number		Page
IV.9	Expansion coefficients for ^8Be obtained with effective Yale interaction, $b = 2.09\text{F}$.	104
IV.10	Expansion coefficients for ^{12}C obtained with effective Yale interaction, $b = 2.09\text{F}$.	105
IV.11(a)	Expansion coefficients for ^{16}O obtained with effective Yale interaction.	106
IV.11(b)	Expansion coefficients for ^{16}O obtained in the HF calculations with effective Yale interaction without coulomb and centre-of-mass corrections.	107
IV.12	Expansion coefficients for ^{10}Be obtained with effective Yale interaction.	108
IV.13(a)	Expansion coefficients for ^{18}O obtained with effective Yale interaction.	109
IV.13(b)	Expansion coefficients for ^{18}O obtained in the HF calculations with effective Yale interaction without coulomb and centre-of-mass corrections.	110
IV.14	Values of the oscillator range parameter (b) giving the best overlap of the HF orbitals for ^{16}O obtained with effective Yale interaction and harmonic oscillator wave functions.	116
IV.15	Matrix elements $\langle n U(\ell j) n' \rangle$ of the HF potential for ^{16}O obtained with effective Yale interaction.	122
IV.16	Sussex relative matrix elements.	132-133
IV.17	Calculated HF properties of ^4He obtained with Sussex interaction.	134

Number		Page
IV.18	Calculated HF properties of ^{12}C obtained with Sussex interaction.	135
IV.19	Calculated HF properties of ^{16}O obtained with Sussex interaction.	136
IV.20	Central, spin-orbit and tensor components of Sussex relative matrix elements.	140-143
IV.21	Effect of central, spin-orbit and tensor parts of Sussex interaction on calculated HF properties of ^{12}O for $b = 2.0\text{F}$.	145
IV.22	Effect of central, spin-orbit and tensor parts of Sussex interaction on calculated HF properties of ^{16}O for $b = 2.0\text{F}$.	146
IV.23	Calculated HF properties for ^{40}Ca obtained with Sussex interaction without coulomb and centre-of-mass corrections, $b = 2.0\text{F}$.	148
IV.24	Single particle energies for ^{16}O obtained in the HF calculations with Sussex interaction without coulomb and centre-of-mass corrections, $b = 2.0\text{F}$.	149
IV.25	Expansion coefficients for ^4He obtained with Sussex interaction, $b = 1.8\text{F}$.	150
IV.26	Expansion coefficients for ^{12}C obtained with Sussex interaction, $b = 2.0\text{F}$.	151
IV.27(a)	Expansion coefficients for ^{16}O obtained with Sussex interaction, $b = 2.0\text{F}$.	152
IV.27(b)	Expansion coefficients for ^{16}O obtained in the HF calculations with Sussex interaction without coulomb and centre-of-mass corrections, $b = 2.0\text{F}$.	153

IV.28	Expansion coefficients for ^{40}Ca obtained in the HF calculations with Sussex interaction without coulomb and centre-of-mass corrections, $b = 2.0\text{F}$.	154
IV.29	Variation of expansion coefficients for ^{16}O obtained with Sussex interaction with the oscillator range parameter b .	155
IV.30	Comparison of our results for the HF binding energy and r.m.s. radius of ^{16}O and ^{40}Ca with the results of other calculations.	159
IV.31	Comparison of our results for the HF single particle neutron energies of ^{16}O with the results of other calculations.	160
IV.32	Comparison of our results for the HF proton single particle energies of ^{16}O with other calculations.	161
IV.33	Comparison of our results for the HF single particle energies for ^{40}Ca with other calculations.	162
IV.34	Weight-factors for ^{16}O .	166
IV.35	Weight-factors for ^{40}Ca .	167-168
IV.36	Binding energies of ^4He , ^{12}C , ^{16}O and ^{40}Ca in the single oscillator configuration approximation.	169
IV.37	Single particle energy levels of ^{16}O obtained in the single oscillator configuration approximation.	171
IV.38	Single particle energy levels of ^{40}Ca obtained in the single oscillator configuration approximation.	172

Number	Page
V.1	Comparison of calculated HF two-body ($\tau=1$) matrix elements in the s-d shell for effective Yale interaction with the results of Kuo and Brown (KB), Clement and Baranger (CB2), Federman and Talmi (FT), and Arima. 189
V.2	Comparison of calculated HF two-body ($\tau=0$) matrix elements in the s-d shell for effective Yale interaction with the results of Kuo and Brown (KB), Clement and Baranger (CB2), Federman and Talmi (FT), and Arima (A1 and A2). 190
V.3	Comparison of calculated two-body matrix elements in the s-d shell for Sussex interaction with the results of Clement and Baranger (CB1). 194

LIST OF FIGURES

Number		Page
IV.1	Hartree-Fock (HF) binding energy per particle for ^4He , ^8Be , ^{12}C and ^{16}O as a function of oscillator range parameter b .	87
IV.2	Variation of neutron single particle energy obtained with effective Yale interaction with the nucleon number A .	98
IV.3	HF $s_{1/2}$ orbitals for ^{16}O obtained with effective Yale interaction. The dotted line represents the calculated HF orbitals while the solid line represents the harmonic oscillator wave functions (HO) for a value of b which gives the same r.m.s. radius as that obtained from HF calculations.	112
IV.4	HF $p_{3/2}$ orbitals for ^{16}O . Other details are same as in Figure IV.3.	113
IV.5	HF $p_{1/2}$ orbitals for ^{16}O . Other details are same as in Figure IV.3.	114
IV.6	$s_{1/2}$ state HF proton wave functions for ^{16}O obtained with effective Yale interaction. Curve A corresponds to wave functions without coulomb and centre-of-mass corrections. Curves B and C are obtained in absence of coulomb and centre-of-mass corrections respectively. Curve D is obtained when both the corrections are taken into account.	117
IV.7	$p_{3/2}$ state HF proton wave functions for ^{16}O obtained with effective Yale interaction. Other details are same as in Figure IV.6.	118

Number	Page
IV.8 $s_{1/2}$ state HF proton wave functions for ^4He obtained with effective Yale interaction. Other details are same as in Figure IV.6.	119
IV.9 HF matter density for the nuclei ^4He , ^8Be , ^{12}C and ^{16}O obtained with effective Yale interaction.	120
IV.10 HF charge density for the nuclei ^4He , ^8Be , ^{12}C and ^{16}O obtained with effective Yale interaction.	121
IV.11 $s_{1/2}$ state HF single particle potential for ^{16}O obtained with effective Yale interaction.	124
IV.12 $p_{3/2}$ state HF single particle potential for ^{16}O obtained with effective Yale interaction.	125
IV.13 $p_{1/2}$ state HF single particle potential for ^{16}O obtained with effective Yale interaction.	126
IV.14 Static limit of the non-local HF potential for ^{16}O obtained with effective Yale interaction.	127
IV.15 $1p_{3/2}$ state wave functions of a local potent- ial which gives same energies for $1p_{3/2}$ and $1p_{1/2}$ states as obtained in HF calculations with effective Yale interaction for ^{16}O . Dashed curve represents the HF wave function and solid curves represent the wave functions of equivalent local potential. Curve P is obtained in absence of non-local correction while curves Q, R and S are obtained with the non-locality range parameter taken as 1.0F, 1.5F and 2.0F respectively.	129

IV.16	$1p_{1/2}$ state wave function of a local potential which gives the same energies for $1p_{3/2}$ and $1p_{1/2}$ states as obtained in HF calculations with effective Yale interaction for ^{16}O . Dashed curve represents the HF wave function and solid curve is the wave function of equivalent local potential.	130
IV.17	HF binding energy per particle obtained with Sussex interaction for 4He , ^{12}C and ^{16}O as a function of oscillator range parameter b .	138
V.1	Positive parity states of ^{18}O obtained with effective Yale interaction and HF wave functions.	182
V.2	Positive parity states of ^{18}F obtained with effective Yale interaction and HF wave functions. Levels with $\tau=1$ are specified with bracketed spin. All other levels have $\tau=0$.	183
V.3	Comparison of calculated HF and HO positive parity levels of ^{18}O for effective Yale interaction with the results of Kuo and Brown (KB), and Clement and Baranger (results with second-order Born correction are referred to as CB2).	186
V.4	Comparison of calculated HF and HO positive parity levels of ^{18}F for Yale interaction with the results of Kuo and Brown (KB), and Clement and Baranger (CB2). Levels with bracketed spin have $\tau=1$. All other levels have $\tau=0$.	187

Number	Page
V.5	Comparison of calculated HF and HO positive parity levels of ^{18}O for Sussex interaction with the results of Clement and Baranger (results without second-order Born correction are referred to as CBl), and experiments. 192
V.6	Comparison of calculated HF and HO positive parity ($\tau = 0$) levels of ^{18}F for Sussex interaction with the results of Clement and Baranger (CBl), and experiments. 193
V.7	^{10}Be levels obtained with effective Yale interaction and HF wave functions. 195

PREFACE

In the present work our main efforts have been to study the static properties of light nuclei ($A \leq 40$) which are obtained from Hartree-Fock calculations with realistic interactions. This work mainly consists of five chapters. Chapter I is mainly an introduction giving a brief account of the independent particle model of the nucleus, and the Hartree-Fock and Brueckner-Hartree-Fock approximations of solving many-body problem. Several Hartree-Fock and Brueckner-Hartree-Fock calculations that have been done in the past are also summarized and the problems taken up for the present work have been mentioned. Chapter II describes the nucleon-nucleon interactions which can be used in nuclear structure studies. We have chosen the following two interactions for our purpose: effective interaction of Shakin, Waghmare and Hull derived from Yale potential by using a unitary-model-operator approach and the Sussex interaction of Elliott et. al. obtained directly from experimental phase shift data by using an auxiliary potential method. Chapter III contains the Hartree-Fock theory in detail and the matrix method of solving the Hartree-Fock equations. The formulae used in the calculations of various ground state properties are also given. Two important corrections due to the coulomb energy and centre-of-mass motion of the nucleus are estimated. Both these corrections are included in a self-consistent manner in our calculations,

unlike the earlier Hartree-Fock calculations of various other authors. These corrections are estimated by those authors externally after solving the Hartree-Fock equations. Single oscillator approximation limit to the Hartree-Fock solutions has also been discussed. In Chapter IV we present the results of spherical Hartree-Fock calculations for the nuclei ^4He , ^8Be , ^{12}C , ^{16}O and ^{40}Ca . The properties calculated are the binding energies, the single particle energies, r.m.s. radius and charge radius, matter and charge densities, spin-orbit splittings, etc. It is found that the binding energy results, obtained with effective Yale interaction for all the nuclei considered are in satisfactory agreement with the corresponding experimental values if all the second-order terms of the Yale potential are accounted for. Sussex matrix elements give better results for the binding energies in the first order compared to the first order in Yale potential. For ^{40}Ca , however, Sussex matrix elements give binding energy in excess of the experimental value. Rest of the properties calculated are in fair agreement with the experimental data. The results obtained in the single oscillator configuration approximation to Hartree-Fock wave functions are also presented. Single particle wave functions and self-consistent single particle potentials obtained in the Hartree-Fock calculations with effective Yale interaction have been studied in detail. The Hartree-Fock single particle wave functions for ^{16}O have been compared with the conventional harmonic oscillator wave functions. The general nature of the wave functions is the

same for all the nuclei. The Hartree-Fock single particle potential is non-local and state-dependent. The static limit to this non-local potential has been discussed.

Finally, in Chapter V we have studied the energy levels of ^{18}O , ^{18}F and ^{10}Be in the Hartree-Fock representation. It is assumed that the nucleons move independently of each other in a Hartree-Fock self-consistent field and the low-lying states of these nuclei may arise due to the excitations of only the last two neutrons to the higher states. The single particle energies and wave functions describing the behaviour of these two nucleons are obtained from Hartree-Fock calculations. The nucleon-nucleon potentials used are the effective Yale interaction of Shakin et. al. and Sussex interaction. It is seen that the HF spectra are compressed compared to experimental levels in all the cases. Probable reasons for this discrepancy have been discussed.

CHAPTER I

INTRODUCTION

I.1 Independent Particle Model

The study of the nucleus is a many-body problem which cannot be solved exactly. Instead, studies of complex nuclei have been carried out by various phenomenological models. There are several nuclear models which can be broadly divided into two classes. First class consists of so-called 'strong interaction models' which treats the nucleus as an assemblage of closely coupled particles, e.g., liquid drop model, Bohr and Mottelson model, etc. These models have been successful in explaining many collective properties of nuclei but we shall not discuss them here. The second class is of 'independent particle models' which assumes that the nucleons move independently of each other in an average potential. Recent evidence suggests that the independent particle model provides a better description for low-energy phenomena though the coupling of nucleons by virtue of their mutual interaction can by no means be neglected. The most successful of these independent particle models are the shell model, the optical model and the Nilsson model. The uniform potential is spherical for shell model, complex for optical model and spheroidal for Nilsson model. Shell model, proposed by Mayer in 1948 and developed since then, has been very successful in explaining some regularities in the binding energies of nuclei, spin and parities of some

of the low-lying nuclear levels, certain multipole transitions, β -decay, etc. The optical model was primarily designed to explain the nuclear reaction phenomena and it successfully accounts for the scattering cross-section data of low and medium energy reactions. Nilsson model can predict well the ground state spins, moments of inertia, energies of excited state rotational bands, equilibrium deformations, and vibrational properties of deformed nuclei, which are not described well on the basis of simple shell model. In all these independent particle models the nucleons fill up the successive lowest quantum levels of the mean potential well and move in definite orbits. This picture provides the qualitative features of many nuclear phenomena. To get the quantitative agreement with experiments the residual interaction between the particles is introduced. It mixes up the orbits to some extent but the basic character of the model is essentially the independent particle motion.

With increasing addition in our knowledge of nucleon-nucleon force from the study of two, three and four nucleons systems, it was thought that there should be a way of correlating the average potential field of the nucleus with the nucleon-nucleon interaction. The strong objection to this was the following. Most of the realistic nucleon-nucleon potentials which fit the two-body data contain a repulsive core. Such a repulsive core will give rise to strong short-range correlations which are not described well by an independent particle model. However, there are many experimental evidences in favour of

independent particle motion, e.g. the nuclear reaction experiments, in which an incident particle knocks out a nucleon from target nuclei, show that single particle structure does prevail for the nucleons inside the nucleus. Besides, elastic scattering shows resonances which are explained in terms of optical potential model. Thus, the fact that independent particle model is successful in explaining a large number of experimental data implies that short-range correlations do not play an important role in many nuclear properties and the nucleons inside the nucleus behave to a certain extent as independent particles in a common potential. Recent advances in the theory of nuclear matter by Moszkowski and Scott (Moi 60) and Gomes et. al. (Gos 58) have explained the mechanisms which reduce the effect of strong interaction on the nuclear motion. In particular, the essential features of Moszkowski-Scott method could be described as follows:

(i) The scattering of two nucleons inside a nuclear medium is characteristically different from the collision of free nucleons. The reason for this is that inside the nuclear medium Pauli principle forbids scattering to states which are already occupied and thus, the number of available final states is limited. The nucleons far apart can interact through low Fourier components of the force. Such interactions are generally forbidden inside the nucleus since the momentum transfer is insufficient to raise the particles above the Fermi sea. The short-range part of the potential corresponds to high

momentum transfer and scatters the particles to unfilled states. Thus, beyond a certain healing distance the relative wave function of two nucleons approaches that of noninteracting particles. This is in sharp contrast to scattering of free nucleons where the wave function never heals up and is phase shifted relative to free particle wave function even at infinity. The healing distance is of the order of $1F$ and the average separation of the nucleons in nuclear matter is approximately $1.66F$. Consequently, the effect of two-body correlations would be small. Besides, the fact that healing distance is smaller than the average separation implies that the probability that more than two particles will simultaneously be at distances smaller than the healing distance would be small and three-body correlations would be unimportant.

(ii) The effect of the attractive part of the potential on the nuclear phase shifts is opposite to that of the repulsive part. Thus, a part of the attractive potential can be combined, with the repulsive core so that the two together give zero phase shifts. Consequently, the phase shifts due to the strong nucleon-nucleon interaction are the same as that due to weak attractive long-range part of the force beyond the healing or cut-off distance.

As a consequence of these two effects particles move almost independently with very weak interactions. This implies

that the nuclear Hamiltonian H of a system of A nucleons can be written as

$$H = H_0 + v, \quad (1.1)$$

where H_0 is the independent particle Hamiltonian and v is the residual interaction. The average potential field, which each nucleon feels, must be some sort of average of the interactions it has with all the other nucleons. The residual interaction between two nucleons must be the interaction left over after this average effect is removed. A systematic way of determining H_0 , starting from fundamental nucleon-nucleon interaction, is the self-consistent Hartree-Fock (HF) method. The ground state of the nucleus is represented, in the first approximation, by a nondegenerate eigenstate $\underline{\Phi}_0$ of H_0 i.e.

$$H_0 \underline{\Phi}_0 = E_0 \underline{\Phi}_0 \quad (1.2)$$

where E_0 is the lowest eigenvalue of H_0 . We shall briefly describe the HF method of determining $\underline{\Phi}_0$ and E_0 .

I.2 Hartree-Fock Method

The Hartree-Fock (HF) method consists in assuming that the wave function $\underline{\Phi}_0$ of the nucleus is an antisymmetrized product of single particle wave functions. To determine the best single particle wave functions there are many equivalent criteria. For example, one can minimize the total energy or one can require self-consistency between the single particle potential field of H and the average potential seen by the particle as a result

of its interaction with all the other nucleons. The single particle wave functions which minimize the total energy are the solutions of following HF equations

$$\langle \alpha | T | \beta \rangle + \langle \alpha | U | \beta \rangle = \epsilon_{\alpha} \delta_{\alpha\beta} , \quad (1.3)$$

where α and β specify the single particle states, T is the kinetic energy and U the HF single particle potential which is related to the nucleon-nucleon potential V by the following equation,

$$\langle \alpha | U | \beta \rangle = \sum_{\gamma=1}^A \langle \alpha \gamma | V | \beta \gamma \rangle . \quad (1.4)$$

Thus, the HF single particle potential U is calculated in terms of V by a sum over occupied single particle states, but the latter cannot be obtained without a prior knowledge of U . This is the HF self-consistency problem and is solved by an iteration interpolation procedure, starting from a trial guess and improving the wave functions until self-consistency is achieved. The HF field may be spherical or deformed depending upon the nuclei studied. Thus, for example, the HF field is spherical for the doubly closed shell nuclei ^4He , ^{16}O , ^{40}Ca and ^{208}Pb . The ground state Φ_0 is a Slater determinant wherein all the single particle states are occupied up to Fermi level ϵ_F . For deformed nuclei single particle states are described in a deformed HF field. The ground state Φ_0 is again a Slater determinant in which all the deformed orbitals are occupied up to Fermi level.

The HF method not only describes the independent particle picture of the nucleus but can also be used in the discussion of collective motion of the nucleons, e.g., the vibration and rotation of the nucleons as a whole can be explained by letting the self-consistent HF field become time-dependent. Besides, the pairing correlations of the two-body force can be taken into account in an extended HF theory, known as Hartree-Fock-Bogoliubov-Valatin theory. This method extends the variational principle to a class of trial wave functions of independent excitations of quasi particles which include pairing correlations. In this case the total Hamiltonian H can be written as

$$H = H_0^{QP} + v^{QP}, \quad (1.5)$$

where H_0^{QP} is the independent quasi particle Hamiltonian and v^{QP} is the residual interaction between these quasi particles.

HF theory has been successfully applied in atomic and solid state physics. In fact, the idea of self-consistent field was first intuitively introduced by Hartree and was successfully applied to electronic structure of atoms. Later this was extended by Fock who included the exchange effects and established the HF equations using a variational method. Thus, the HF method in nuclear physics is essentially borrowed from atomic physics, but the application of this method to nuclear structure calculations is much more tedious than in the case of atoms because of the following reasons:

- (i) The nucleon-nucleon interaction V is not known uniquely.
- (ii) Most of the realistic nucleon-nucleon potentials which fit the two-body data contain a hard core. The matrix element of such a potential in a basis of independent particle wave functions is infinite.
- (iii) Complete HF calculations are very time-consuming and cannot be carried out without high-speed computers.

In spite of all these difficulties several spherical and deformed HF calculations have been done during the last few years. A detailed survey of all these calculations is not possible here. For an excellent review of deformed HF calculations we refer to an article by Ripka (Ria 68). Since our main interest lies in the spherical HF calculations, we shall briefly review only such calculations that have been carried out in the past. Spherical HF calculations by Davies et. al. (Das 66) have been carried out using simple velocity-dependent force acting only in relative s-state. They have studied the nuclei ^{12}C , ^{16}O , ^{28}Si , ^{40}Ca and ^{80}Zr and obtained qualitative agreement for various calculated ground state properties with experiment. In the calculations of Muthukrishnan et. al. (Mun 65), Yamaguchi potential has been used and the results obtained for various nuclei are very similar to those of Davies et. al. (Das 66). Abgrall and Monsonego (Abl 66) have used a central force with a nonsaturating exchange mixture. Also,

there are calculations done by Krieger et. al. (Krr 66), whose effective interaction includes three-body contact term proportional to cube of density. In their later calculations, Davies et. al. (Dav 68) have employed a more complete two-body potential including both even and odd noncentral potentials and giving a fair fit to two-body data. They have studied in detail a number of closed shell nuclei in the range $16 \leq A \leq 208$. Although, in some of these calculations the calculated HF properties are in reasonable agreement with experiments, the major drawback of these calculations is that they were carried out with nucleon-nucleon potentials especially designed for use in HF calculations. The parameters of these potentials were adjusted to fit the nuclear matter data so that they gave a fair fit for the binding energies of various nuclei (particularly heavy nuclei) with the experimental data, but they did not fit the two-body data. In fact these effective potentials do not contain any features of the realistic nucleon-nucleon potentials, such as hard core or nonlocality, one-pion-exchange behaviour at large distances, etc. First time a realistic potential (Tabakin potential) in the HF calculations has been used by Kerman and co-workers (Ken 66). These authors have studied the nuclei ^{16}O and ^{40}Ca in considerable detail and find that Tabakin potential fails to give adequate binding in first-order and gives too large a value for the spin-orbit splittings. Later on, Pal et. al. (Pal 66) have improved the agreement for the binding energy by calculating the contribution of second

order term. In all the HF calculations described above the nucleon-nucleon interaction was smooth and did not contain any hard core singularity. The first theoretical foundation for the use of singular potential in HF calculations has been laid by Shakin et. al. (Shn 66, 67a). Their theory is based on the unitary-model-operator approach of Villars (Vis 63) and is applicable to any general singular interaction. The fact that short-range correlations do not play an important role in many nuclear properties implies that independent particle HF wave functions are significant and can be obtained from an effective interaction from which the effect of hard core has been removed. This was the philosophy adopted by Shakin et. al. in deducing a smooth effective interaction for use in HF calculations. Thus, all the problems from (i) to (iii) have now largely been solved. There is another approximation method proposed by Brueckner and co-workers for dealing with the problem of hard cores. We describe it very briefly below.

I.3 Brueckner Theory

In the Brueckner theory motion of a pair of nucleons is described by means of a correlated wave function $\Psi_{\alpha\beta}(\vec{r}_1, \vec{r}_2)$, which vanishes inside the core region $|\vec{r}_1 - \vec{r}_2| \ll r_c$ and asymptotically approaches the unperturbed wave function $\Phi_{\alpha\beta}$:

$$\Psi_{\alpha\beta}(\vec{r}_1, \vec{r}_2) \rightarrow \Phi_{\alpha\beta}(\vec{r}_1, \vec{r}_2) = \frac{1}{\sqrt{2}} (\varphi_{\alpha}(\vec{r}_1)\varphi_{\beta}(\vec{r}_2) - \varphi_{\alpha}(\vec{r}_2)\varphi_{\beta}(\vec{r}_1)) . \quad (1.6)$$

$\underline{\Psi}$ is the solution of a modified form of two-nucleon Schrödinger equation known as Brueckner-Bethe-Goldstone equation (Bee 57), and is related to $\underline{\Phi}$ through a reaction matrix (K-matrix) defined as

$$K \underline{\Phi}_{\alpha\beta} = V \underline{\Psi}_{\alpha\beta} . \quad (1.7)$$

Because of the strong short-range correlations, generated by the two-nucleon potential, it is assumed that the motion of the pair will not be affected by the other nucleons through any multiparticle clustering, the other nucleons only modify the energy of the interacting pair through HF potential, and Pauli principle forbids scattering to states which are occupied by other nucleons. This is known as independent pair approximation. The interaction between the nucleons inside the nuclear medium is determined by a reaction-matrix which differs from the two-body potential over the short-range of correlation distances in the nuclear wave functions. The defining equation for K-matrix is

$$K = V + V \frac{Q}{e} K , \quad (1.8)$$

Q is the Pauli operator which takes care of exclusion principle and e is the energy denominator which takes into account the binding effects of average nuclear field. In a basis of independent particle wave functions ϕ_α 's together with associated eigenvalues E_α 's, the matrix elements of K can be written as

$$K_{\alpha\beta, \gamma\delta} = V_{\alpha\beta, \gamma\delta} + \sum_{\sigma\tau} V_{\alpha\beta, \sigma\tau} (E_{\gamma} + E_{\delta} - E_{\sigma} - E_{\tau})^{-1} K_{\sigma\tau, \gamma\delta} \quad (1.9)$$

The sum over σ and τ is to be carried out over empty states only.

The single particle energies E_{α} occurring in equation (1.9) are

$$E_{\alpha} = \left(\frac{p^2}{2m}\right)_{\alpha\alpha} + \sum_{\gamma(\text{occ})} (K_{\alpha\gamma, \alpha\gamma} - K_{\alpha\gamma, \gamma\alpha}) \quad (1.10)$$

The second term in equation (1.10) defines the single particle potential U , i.e.

$$U_{\alpha\alpha} = \sum_{\gamma(\text{occ})} (K_{\alpha\gamma, \alpha\gamma} - K_{\alpha\gamma, \gamma\alpha}) \quad (1.11)$$

In the limit of a weak interaction K can be replaced by the potential V and the single particle potential defined by equation (1.11) is the HF potential. Starting from a given set of eigenstates ϕ_{α}^n (n means n^{th} iterate) the new set ϕ_{α}^{n+1} obtained from the single particle potential $U_{\alpha\alpha}^n$ will in general not agree with the input. The problem of obtaining agreement is the self-consistency problem of HF. In the Brueckner theory a new self-consistency problem arises since a change in the representation $\phi_{\alpha}^n \rightarrow \phi_{\alpha}^{n+1}$ not only changes the single particle potential, but also through the change in the energy spectrum changes the reaction-matrix. This in turn reacts back on the single particle potential and eigenfunctions. This is the Brueckner self-consistency problem of obtaining self-consistent energy spectrum and reaction-matrix. In infinite nuclear

matter the eigenstates are plane waves and only Brueckner self-consistency problem exists. In finite nuclei Brueckner and HF self-consistency problems are coupled together and exact Brueckner-Hartree-Fock (BHF) calculations become quite complicated. Besides, in finite nuclei exact treatment of Pauli operator causes some difficulties and various approximation methods are used to calculate the reaction-matrix. Many authors have bypassed the HF self-consistency problem by using pure oscillator wave functions (Wog 67, 68: Kör 66, 67: Mar 66). Such calculations encounter only Brueckner self-consistency problem and are called Brueckner-type calculations. In his calculations Wong (Wog 67) has studied qualitatively the ground state properties of ^{40}Ca , ^{16}O and ^4He using a number of hard core potentials. It is found that realistic potentials underbind these nuclei by 2-4 MeV per particle, a result similar to that obtained in pure HF calculations with realistic potentials (Ken 66: Shn 67b). Some BHF calculations for finite nuclei have also been reported in the literature. First few BHF calculations (Brr 58, 61: Man 63: Kör 65) have been done in coordinate representation, but none of them are exact. Calculations by Brueckner and coworkers have been done in the local density approximation. In this approximation, the reaction-matrix elements for finite nuclei are taken to be simple averages over matrix elements for nuclear matter, calculated for the density at the centre-of-mass position of the two interacting nucleons. In the calculations carried out with Gammel-Thaler potential, light nuclei are found to be underbound by

2-4 MeV per particle but discrepancy decreases with increasing A. However, the equilibrium nuclear radius becomes too small for heavy nuclei. The results for ^{16}O , ^{40}Ca , ^{90}Zr and ^{208}Pb are summarized in references (Brr 61) and (Man 63). BHF calculations in an oscillator basis have been recently reported by Davies et. al. (Das 69). As in the pure HF calculations, the single particle wave functions are expanded in terms of harmonic oscillator wave functions and the calculations have been carried out with Hamada-Johnston potential for the nuclei ^{16}O , ^{40}Ca , ^{48}Ca and ^{208}Pb . Their main conclusions are that nuclei are too small and underbound.

We thus see that HF is very much alive even when the nucleon-nucleon interaction is singular, if not the simple HF something more sophisticated like BHF is valid. In fact, it has been shown (Grg 68) that the effective interaction of Shakin et. al., obtained by the method of canonical transformations, can also be expressed in terms of K-matrix. However, in the HF calculations carried out with this effective interaction (Shn 67b) there is no Brueckner-self-consistency involved since in the calculation of second-order terms in the effective interaction these authors have used an average value for the energy denominator ϵ and angle averaged Pauli operator Q . For the purpose of present work we come back to simple HF calculations which do not involve any Bruckner-self-consistency problem.

I.4 Problems for Present Work

The following problems have been undertaken in the present work:

(i) Spherical HF calculations with effective Yale interaction have been carried out for ^4He , ^8Be , ^{12}C and ^{16}O . This interaction has been widely used in several spherical and deformed HF calculations of various nuclei. Spherical HF calculations for ^{16}O and ^{40}Ca with this interaction have been done by Shakin et. al. (Shn 67b). Present work is an extension of their calculations to other lighter nuclei. We have also included coulomb and centre-of-mass corrections in our calculations in a self-consistent manner whereas in the calculations of Shakin et. al. the effect of these corrections on the total ground state energy was estimated externally. The effect of these corrections on various ground state properties has also been studied in detail. The results are presented in Section IV.2 of Chapter IV.

(ii) Elliott et. al. at Sussex (Elt 68a) have recently published relative matrix elements of the nucleon-nucleon interaction in an oscillator basis obtained directly from experimental phase shift data. As a test of their matrix elements Elliott et. al. (Elt 67) have calculated the spin-orbit splittings of light nuclei ($A \leq 41$) and obtained reasonable values. A number of deuteron (Elt 68b) and triton and alpha particle properties (Jan 69) have also been calculated and satisfactory

agreement with experiments has been obtained. The success of these calculations suggests that Sussex matrix elements are reliable and can be used in the calculations of more complicated nuclei. We have used these matrix elements in the spherical HF calculations for the nuclei ^4He , ^{12}C , ^{16}O , and ^{40}Ca . The results are given in Section IV.3 of Chapter IV. A detailed comparison of the Sussex matrix elements results with those of several other calculations, particularly with those of potentials obtained from a fit to experimental phase shifts, has been made in Section IV.4 of Chapter IV. Since the HF formalism is well-known to give a good account of the ground state properties, our calculations also serve as a test of the saturation properties of Sussex matrix elements.

(iii) We have calculated the low-lying excited states of ^{10}Be , ^{18}O and ^{18}F using HF wave functions. As in the pure shell model calculations, it is assumed that low-lying states of these nuclei arise due to the interaction of last two nucleons and remaining nucleons are treated as inert. The single particle parameters needed in the calculation are obtained from self-consistent HF calculations.

Several shell model spectroscopy calculations for the energy spectra of these nuclei have been reported in the literature. In most of the earlier calculations the residual interaction between the last two nucleons was taken to be purely phenomenological, e.g. some simple exchange force with Gaussian

or Yukawa radial dependence. The adjustable parameters of the potential were determined from best fit to experimental data on one or more nuclei. Such calculations have been done by Waghmare (Wae 64), Elliott and Flowers (Elt 57), and many others. The residual interaction so obtained depends upon the configurations taken into account and the energy levels which are included in the calculation and cannot be compared with any standard realistic potentials. A realistic interaction in the energy level calculations for $A = 18$ nuclei was first used by Kuo and Brown (Kuo 66). These authors, starting from Hamada-Johnston potential, have obtained an effective interaction which when used in the standard spectroscopy calculation, gives a good description of the energy levels of these nuclei. Clement and Baranger (Clt 68) using Tabakin potential have obtained results for $A = 18$ nuclei very close to those of Kuo and Brown. In all the calculations described above pure harmonic oscillator wave functions and experimental single particle energies have invariably been used. The use of harmonic oscillator wave functions is preferred because in this representation separation between relative and centre-of-mass coordinates can be made exactly and two-body matrix elements of the nucleon-nucleon potential can be easily calculated. Very recently, Kahana (Kaa-Preprint) has reported energy level calculations for $A = 18$ nuclei using Woods-Saxon wave functions. No attempt till now has been made to obtain the single particle energies and single particle wave functions from some self-consistent calculations. HF calculation gives

us a picture very close to shell model, i.e., it provides us with a self-consistent single particle level spectrum and associated with each level is the single particle wave function. These single particle parameters serve as a basis for any shell model spectroscopy calculation and the residual interaction would be same as that used in the self-consistent HF calculation to obtain the single particle parameters. We have carried out the calculations with effective Yale interaction and Sussex interaction. The details of the calculations and the results are presented in Chapter V.

In a somewhat different approach followed by some authors one tries to dispense with any potential picture and the two-body matrix elements which enter any shell model spectroscopy calculations are treated as arbitrary parameters and adjusted to give best possible fit to spectra of several nuclei. Such calculations have been done by Arima (Ara 68) for oxygen isotopes ^{18}O , ^{19}O , ^{20}O . In his calculations ^{16}O is regarded as inert core and low-lying states of these nuclei are assumed to arise from neutrons in $(1d_{5/2} 2s_{1/2})$ configuration. $T = 1$ matrix elements have been calculated from least square fit to these levels. $T = 0$ matrix elements have been calculated by extending the calculations to cover the nuclei ^{18}F , ^{19}F and ^{20}Ne as well. Similar calculations have also been done by Federman and Talmi (Fen 65). It would be interesting to compare the empirically determined two-body matrix elements with those calculated from a realistic potential for this configuration

space. Such a comparison has been made in Chapter V.

In Chapter II we describe various types of nucleon-nucleon interactions available for use in any nuclear structure calculations. The prescription used to obtain the effective Yale interaction from Yale potential by Shakin et. al. and Sussex matrix elements directly from phase shift data by Elliott et. al. has also been described briefly. The details of the HF theory and various formulae used in the calculations are given in Chapter III. The results of HF calculation are presented in Chapter IV. The results obtained for the energy levels of various nuclei obtained with HF wave functions and different types of residual interactions are given in Chapter V.

All calculations have been carried out on IBM 7044 computer at Indian Institute of Technology, Kanpur.

CHAPTER II

NUCLEON-NUCLEON INTERACTIONS

The exact nature of the nucleon-nucleon interaction is still not known and it is not possible to present it in a close deductive form. However, the nucleon-nucleon interaction in its nonrelativistic version can be represented in terms of a potential. The nucleon-nucleon potentials, available for use in nuclear structure calculations, can be broadly classified into following categories:

- (i) Realistic potentials
- (ii) Effective potentials
- (iii) Potential matrix elements obtained directly from phase shifts.

We shall describe these potentials in the following sections.

II.1 Realistic Potentials

Realistic potentials are obtained directly from an analysis of the deuteron and two-body scattering data. The available data (Marr 68: Nos 67) consist of in pp and np scattering: total cross-sections, angular distributions, and different types of polarization measurements and also s-wave scattering lengths. The two-body bound state data are deuteron binding energy, quadrupole moment, D-state probability, etc. In the energy range 0 to 300 MeV there are about one thousand pieces of data left to be fitted, after discarding quite a few of them considered unrealistic. There are two ways of handling the

problem. One can either try to fit the data as they come from the experiments or one can use a phase shift parameterization of the data and compare these phase shifts with those extracted from potentials. The latter procedure is generally preferred. Phase shift analysis of the experimental data has been carried out mainly by two groups: one at Yale led by Breit (Brt 62) and the other at Livermore (Marr 68). Signell and co-workers (Sil 65) have also made a number of useful analyses. Only one set of phase shifts emerges and the phases are fairly well determined. It is to these phase shifts that the potential parameters are fitted in most of the models. No attempt is made to fit the data at energies above about 300 MeV. At higher energies pion production and other relativistic effects become important and two-nucleon Schrödinger equation is inadequate. However, the energies of nucleons in collision in nuclei are expected to be of the order of 160 MeV or so. Thus, we have reasonably accurate information about most of the partial waves which would play a dominant role in nuclear phenomena.

The long-range part of the interaction is rather unambiguously known from meson-theory. It is determined by the one-pion exchange potential (Hun 57) corresponding to the lightest meson which can be exchanged between two nucleons. The pion-nucleon coupling constant is measured from pion experiments or by nucleon-nucleon scattering data. However, at the pion range other terms corresponding to the exchange of heavier mesons, such as ρ , ω , η -mesons (Bra 67; Lon 68), dominate one-pion

exchange potential (OPEP) by a factor of two or three. Again, the one boson exchange strength (OBEP) is determined by the nucleon-nucleon scattering or alternatively by calculating the meson-nucleon coupling constants, for example from SU_3 symmetry.

The nature of the short-range part of the interaction is not exactly known. The most general two-body interaction is a non-local one, which, to be translational invariant, must have the form

$$V(\vec{r}_1, \vec{r}_2 | \vec{r}'_1, \vec{r}'_2) = \delta(\vec{R} - \vec{R}') V(\vec{r} | \vec{r}'). \quad (2.1)$$

The relative and centre-of-mass coordinates are defined by

$$\vec{r} = \vec{r}_1 - \vec{r}_2, \quad \vec{R} = \frac{1}{2}(\vec{r}_1 + \vec{r}_2) \text{ etc.} \quad (2.2)$$

Meson-theory indicates that the correct two-body interaction may be non-local at short-range, but most of the potential models are local potentials, for which

$$V(\vec{r} | \vec{r}') = \delta(\vec{r} - \vec{r}') V(\vec{r}). \quad (2.3)$$

II.1a Local Potentials

The first group of local potentials contains a repulsive core of infinite magnitude — the so-called hard core. The assumption that nucleon-nucleon potential becomes repulsive at short distances was first made by Jastrow (Jaw 51). It was strongly supported by the two-nucleon scattering data through the change in sign of the 1S_0 -state phase shift from its low-energy positive sign (attractive potential) to a negative sign

characteristic of a repulsive potential above 200 MeV. Two such most widely known potentials are of Yale group of Breit and collaborators (Laa 62) and of Hamada and Johnston (Haa 62). Yale potential is of the following form:

$$V(x) = V^{(2)}(x) + V_c(x) + \hat{S}_{12} V_T(x) + \vec{t} \cdot \vec{S} V_{LS}(x) - l(l+1) V_q(x) \delta_{lJ}, \quad (2.4)$$

where x is the internucleon distance measured in units of pion Compton wave length μ , i.e.

$$x = \mu^{-1} r, \quad (2.5)$$

$V^{(2)}(x)$ = one-pion exchange potential,

$$= \frac{1}{3} \mu (\vec{\tau}_1 \cdot \vec{\tau}_2) \frac{f^2}{4\pi} \left\{ [\vec{\sigma}_1 \cdot \vec{\sigma}_2 + \hat{S}_{12} (1 + \frac{3}{x} + \frac{3}{x^2})] \frac{e^{-x}}{x} + \vec{\sigma}_1 \cdot \vec{\sigma}_2 \delta(x) \right\}, \quad (2.6)$$

where $\vec{\sigma}$ and $\vec{\tau}$ are the spin and isospin vectors for the two nucleons, \hat{S}_{12} is the usual tensor-operator defined as,

$$\hat{S}_{12} = \frac{3}{x^2} (\vec{\sigma}_1 \cdot \vec{x}) (\vec{\sigma}_2 \cdot \vec{x}) - (\vec{\sigma}_1 \cdot \vec{\sigma}_2), \quad (2.7)$$

$$\frac{f^2}{4\pi} \simeq \frac{g_0^2}{14^2} = \frac{0.94}{14} \quad \text{for singlet even states,}$$

$$= \frac{1}{14} \quad \text{otherwise.} \quad (2.8)$$

Here V_i ($i=c, T, LS, q$) are the central, tensor, spin-orbit and quadratic spin-orbit potentials defined by

$$V_i(x) = +\infty \text{ for } x \leq x_c ,$$

$$V_i(x) = \sum_{n=0}^7 a_n e^{-2x/x^n} \text{ for } x > x_c , \quad (2.9)$$

x_c is 0.35. The radius of the hard core is

$r_c = 0.5116F$ for singlet even and triplet odd,

$= 0.5002F$ for singlet odd and triplet even

states. (2.10)

The parameters of the potential can be found in reference (Mar 66). In some cases the idealized hard core is replaced by softer repulsive core which is quite strong but not infinitely large. The examples of soft core potentials are those of Bressel, Kerman and Lomon (Brl 65) and of Reid (Red 68). Outside the repulsive core BKL potential has nearly the same form as that of Hamada-Johnston (HJ) with a few changes in parameters.

The next group of local potentials is typified by the boundary-condition model of Feshbach, Lomon and Tubis (Feh 64). In this the one-pion and two-pion exchange potentials are used outside a radius r_c at which an energy dependent boundary condition is specified to fit the high-energy scattering data.

Another group consists of meson-theoretic potentials which take into account exchange of several bosons in addition to π -meson, such as ρ , ω , η and σ -mesons. Different combinations of masses and coupling constants give a variety

of potentials. Recent attempts in developing such potentials have been done by Bryan and Scott (Bry 67) and Green and collaborators (Grn 67).

II.1b Non-local Potentials

A non-local potential is a non-diagonal operator, which implies that the potential energy is a matrix in coordinate space. The Schrödinger equation then has the form,

$$-\frac{\hbar^2}{2m} \nabla^2 \psi(\vec{r}) + \int v(\vec{r}, \vec{r}') \psi(\vec{r}') d\vec{r}' = E \psi(\vec{r}), \quad (2.11)$$

where m is the nucleon mass. Because of hermiticity, $v(\vec{r}, \vec{r}')$ must be a symmetric matrix, real in the energy range $0 \leq E \leq 300$ MeV. Such potentials are developed by Yamaguchi (Yai 54), Tabakin (Tab 64), Mitra and co-workers and others. Yamaguchi potential is a simple separable potential of the form,

$$v(\vec{r}, \vec{r}') = -\lambda U(\vec{r}) U(\vec{r}'). \quad (2.12)$$

Tabakin potential is a series of separable terms of Yamaguchi type and is of the form:

$$v(\vec{r}, \vec{r}') = \sum_{M, S, J, M'} P_{\ell} [-g(r)g(r') + h(r)h(r')] Y_{\ell S J}^M(\hat{r}) Y_{\ell' S J}^{M*}(\hat{r}')$$

with $\ell \leq 2$. (2.13)

Here, $\zeta = \frac{\hbar^2}{m}$, $Y_{\ell S J}^M(\hat{r})$ are the vector spherical harmonics,

defined in terms of the spherical harmonics $Y_{\ell}^m(\hat{r})$ and spin states $\chi_S^{m_S}$ by

$$Y_{\ell S J}^M(\hat{r}) = \sum_{m_S, m_S} (l_S m_S | JM) Y_{\ell}^{m_S}(\hat{r}) \chi_S^{m_S}, \quad (2.14)$$

$(l_S m_S | JM)$ is the Clebsh-Gordon coefficient defined on page 37 of reference (Eds 57). In expression (2.13) because the summation is done over ℓ and ℓ' , it allows ℓ -mixing, i.e., especially S-D mixing. P_{ℓ} is the isospin projection operator. The g-term is attractive and h-term is repulsive. Tabakin has given the form of g and h in momentum space. This potential gives only a qualitative fit to the two-body data. Moreover, it does not have the one-pion exchange feature for the long-range part of the potential. Thus, the Tabakin potential is not very realistic but it has been very useful in nuclear structure calculations because of the ease with which its matrix elements can be calculated.

III.1c Velocity-Dependent Potentials

Such potentials are of the form

$$V = V(r, p) + \text{constraints for hermiticity}, \quad (2.15)$$

where p is the momentum operator. The most commonly used velocity-dependent potential is that due to Green (Grm 62) and is of the form

$$V(r, p) = V(r) + [p^2 U(r) + U(r) p^2]. \quad (2.16)$$

$W(r)$ and $U(r)$ have the Gaussian radial dependence.

II.2. Effective Potentials

It is well known that the approximation in which one considers nuclear particles moving in some average potential field and interacting with a weak residual interaction is highly successful in the study of nuclear properties. In an independent particle model calculation one usually considers the effects of only few shells. The neglected shells renormalize the interaction in the space of the shells considered in one's calculation. Renormalization of the nucleon-nucleon interaction also takes place due to admixture of very high energy orbitals into the nuclear wave functions. This results from strongly repulsive nature of the nuclear force at short distances and also from specific characteristic of tensor force. In fact, the singular nature of the nucleon-nucleon interaction at short distances gives rise to strong short-range correlations which are not properly described by an independent particle wave function. Thus, in the nuclear structure calculations one must use the unmodified or the free nucleon-nucleon interaction in a configuration space described by wave functions which properly take into account short-range correlation effects. Alternatively, one can use a modified or effective interaction in a truncated configuration space consisting of independent particle wave functions. Thus, the problem is to find an effective interaction V_{eff} which would give the same results when used with uncorrelated wave functions in a limited

configuration space, as the true interaction V would give with correlated wave functions in an unlimited configuration space. For many years, in some simple minded calculations V_{eff} was chosen in an empirical manner and only a vague idea existed about its possible dependence on the choice of single particle orbitals and configuration space and its relationship to the realistic two-body interaction. It was only after the development of Brueckner theory (Brr 55) that several different approaches to the relationship of V_{eff} and V were given. In the Brueckner theory the nucleon-nucleon interaction V is replaced by an effective interaction, commonly known as K-matrix and is defined in equation (1.8). Several different approaches to relationship of V_{eff} and V , based on Brueckner theory, have been given by various authors. To name a few are the separation method of Moszkowski and Scott (Moi 60), reference-spectrum method of Bethe, Brandow and Petschek (Bee 63), Eden-Emery method (Edn 59), etc.

The reaction-matrix differs from the two-body potential over the short-range of correlation distance in the nuclear wave functions. There is an alternative way of introducing the effect of short-range correlations in the effective interaction, namely the method of canonical transformation. This approach (which in essence is close to Moszkowski-Scott technique) has been followed by Shakin, Waghmare and co-workers (Shn 67a). We shall briefly describe below their method of obtaining the effective interaction. In their method, the

25

correlations in the wave function are introduced via a unitary-model-operator such that if the long-range properties of the wave function are specified by a function $\bar{\bigcirc}(\vec{r}_1, \vec{r}_2 \dots \vec{r}_n)$, the corresponding correlated state is,

$$\Psi(\vec{r}_1, \vec{r}_2 \dots \vec{r}_n) = e^{iS} \bar{\bigcirc}(\vec{r}_1, \vec{r}_2 \dots \vec{r}_n) . \quad (2.17)$$

An effective Hamiltonian is defined in the space of the uncorrelated functions as

$$H_{\text{eff}} = e^{-iS} H e^{iS} , \quad (2.18)$$

where H is the true nuclear Hamiltonian. Since a transformation of the form described in equation (2.18) leaves the eigenvalue spectrum unchanged, H and H_{eff} are completely equivalent with respect to energy calculations. But, besides the desired two-body terms, H_{eff} contains many-body terms induced by the unitary transformation. Carrying out the expansion of H_{eff} and neglecting three and many-body terms, one finds that the effective Hamiltonian is,

$$H_{\text{eff}} = \sum_{n_1 n_2} \langle n_1 | T | n_2 \rangle a_{n_1}^+ a_{n_2}^+ + \frac{1}{2} \sum_{n_1 n_2 n_3 n_4} a_{n_1}^+ a_{n_2}^+ \langle n_1 n_2 | e^{-iS} \times \\ \times (T_1 + T_2 + U_1 + U_2 + V_{12}) e^{iS} - (T_1 + T_2 + U_1 + U_2) | n_3 n_4 \rangle a_{n_4} a_{n_3} , \quad (2.19)$$

where H_{eff} has been expressed in the second-quantized notation.

The operators a^\dagger and a are the usual creation and annihilation operators for the single particle states. The subscripts n_1 and n_2 refer to the quantities (n, l, j, m) necessary to specify the orbitals for particle motion in harmonic oscillator potential. T is the kinetic energy operator and V_{12} is the nucleon-nucleon interaction which may or may not have a hard core. The potentials U_1 and U_2 are used to generate the single particle wave functions. The form of U is generally taken to be of harmonic oscillator type to simplify the calculations, i.e., $U = \frac{1}{2} kr^2$. The operator S is assumed to introduce only central short-range two-body correlations in which case equation (2.17) becomes

$$e^{iS} \underline{\Psi}_{n_1 n_2} = \underline{\Psi}_{n_1 n_2}, \quad (2.20)$$

where $\underline{\Psi}$'s are the uncorrelated wave functions and $\underline{\Psi}$'s are the correlated wave functions occurring in equation (2.19). V_{12} can be written as a sum of two parts, v_{12} which is diagonal in relative orbital angular momentum l and v_T^{OD} which is off-diagonal in l , i.e.

$$V_{12} = v_{12} + v_T^{OD}. \quad (2.21)$$

Clearly v_T^{OD} receives contributions only from tensor part of the nucleon-nucleon interaction. v_{12} is separated into a long-range part v_{12}^l and a short-range part v_{12}^s such that the short-range part produces no energy shift in the pair state. This is a natural extension to finite nuclei of the zero phase shift condition of Moszkowski and Scott (Moi 60)

for nuclear matter calculations. The main effect of v_T^{OD} is to admix high-momentum orbitals into nuclear wave function. This admixture is not readily treated by the separation method used for v_{12} . Thus, the tensor correlations are treated on a different footing than the correlations due to short-range part of v_{12} and the separation of v_{12} into v_{12}^S and v_{12}^T is achieved by solving the following two equations:

$$(T_1 + T_2 + U_1 + U_2 + v_{12}^S) \bar{\Psi}_{n_1 n_2} = (\varepsilon_{n_1} + \varepsilon_{n_2}) \bar{\Psi}_{n_1 n_2} \quad (2.22)$$

$$\text{and } (T_1 + T_2 + U_1 + U_2) \bar{\Phi}_{n_1 n_2} = (\varepsilon_{n_1} + \varepsilon_{n_2}) \bar{\Phi}_{n_1 n_2} , \quad (2.23)$$

ε_{n_1} and ε_{n_2} are the energies of single particle states n_1 and n_2 respectively. For hard core potentials such as the Yale or the HJ potential it is necessary to introduce a short-range pseudopotential (VP) to carry out this separation procedure. In that case

$$v_{12} = (v_{12}^S + VP) + (v_{12}^T - VP) , \quad (2.24)$$

and one requires that

$$(T_1 + T_2 + U_1 + U_2 + v_{12}^S + VP) \bar{\Psi}_{n_1 n_2} = (\varepsilon_{n_1} + \varepsilon_{n_2}) \bar{\Psi}_{n_1 n_2} . \quad (2.25)$$

In general, therefore, one has

$$H_{eff} = \overbrace{\sum_{n_1 n_2} \langle n_1 | T | n_2 \rangle a_{n_1}^+ a_{n_2}^+} + \overbrace{\sum_{n_1 n_2 n_3 n_4} a_{n_1}^+ a_{n_2}^+ a_{n_4}^+ a_{n_3}^+} \\ \langle \bar{\Psi}_{n_1 n_2} | (v_{12}^T - VP) + v_T^{OD} | \bar{\Psi}_{n_3 n_4} \rangle . \quad (2.26)$$

If the shell-model or Hartree-Fock calculations are limited to orbitals having only fairly low-momentum components, almost all of the contribution of v_T^{OD} to the binding energy and to the effective interaction would be missed. Most of the contribution of v_T^{OD} may be taken into account by renormalizing the effective Hamiltonian in the independent pair approximation (Kuo 65):

$$H_{eff} = \sum_{n_1 n_2} \langle n_1 | T | n_2 \rangle a_{n_1}^+ a_{n_2}^+ + \frac{1}{2} \sum_{n_1 n_2 n_3 n_4} a_{n_1}^+ a_{n_2}^+ a_{n_4} a_{n_3}$$

$$\langle \Psi_{n_1 n_2} | (v_{12}^l - VP) + v_T^{OD} + v_T^{OD} \frac{Q}{e} v_T^{OD} \Psi_{n_3 n_4} \rangle. \quad (2.27)$$

If the second-order term in the pseudopotential is also included, a term $VP \frac{Q}{e} VP$ should be added to H_{eff} in equation (2.27).

The prescription described above is quite general and is applicable to any singular interaction. Using expression (2.27), Shakin et. al. (Shn 67a,67b) have evaluated the matrix elements of the Yale potential for various states of relative angular momentum. An attractive square-well type of pseudopotential (VP) has been used for those states of relative motion where the interaction is repulsive and also in 1S_0 and 3S_1 states (to keep the separation distance constant at 1.0F). For the treatment of intermediate states in the calculation of second-order terms the approximation of Kuo and Brown (Kuo 65) is used, which consists of using

plane-wave intermediate states and an angle averaged operator to take account of the Pauli principle in the intermediate states. A simple parameterization of the energy denominator e is made. The details of these calculations can be found in references (Shn 67a, 67b). Results for the relative matrix elements of effective Yale interaction are tabulated (Shn 67b) and will be used in the present work.

It can be seen that the unitary-model-operator method of obtaining the effective interaction is in some sense analogous to Brueckner theory. In fact it is possible to find a unitary transformation (Grg 68) for which the transformed two-body potential V_{eff} is

$$V_{\text{eff}} = \frac{1}{2}(K + K^+) \quad (2.28)$$

Expansion of H_{eff} defined in equation (2.18) is

$$H_{\text{eff}} = H^{(1)} + H^{(2)} + H^{(3)} + \dots, \quad (2.29)$$

where $H^{(n)}$ is an n -body operator. In first-order

$$H_{\text{eff}} = H^{(1)} + H^{(2)}, \quad (2.30)$$

when many-body terms are neglected. Applying the Hartree-Fock formalism to H_{eff} in equation (2.30), one finds the same expression for the ground state energies as in the first-order of Brueckner theory, except for the replacement of K by the hermitian combination $\frac{1}{2}(K+K^+)$. The higher-order corrections in both cases arise due to many particle effects,

more accurately, the many-body terms in the result of a unitary transformation have their counterparts in the cluster corrections of Brueckner theory.

There are quite a few other effective interactions obtained directly from realistic interactions, for example, the effective interaction of Kuo and Brown (Kuo 66) derived from HJ potential and later improved by Kuo (Kuo 67). Their effective interaction includes the contribution of renormalization effects due to core-polarization and has been widely used in nuclear-structure studies. To name a few other effective interactions used in the literature, are those of Wong (Wog 68) obtained from HJ potential and of Clement and Baranger (Clt 68) derived from Tabakin potential. These effective interactions have been obtained following the lines of Brueckner theory.

Of late, there has been a tendency to develop potentials primarily for the use in nuclear structure calculations. The principal aim of these works is to determine an effective potential having no hard core singularity and giving the correct energy, density and perhaps the symmetry energy in nuclear matter. Only a moderate fit to the two-body data is required. An additional requirement is that second and higher-order contributions to the energy of nuclear matter be small in order to improve convergence of perturbation expansion. These potentials are effective potentials in some sense and it is presumed that they are

not very different from the realistic potentials so that two-body data still have some significance even for the effective ones. We mention in this category the work done by Davies, Krieger and Baranger, Nestor and co-workers and Donelly, etc.

The potential of Davies et. al. (Das 66) is a simple velocity-dependent potential of the form given by Green (see equation 2.16). Their potential acts only in relative S-state. The parameters are determined from a fit to nuclear matter data but such a potential is in strong disagreement with the two-body data. In an attempt to improve the agreement with the two-body data Krieger and co-workers (Krr 66) have introduced a density-dependent term in Davies potential. The strength and range parameters of their potential are determined from a fit to the two-body data, while the density-dependent term takes care of nuclear matter saturation properties. The potential of Nestor et. al. (Ner 68) is also of the form given by Green but contains additional spin-orbit and tensor terms. These potentials have been used in the calculations of finite nuclei (Das 66: Krr 66: Ner 68) in the Hartree-Fock approximation and found to give reasonable results.

Brink and Boeker (Brk 67) have investigated various effective interactions of different forms, e.g. a sum of two Gaussians, a sum of a Gaussian and a delta function, and a velocity-dependent interaction. The parameters of each potential are adjusted so as to give the experimental binding

energies of ^4He and nuclear matter at about the experimental densities. With the resulting forces the binding energies and densities of intermediate nuclei are calculated. But no force could reproduce all the experimental data at the same time.

II.3 Potential Matrix Elements Obtained Directly from Phase Shifts

In most of the nuclear structure calculations the primary input needs matrix elements of nuclear force between states of two nucleons in nuclei. The usual procedure described above is to construct a potential model from nucleon-nucleon scattering data and then use this potential to calculate matrix elements needed for nuclear structure studies. In an alternative approach relative matrix elements of the two-body potential are obtained directly from experimental phase shifts data without attempting to establish a realistic potential form as an intermediate step. This method has been used by Kallio (Kao 65), Koltun (Kon 67), Elliott and co-workers (Elt 67, 68a). Elliott et. al. have obtained the relative matrix elements of the two-body potential in an oscillator basis by using an auxiliary potential method. Their matrix elements are commonly known as Sussex matrix elements. We shall briefly describe below their prescription used to obtain these matrix elements.

The potential V is regarded as a most general non-singular potential consistent with the general conservation

laws of spin, parity and isospin. It may be written as

$$V = \sum_{S \ell J} V^{S \ell J} (r, \frac{\partial}{\partial r}) |S \ell J\rangle \langle S \ell J|, \quad (2.31)$$

where $S \ell J$ denotes the particular spin and angular momentum state of the pair and n the oscillator radial quantum number describing the relative radial wave function $R_{n \ell}(r)$ of the pair. The $S \ell J$ labels are referred to as a particular channel. Thus, the set of the matrix elements $\langle n' S \ell J | V | n S \ell J \rangle$ are

$$\langle n' S \ell J | V | n S \ell J \rangle = \int_0^{\infty} R_{n' \ell}^* (r, \frac{\partial}{\partial r}) V^{S \ell J} (r, \frac{\partial}{\partial r}) R_{n \ell} r^2 dr. \quad (2.32)$$

In a particular channel V (the label $S \ell J$ can be dropped for brevity if one is confined to a chosen channel) is written as the sum of two terms $V = V_0 + V_1$, where V_0 is the auxiliary potential and V_1 is small in the sense that it can be treated in Born approximation at some energy $E = \frac{\hbar^2 k^2}{m}$, where k is the relative momentum and m is the nucleon mass. If δ is the observed phase shift and δ_0 that calculated with the auxiliary potential at the same energy E , then it is shown by Morse and Feshbach (Moe 53) that

where $u_k(r)$ is the radial wave function for scattering by the auxiliary potential with the usual asymptotic normalization

$$u_k(r) = \frac{1}{r} \sin \left(kr - \frac{1}{2} \ell \pi + \delta_0 \right) . \quad (2.34)$$

The auxiliary potential is taken to be a cut-off oscillator

$$\begin{aligned} V_0 &= -\frac{\hbar^2}{m} (D - r^2/4b^4) \quad \text{in } r \leq a \\ &= 0 \quad \text{in } r \geq a \end{aligned} \quad (2.35)$$

with depth D , range a and shape or range parameter b . The radial wave function $u_k(r)$ is then a solution of the following Schrödinger equation

$$\left(\frac{d^2}{dr^2} + \frac{2}{r} \frac{d}{dr} - \frac{\ell(\ell+1)}{r^2} + D + k^2 - \frac{r^2}{4b^4} \right) u_k(r) = 0 \quad (2.36)$$

for $r \leq a$ and is the free nucleon scattering wave function for $r \geq a$. For energy

$$E = \left(2n + \ell - \frac{1}{2} \right) \frac{\hbar^2}{mb^2} - \frac{\hbar^2 D}{m} = \frac{\hbar^2 k^2}{m} , \quad (2.37)$$

the radial part $u_k(r)$ is given by

$$\begin{aligned} u_k(r) &= B R_{n\ell}(r) & r \leq a \\ &= k(\cos \delta_0 j_\ell(kr) - \sin \delta_0 n_\ell(kr)) \quad r \geq a , \end{aligned} \quad (2.38)$$

$j_\ell(kr)$ and $n_\ell(kr)$ are the spherical Bessel and Neumann functions defined on page 621 of reference (Mo 53), $R_{n\ell}$ is the radial

of the bound state wave function of an infinite oscillator potential $u_k(r)$ has the required asymptotic normalization given in equation (2.34). Constants B and δ_0 are determined by the matching conditions

$$B R_{nl}(a) = k(\cos \delta_0 j_l(ka) - \sin \delta_0 \eta_l(ka)) , \quad (2.39)$$

$$\frac{R'_{nl}(a)}{R_{nl}(a)} = \frac{(\cos \delta_0 j'_l(ka) - \sin \delta_0 \eta'_l(ka))}{(\cos \delta_0 j_l(ka) - \sin \delta_0 \eta_l(ka))} , \quad (2.40)$$

where the prime denotes differentiation with respect to r . Combining equations (2.33) and (2.38) we have

$$\begin{aligned} \int_0^\infty R_{nl}(r) V_1 R_{nl}(r) r^2 dr &= - \frac{\hbar^2 k}{m B^2} \operatorname{tg}(\delta - \delta_0) \\ &+ \int_a^\infty \left\{ R_{nl}(r) V R_{nl}(r) - B^{-2} u_k(r) V u_k(r) \right\} r^2 dr . \end{aligned} \quad (2.41)$$

The second term on the right-hand-side of equation (2.41) is referred to as long-range correction. It arises due to the fact that $u_k(r)$ is not an oscillator function beyond $r > a$. However, this is very small if a is chosen to be near the range of nuclear forces and can be neglected. The matrix elements of the total potential V are obtained by adding the matrix elements of V_0 in the range $0 \leq r \leq a$ in equation (2.41). In the range $a \leq r \leq \infty$, V is same as V_1 . Thus,

$$\int_0^a R_{n\ell}(r) V R_{n\ell}(r) r^2 dr = \int_0^a R_{n\ell}(r) V_0 R_{n\ell}(r) r^2 dr - \frac{\hbar^2 k}{mB^2} \operatorname{tg}(\delta - \delta_0)$$

or more compactly

$$\langle R_{n\ell} | V | R_{n\ell} \rangle = \langle R_{n\ell} | V_0 | R_{n\ell} \rangle - \frac{\hbar^2 k}{mB^2} \operatorname{tg}(\delta - \delta_0) . \quad (2.42)$$

The matrix elements of V are insensitive to the choice of auxiliary potential as long as δ is close to δ_0 . Equation (2.42) gives matrix elements diagonal in radial quantum number. The off-diagonal matrix elements are obtained by differentiating the diagonal matrix elements with respect to b . The theory described above has been extended to cover the mixing of channels so that the matrix elements in the coupled channel can also be calculated. The details can be found in reference (Elt 68a).

Thus, the auxiliary potential method described above consists in assuming that the difference between a roughly chosen, smooth auxiliary potential, and the real potential may be treated in Born approximation. In the earlier work of Elliott et. al. (Elt 67) and in Kallio method it is assumed that the entire potential V is small enough to be treated in Born approximation. Thus, the auxiliary potential $V_0 = 0$ and the radial wave function $u_k(r)$ will be spherical Bessel

functions for all r ,

$$u_{\frac{1}{2}}(r) = k j_{\frac{1}{2}}(kr) \quad (2.43)$$

Kallio uses an approximate relation between spherical Bessel functions and harmonic oscillator radial functions given, by

$$R_{nl}(r) = B' k j_{\frac{1}{2}}(kr), \quad (2.44)$$

$$E = \frac{\hbar^2 k^2}{m} = (2n+1+\frac{1}{2})\hbar\omega. \quad (2.45)$$

The above approximation is valid at short distances and improves with increasing n . Thus, Kallio matrix elements are given by

$$\langle R_{nl} | V | R_{n'l} \rangle = - \frac{\hbar^2}{m} \frac{k}{B'^2} \operatorname{tg}\delta. \quad (2.46)$$

Kallio technique breaks down at $\delta = \pi/2$ since the matrix elements become infinite. In fact Kallio method can be regarded as the limiting case of the auxiliary potential method described above.

The Sussex matrix elements are obtained using experimental phase shifts of Breit et. al. (Brt 62) and are tabulated in reference (Elt 68a). The range of the oscillator length parameter is $1.4 \leq b \leq 2.6$. At each value of b , the complete matrix, i.e. for all (n, n') would define the potential uniquely. A connection between the n value of a diagonal matrix element and the energy of the phase shift, which governs its value, is defined in equation (2.37).

Consequently, an upper limit of 300 MeV, up to which experimental phase shifts are reliably known, imposes an upper limit on n . Moreover, since the accuracy of the successive differentiation on a curve determined numerically over a finite range goes on decreasing, there is a maximum limit of the size of the difference $n' - n$, for which reliable matrix elements can be deduced. However, the matrix elements which can be obtained reliably are the ones which are of importance in most of the nuclear structure calculations.

In obtaining the Sussex matrix elements it was assumed that V is non-singular. However, the matrix elements calculated by the auxiliary potential method give a first-order approximation to the reaction matrix elements even when the true potential is singular. This has been shown explicitly by Mavromatis et. al. (Mas 69). These authors start with a reaction matrix (t -matrix) associated with a two-body interaction V and defined as

$$t = V + V \frac{Q}{e} t . \quad (2.47)$$

The energy denominator e is

$$e = \hat{H}_0 - E , \quad (2.48)$$

\hat{H}_0 is the unperturbed Hamiltonian of relative motion

$$\hat{H}_0 = T + U \quad (2.49)$$

with eigenstate ϕ and E is energy of the perturbed state

Ψ which φ approximates. Q is the Pauli operator as defined earlier. If the normalization is chosen such that

$$\langle \varphi | \Psi \rangle = \langle \varphi | \varphi \rangle , \quad (2.50)$$

then $t\varphi = V\varphi$ (2.51)

and $\langle \varphi | t | \varphi \rangle = \langle \varphi | V | \varphi \rangle$ (2.52)

The matrix elements $\langle \varphi | t | \varphi \rangle$ remain finite even when V has a hard core. Of interest for nuclear structure calculations are those t -matrix elements for which \hat{H}_0 is the harmonic oscillator Hamiltonian,

$$\hat{H}_0 = T + \frac{1}{4} m\omega^2 r^2 \quad (2.53)$$

and the basis function φ is the complete set of harmonic oscillator wave functions. Such a t -operator is defined as t_n . In the auxiliary potential method of obtaining reaction matrix elements, one divides the potential V into two parts, the low-energy part \hat{V} for which the exclusion principle is significant, and the high-energy part $(V - \hat{V})$. For high-energy part Q is approximated by Q_A , the appropriate operator for the two particle system. This is justified since intermediate states of high-energy are largely unfilled in the nucleus and so exact treatment of Q is not very important. One defines the reaction matrix associated with the high-energy part as

$$t_A(\hat{V}) = (V - \hat{V}) + (V - \hat{V}) \frac{Q_A}{e_A} t_A(\hat{V}) , \quad (2.54)$$

$$\text{with } e_A = T + \hat{V} - E. \quad (2.55)$$

Keeping terms to second-order in t_A and V the perturbative expansion (Bron 64) of t_n is

$$t_n = t_A + \hat{V} + \hat{V} \frac{Q}{e_n} \hat{V} + \hat{V} \frac{Q}{e_n} t_A + t_A \frac{Q}{e_n} \hat{V} + t_A \left(\frac{Q}{e_n} - \frac{Q_A}{e_A} \right) t_A, \quad (2.56)$$

$$\text{with } e_n = T + \frac{1}{4} m \omega^2 r^2 - E \quad (2.57)$$

In Elliott method, $\hat{V} = V_0$ is taken to be a cut-off harmonic oscillator defined in equation (2.35). The basis functions ϕ associated with t_n have the radial part $u_k(r)$ defined in equation (2.38). If the radial part of the wave function Ψ is denoted as $w_k(r)$, the matrix elements

$$\langle u_k(r) | t_A(V_0) | u_k(r) \rangle = \langle u_k(r) | (V - V_0) | w_k(r) \rangle$$

may be obtained from the solution of following Schrödinger equations for $u_k(r)$ and $w_k(r)$:

$$\left[-\frac{\hbar^2}{m} \frac{d^2}{dr^2} + \frac{\hbar^2}{m} \frac{l(l+1)}{r^2} + V_0 - E \right] (r u_k(r)) = 0,$$

$$\left[-\frac{\hbar^2}{m} \frac{d^2}{dr^2} + \frac{\hbar^2}{m} \frac{l(l+1)}{r^2} + V - E \right] (r w_k(r)) = 0. \quad (2.58)$$

One obtains

$$\begin{aligned}
 \langle u_k | t_A(v_0) | u_k \rangle &= \int_0^\infty dr \, r u_k(r) (V - V_0) r w_k(r) \\
 &= \frac{\hbar^2}{m} [(r u_k) \frac{d}{dr} (r w_k) - \frac{d}{dr} (r w_k) (r u_k)] \\
 &= - \frac{\hbar^2}{m} k \, \operatorname{tg}(\delta - \delta_0) \tag{2.59}
 \end{aligned}$$

Thus, using equations (2.38), (2.56), (2.59) and neglecting any long-range corrections we have, to first-order in t_A and V_0 ,

$$\begin{aligned}
 \langle R_{nl} | t_n | R_{nl} \rangle &= - \frac{\hbar^2}{m} \frac{k}{B^2} \operatorname{tg}(\delta - \delta_0) + \langle R_{nl} | V_0 | R_{nl} \rangle \\
 &\quad + \text{higher-order terms.} \tag{2.60}
 \end{aligned}$$

With a suitable choice of V_0 , it is generally possible to make $\delta_0 = \delta$ for any particular value of k in which case the first term in equation (2.60) vanishes and $\langle R_{nl} | t_n | R_{nl} \rangle$ is given in first order by $\langle R_{nl} | V_0 | R_{nl} \rangle$ even when the true potential is singular. This is precisely the prescription used in the auxiliary potential method where, however, it is assumed that V is well behaved and the two first terms on the right-hand-side of equation (2.60) together then give the potential matrix elements $\langle R_{nl} | V | R_{nl} \rangle$. Thus, in any case the Sussex matrix elements can be regarded as a first-order approximation to nuclear reaction matrix elements $\langle R_{nl} | t_n | R_{nl} \rangle$.

There is a direct analogy between the Moszkowski-Scott separation method and the auxiliary potential method of calculating reaction matrix elements. In the separation method V is divided into a short-range part V^S and the long-range part V^L such that the matrix elements of the reaction matrix t_s associated with V^S vanish and in first-order t_n is replaced by V^L . In the auxiliary potential method V^S can be associated with $V - \hat{V}$ and V^L with \hat{V} . Matrix elements of t_A associated with $(V - \hat{V})$ can be made equal to zero in which case t_n is replaced by \hat{V} . However, the separation in the auxiliary potential method is not spatial but is energy separation. Unlike the separation method the auxiliary potential method can be applied equally well whether the potential V is attractive or repulsive.

In Kallio method $\hat{V} = 0$ so that

$$\langle R_{nl} | t_n | R_{nl} \rangle = - \frac{\hbar^2}{m} \frac{k}{B^2} \operatorname{tg} \delta . \quad (2.61)$$

This is also the expression to which right-hand-side of equation (2.60) reduces in the limit $\delta_0 \rightarrow 0$. In fact Sussex matrix elements with $\delta_0 \neq 0$ are substantially in agreement with Kallio matrix elements. Koltun phase shift method is a calculation of t -matrix for the free two nucleon system in an oscillator basis, but we shall not go into the details of his method. The work done by Elliott and co-workers is most intensive and complete. The matrix elements have been

tested in some of the nuclear structure calculations for finite nuclei and found to give reasonable results. In the present work these matrix elements have been employed in the HF calculations of light nuclei in the range $4 \leq A \leq 40$.

II.4 Summary

To summarize, the situation is as follows. The experimental information about the nucleon-nucleon potential comes from the two-body scattering and two-nucleon bound state data. Most of the potential models nowadays use the results of meson theory, mainly to determine the long-range part of the potential. The short-range part is left to phenomenology and the uncertainty in it is mainly due to the necessity of working below an upper energy limit of 300 MeV. The adjustable parameters of the model are determined from a fit to two-body data. One important characteristic of these potentials which fit the two-body data, is that they do not fit the nuclear matter data, e.g. in the binding energy calculation of nuclear matter Yale and Hamada-Johnston potentials give (Brr 62: Ray 63) a minimum of -8.3 MeV per particle at a density corresponding to Fermi momentum $k_F = 1.19 F^{-1}$ and -7.8 MeV per particle at $k_F = 1.12 F^{-1}$ respectively, compared to the experimental values of B.E. per particle = -15.75 MeV, $k_F = 1.5 F^{-1}$. According to Brueckner theory, following features of the nucleon-nucleon potential are responsible for the smaller values of energy and density:

- (i) large core-radius
- (ii) strong odd-state repulsion
- (iii) quadratic-spin-orbit term
- (iv) weak even triplet central force.

However, these are just the same features necessary for a good fit to high-energy scattering data. Tabakin potential also gives only ~ 8 MeV per particle, $k_F = 1.6F^{-1}$ in nuclear matter calculations, in first order. These potentials when used in any perturbation theory treatment of finite nuclei fail to give adequate binding in first-order (Ken 66: Shn 67b). It has been found that second-order corrections for these potentials are quite important and reasonable values of binding energies of finite nuclei and infinite nuclear matter can be obtained only when the contributions of second-order terms are taken into account (Tan 64: Pal 66).

On the other hand there are some effective potentials, available for use in binding energy calculations, which are computationally easy to handle. The most important criteria in choosing these potentials are that they fit the nuclear matter data and the second-order corrections to the binding energy of nuclear matter are small. Binding energy results obtained with these potentials are, in some cases, better than those obtained with realistic potentials (Das 66: Krr 66) at least in first-order, but then the fit to the two-body data is poor. Thus, the question still remains open whether a potential model can be constructed

which would fit the scattering data as well as the nuclear matter and finite nucleus data at one and the same time.

The fact, that different realistic interactions which fit the two-body data quantitatively give similar results in nuclear structure calculations (Lyh 67), suggests that one can avoid the complicated procedure of constructing a potential model and obtaining the parameters from a fit to two-body data. Instead, one can obtain the matrix elements of nucleon-nucleon potential in some suitable basis directly from experimental phase shift data as done by Elliott et. al. and others. However, the results of such calculations would be expected to be close to those made with realistic potentials (see Chapter IV).

CHAPTER III

HARTREE-FOCK THEORY FOR FINITE NUCLEI

III.1 Hartree and Hartree-Fock Equations

Present microscopic theories of nuclei are based on two postulates:

- (i) The degrees of freedom associated with the meson fields in nuclei may be replaced by the potentials (including exchange forces) between nucleons.
- (ii) Two-body forces are most important. Thus, the Hamiltonian of the nucleus consisting of A nucleons is of the form

$$H = \sum_{i=1}^A T_i + \sum_{i < k}^A v_{ik} , \quad (3.1)$$

where T_i is the kinetic energy $\frac{p_i^2}{2m_A}$ of the i^{th} nucleon, v_{ik} is the interaction potential between the pair of particles i and k , and m_A is the nucleon mass. To understand the nuclear structure one has to solve the many-nucleon Schrödinger equation

$$H\Psi(\vec{r}_1, \vec{r}_2 \dots \vec{r}_A) = E\Psi(\vec{r}_1, \vec{r}_2, \dots \vec{r}_A) , \quad (3.2)$$

where $\vec{r}_1, \vec{r}_2 \dots \vec{r}_A$ define the coordinates of the particles. This is a non-separable differential equation in $3A$ independent variables and needs some simplification for its practical

treatment. Hartree and Hartree-Fock (HF) approximations (Slr 60) consist of obtaining approximate solutions of equation (3.2) using variational principle. In Hartree method, the approximate ground state solution Ψ_H of the above equation is assumed to be given by the simple product of A single particle wave functions (orbitals) $\Psi_1(\vec{r}_1)$, $\Psi_2(\vec{r}_2)$ $\Psi_A(\vec{r}_A)$, the first A states being regarded as occupied so that,

$$\Psi_H(\vec{r}_1, \vec{r}_2 \dots \vec{r}_A) = \Psi_1(\vec{r}_1) \Psi_2(\vec{r}_2) \dots \Psi_A(\vec{r}_A) . \quad (3.3)$$

The set of functions $\{\Psi_\alpha\}$ is varied to minimize the average energy $E_H = \langle \Psi_H, H \Psi_H \rangle$ of the system. The minimum condition $\delta \langle \Psi_H, H \Psi_H \rangle = 0$ leads to the following Hartree equation for the single particle wave function Ψ_α ,

$$\int \Psi_\alpha^*(\vec{r}_\alpha) T_\alpha \Psi_\alpha(\vec{r}_\alpha) d\vec{r}_\alpha + \sum_{\gamma \neq \alpha} \left(\langle \Psi_\alpha^*(\vec{r}_\alpha) \Psi_\gamma^*(\vec{r}_\gamma) | V(\vec{r}_\alpha, \vec{r}_\gamma) | \vec{r}_\alpha', \vec{r}_\gamma' \rangle \right) \Psi_\alpha(\vec{r}_\alpha') \Psi_\gamma(\vec{r}_\gamma') d\vec{r}_\alpha' d\vec{r}_\gamma' = \epsilon_\alpha^H , \quad (3.4)$$

where the summation γ runs over only the occupied single particle states. It can be seen that Hartree product function Ψ_H does not satisfy the Pauli principle according to which the wave function must be antisymmetric under the exchange of any two nucleons. In the HF approximation many-body

wave function Ψ is taken to be fully antisymmetrized product of an orthonormal set of single particle wave functions $\{\psi_\alpha\}$,

$$\Psi(\vec{r}_1, \vec{r}_2, \dots, \vec{r}_A) = \frac{1}{\sqrt{A!}} \begin{vmatrix} \psi_1(\vec{r}_1) & \psi_1(\vec{r}_2) & \dots & \psi_1(\vec{r}_A) \\ \psi_2(\vec{r}_1) & \psi_2(\vec{r}_2) & \dots & \psi_2(\vec{r}_A) \\ \vdots & \vdots & \ddots & \vdots \\ \psi_A(\vec{r}_1) & \psi_A(\vec{r}_2) & \dots & \psi_A(\vec{r}_A) \end{vmatrix} \quad (3.5)$$

ψ_α 's are varied to minimize the energy $E = \langle \Psi, H\Psi \rangle$ of the system maintaining the subsidiary conditions, namely, the normalization of all ψ_α 's and the orthogonality of any two ψ_α 's i.e.

$$\int \psi_\alpha^*(\vec{r}) \psi_\beta(\vec{r}) d\vec{r} = \delta_{\alpha\beta} \quad (3.6)$$

Thus, the HF equations are gotten by demanding

$$\delta[\langle \Psi, H\Psi \rangle \langle \Psi, \Psi \rangle] = 0 \quad (3.7)$$

The details of the variational calculation are not presented here and can be found in any book on many-body theory (Len 64: Bron 67). The result is that single particle wave functions ψ_α 's satisfy the following HF equations.

$$\langle \alpha | T | \beta \rangle + \sum_{\gamma=1}^A \langle \alpha\gamma | V_{AN} | \beta\gamma \rangle = \epsilon_\alpha \delta_{\alpha\beta} \text{ for } \alpha \leq A, \beta \leq A ,$$

where the antisymmetrized matrix element of V is

$$\langle \alpha\gamma | v_{AN} | \beta\delta \rangle = \langle \alpha\gamma | v | \beta\delta \rangle - \langle \alpha\gamma | v | \delta\beta \rangle$$

and $\langle \alpha | T | \beta \rangle = \int \Psi_{\alpha}^*(\vec{r}_1) T_1 \Psi_{\beta}(\vec{r}_1) d\vec{r}_1 ,$

$$\langle \alpha\gamma | v | \beta\delta \rangle = \int (\Psi_{\alpha}^*(\vec{r}_1) \Psi_{\gamma}^*(\vec{r}_2) v(\vec{r}_1, \vec{r}_2 | \vec{r}_1', \vec{r}_2') \Psi_{\beta}(\vec{r}_1') \Psi_{\delta}(\vec{r}_2')) d\vec{r}_1 d\vec{r}_2 d\vec{r}_1' d\vec{r}_2' . \quad (3.8)$$

The HF self-consistent single particle potential is defined as

$$\langle \alpha | U | \beta \rangle = \sum_{\gamma=1}^A \langle \alpha\gamma | v_{AN} | \beta\gamma \rangle \quad (3.9)$$

Thus,

$$\langle \alpha | h | \beta \rangle = \langle \alpha | T | \beta \rangle + \langle \alpha | U | \beta \rangle = \epsilon_{\alpha} \delta_{\alpha\beta} , \quad (3.10)$$

where h is the HF single particle Hamiltonian. It can be shown that the unoccupied HF single particle orbitals, which correspond to the states $\alpha > A$, $\beta > A$, also satisfy equations similar to (3.10). That is,

$$\langle \alpha | h | \beta \rangle = \epsilon_{\alpha} \delta_{\alpha\beta} \quad \text{for } \alpha > A, \beta > A ,$$

but $\langle \alpha | h | \beta \rangle = 0$, if only one of the two states α and β are occupied and the other one is unoccupied. Thus, the HF Hamiltonian h has no matrix elements between occupied and unoccupied levels. The ground state energy E_0 of the system

is then given by

$$\begin{aligned}
 E_0 &= \sum_{\gamma=1}^A \varepsilon_{\gamma} - \frac{1}{2} \sum_{\gamma=1}^A \langle \gamma | U | \gamma \rangle \\
 &= \sum_{\gamma=1}^A [\langle \gamma | T | \gamma \rangle + \frac{1}{2} \langle \gamma | U | \gamma \rangle] . \quad (3.11)
 \end{aligned}$$

Equation (3.10) looks like a one-body Schrödinger equation but the potential U depends upon the very single particle wave functions one has set out to find. To carry the summation over γ in equation (3.9) we need to know the wave functions of all the states which are occupied in Ψ . Hence, the solution of HF single particle equation is obtained by the method of self-consistency (iterations) over the wave functions. These equations can be solved by choosing any one of the following two representations for wave functions Ψ_{α} 's, described in next section.

III.2 Different Ways of Doing HF

HF equations can be solved in two different representations.

III.2a Coordinate-Space Representation

In the coordinate-space representation the single particle wave functions are just written as functions of \vec{r} : equations (3.8) and (3.9) lead to the following Schrödinger

equation when V is local

$$\frac{p_1^2}{2m_A} \Psi_\alpha(\vec{r}_1) + \left[\sum_{\gamma=1}^A \left(\vec{d}\vec{r}_2 \Psi_\gamma^*(\vec{r}_2) V(\vec{r}_1 - \vec{r}_2) \Psi_\gamma(\vec{r}_2) \right) \right] \Psi_\alpha(\vec{r}_1)$$

$$- \sum_{\gamma=1}^A \left[\left(\Psi_\gamma^*(\vec{r}_2) V(\vec{r}_1 - \vec{r}_2) \Psi_\alpha(\vec{r}_2) \vec{d}\vec{r}_2 \right) \Psi_\gamma(\vec{r}_1) \right] = \epsilon_\alpha \Psi_\alpha(\vec{r}_1) . \quad (3.12)$$

The first term is a local one-body potential (the direct, or Hartree potential), whereas the second yields the exchange term, a non-local one-body potential (exchange potential). If the two-body interaction is already non-local, all one-body potentials will also be non-local.

Calculations in this representation have been done by Kerman and Lockett (Ken 64), and Vautherin and Vénéroni (Van 67). However, they have used a purely central two-body potential. Inclusion of a spin-orbit term or a non-locality in two-body potential makes the calculations enormously complicated. This representation has also been used in all calculations of Brueckner et. al. (Brr 61) and Köhler (Kör 65).

III.2b Oscillator Representation

The HF single particle wave functions are expanded in a convenient set of orthonormal functions

$$\Psi_\alpha(\vec{r}) = \sum_\mu C_\mu^\alpha \phi_\mu(\vec{r}) , \quad (3.13)$$

where α and μ denote the angular momentum and isospin quantum numbers of single particle states, i.e. $\alpha = (aljm\tau)$, $(\mu = nljm\tau)$: a , n are radial quantum numbers. Combining equations (3.13) and (3.10), we get

$$\sum_{\mu'_1} [\langle \mu_1 | T | \mu'_1 \rangle + \langle \mu_1 | U | \mu'_1 \rangle] c_{\mu'_1}^\alpha = \varepsilon_\alpha c_{\mu_1}^\alpha$$

$$\text{or } \sum_{\mu'_1} \langle \mu_1 | h | \mu'_1 \rangle c_{\mu'_1}^\alpha = \varepsilon_\alpha c_{\mu_1}^\alpha, \quad (3.14)$$

$$\text{where } \langle \mu_1 | U | \mu'_1 \rangle = \sum_{\mu_2 \mu'_2} \rho_{\mu_2 \mu'_2} \langle \mu_1 \mu_2 | V_{AN} | \mu'_1 \mu'_2 \rangle \quad (3.15)$$

$$\text{and } \rho_{\mu_2 \mu'_2} = \sum_{\gamma=1}^A c_{\mu_2}^\gamma c_{\mu'_2}^\gamma. \quad (3.16)$$

ρ is the density of single particle levels and the summation runs over the occupied states only. The total energy E_0 is then given by,

$$E_0 = \sum_{\mu_1 \mu'_1} \rho_{\mu_1 \mu'_1} [\langle \mu_1 | T | \mu'_1 \rangle + \frac{1}{2} \langle \mu_1 | U | \mu'_1 \rangle]. \quad (3.17)$$

The expansion coefficients c_μ^α 's can be found by diagonalizing a matrix whose elements are $\langle \mu_1 | h | \mu'_1 \rangle$. Thus, this is also known as the matrix method (Bar 63: Net 63) of solving HF equations. The choice of the basis ϕ in equation (3.13)

is completely arbitrary but the choice of three-dimensional harmonic oscillator wave functions is preferred for two reasons:

(i) The HF single particle functions are expected to be close to oscillator ones, so that a few terms of the series may be needed to get a good representation. In other words, the set of oscillator functions used need not have a large dimensionality and instead of solving integro-differential equations of the type (3.12) one has to diagonalize small real symmetric matrices. Thus, the calculations are much easier. The coefficients C_{μ}^{α} 's and energies ϵ_{α} 's are always real since they are the eigenvalues and eigenvectors of a real symmetric matrix.

(ii) In this representation the separation between the relative and centre-of-mass coordinates can be done exactly. Thus, the calculation of two-body matrix elements of nucleon-nucleon potential is easy since the latter generally depends only on the relative coordinates of two nucleons.

This representation has been used in most of the earlier HF calculations described in Chapter I as well as in the present work. The function φ_{μ} is the normalized solution of the three-dimensional isotropic harmonic oscillator:

$$\varphi_{\mu}(\vec{r}) = \varphi_{n\ell jm\tau}(\vec{r}) = \frac{R'_{n\ell}(r)}{r} \sum_{j=1}^M \chi_{\frac{j}{2}}^{\tau}, \quad (3.18)$$

$\psi_{\frac{1}{2}j}^m$ is the eigen function of total angular momentum defined in (2.14), $\chi_{\frac{1}{2}}^{\tau}$ is an isospin function and the radial function is

$$R'_{n\ell}(r) = \left[\frac{2\sqrt{\beta_0}(n-1)!}{\Gamma(n+\ell+\frac{1}{2})} \right]^{\frac{1}{2}} (\sqrt{x})^{\ell+1} e^{-x/2} L_{n-1}^{(\ell+\frac{1}{2})}(x) , \quad (3.19)$$

$x = \beta_0 r^2$, $n = 1, 2, 3 \dots$, $L_n^{\alpha}(x)$ is a Laguerre Polynomial, defined on page 784 of reference (Moe 53) and $\beta_0 = \frac{m_A \omega}{\hbar}$, ω being the oscillator frequency. The energy eigenvalue associated with this state is $\epsilon_{n\ell} = (2n+\ell-\frac{1}{2})\hbar\omega$.

In general, the summation over μ in equation (3.13) is over all the quantum numbers. However, the HF Hamiltonian h can have various symmetries, such as spherical, ellipsoidal, axial, etc. which when considered in the initial step, can reduce the vast variational space in expansion (3.13). If we consider the HF field to be spherically symmetric, then the single particle HF states have good angular momentum and the C_{μ}^{α} (and hence $P_{\mu_2 \mu_2^*}$) are diagonal in ℓ , j and independent of m (z-projection of \vec{j}). Thus, the expansion (3.13) can be rewritten as:

$$\Psi_{\alpha}(\vec{r}) = \Psi_{\alpha \ell j m \tau}(\vec{r}) = \sum_{n=1}^N C_n^{\alpha}(\ell j \tau) \psi_{n \ell j m \tau}(\vec{r}) , \quad (3.20)$$

where N specifies the maximum number of terms which are

included in the summation in equation (3.13), and is same as the maximum number of relative nodes in functions ϕ_μ occurring in the summation. The mixing of neutron and proton states in a given orbit has not been considered so that expansion of equation (3.20) is limited to a single value of third component of isospin τ which distinguishes the neutron and proton orbits. Also, if there is no coulomb force $C_\mu^{\alpha\beta}$'s are independent of τ .

III.3 Calculation of the Matrix Elements in Oscillator Basis

III.3a One-Body Matrix Elements, $\langle \mu_1 | T | \mu_1' \rangle$:

The matrix elements of the kinetic energy operator T in the oscillator basis is given by

$$\langle n_1 l_1 j_1 m_1 \tau_1 | T | n_1' l_1' j_1' m_1' \tau_1' \rangle = \delta(l_1 l_1') \delta(j_1 j_1') \delta(m_1 m_1') \times \times \delta(\tau_1 \tau_1') \langle n_1 | T(l_1) | n_1' \rangle ,$$

where

$$\langle n_1 | T(l_1) | n_1' \rangle = \frac{\pi \omega}{2} \times \begin{cases} (2n_1 + l_1 - \frac{1}{2}), & n_1 = n_1' \\ \sqrt{n(n + l_1 + \frac{1}{2})}, & |n_1 - n_1'| = 1, n = \min(n_1, n_1') \\ 0 & , |n_1 - n_1'| > 1 \end{cases} . \quad (3.21)$$

III.3b Two-Body Matrix Elements, $\langle \mu_1 \mu_2 | V_{AN} | \mu_1' \mu_2' \rangle$:

Since most of the two-body interactions depend only on the relative coordinates of the two nucleons, it

is convenient to express the two-body matrix elements in terms of relative and centre-of-mass coordinates of the two particles. The following procedure is used. The two-body uncoupled states $|\mu_1\mu_2\rangle = |n_1\ell_1j_1m_1\tau_1, n_2\ell_2j_2m_2\tau_2\rangle$ are coupled to a total angular momentum J and total isospin τ state with the use of 3-j symbols:

$$|n_1\ell_1j_1m_1\tau_1, n_2\ell_2j_2m_2\tau_2\rangle$$

$$\begin{aligned}
 &= \sum_{JM\tau M\tau} (-1)^{2j_1+J+M+M} \tau [J]^{\frac{1}{2}} [\tau]^{\frac{1}{2}} \times \\
 &\quad \times \begin{pmatrix} j_1 & j_2 & J \\ -m_1 & -m_2 & M \end{pmatrix} \begin{pmatrix} \frac{1}{2} & \frac{1}{2} & \tau \\ \tau_1 & \tau_2 & -M \end{pmatrix} \times \\
 &\quad \times |n_1\ell_1j_1, n_2\ell_2j_2: JM, \tau M\tau\rangle, \quad (3.22)
 \end{aligned}$$

where we have used the notation that a number x inside square brackets implies

$$[x] \Rightarrow (2x+1) .$$

The two-particle coupled state in j - j coupling scheme is transformed to the λ - S coupling scheme by means of 9-j symbols in the following way:

$$|n_1 l_1 j_1, n_2 l_2 j_2: JM, \mathcal{T}_{H_T} \rangle$$

$$= \sum_{S} \left([\lambda][S][j_1][j_2] \right)^{\frac{1}{2}} \left\{ \begin{array}{ccc} l_1 & l_2 & \lambda \\ \frac{1}{2} & \frac{1}{2} & S \\ j_1 & j_2 & J \end{array} \right\} \times$$

$$\times |n_1 l_1 n_2 l_2, \lambda: \frac{1}{2} \frac{1}{2}, S: JM, \mathcal{T}_{H_T} \rangle . \quad (3.23)$$

Further, Moshinsky transformation is used to write

$$|n_1 l_1 n_2 l_2, \lambda \rangle = \sum_{n \ell_{NL}} \langle n \ell_{NL} \lambda | n_1 l_1 n_2 l_2 \lambda \rangle | n \ell_{NL}, \lambda \rangle , \quad (3.24)$$

where the $\langle n \ell_{NL} \lambda | n_1 l_1 n_2 l_2 \lambda \rangle$ are the Brody and Moshinsky transformation brackets (Bry 60). The quantum numbers (n ℓ) and (NL) specify the relative motion of the two particles and the motion of the centre-of-mass of the pair respectively. The total orbital angular momentum λ is the result of the coupling of ℓ and L. A simple recoupling procedure yields

$$|n \ell, NL, \lambda: \frac{1}{2} \frac{1}{2}, S: JM \rangle$$

$$= (-1)^{J+S+\lambda} \sum_{J'} ([\lambda][J])^{\frac{1}{2}} \left\{ \begin{array}{ccc} L & \ell & \lambda \\ S & J & J' \end{array} \right\} |NL, n \ell S J': JM \rangle . \quad (3.25)$$

The quantity inside the curly-brackets is the Wigner 6-j

symbol. The final expression for the most general antisymmetrized two-body matrix elements of an interaction V which conserves total spin S and isospin τ is

$$\begin{aligned}
 & \langle n_1 l_1 j_1 m_1 \tau_1, n_2 l_2 j_2 m_2 \tau_2 | V_{AN} | n'_1 l'_1 j'_1 m'_1 \tau'_1, n'_2 l'_2 j'_2 m'_2 \tau'_2 \rangle \\
 &= \sum_{\substack{\lambda \lambda' J J' M \tau \\ M_{AN} n n' l l' \\ NL}} (-)^{\lambda + \lambda'} ([j_1][j_2][j'_1][j'_2])^{\frac{1}{2}} [J'][\lambda][\lambda'][s][J][\tau] \times \\
 & \quad \times \langle n l NL \lambda | n_1 l_1 n_2 l_2 \lambda \rangle \langle n' l' NL \lambda' | n'_1 l'_1 n'_2 l'_2 \lambda' \rangle \times \\
 & \quad \times \begin{pmatrix} j_1 & j_2 & J \\ -m_1 & -m_2 & M \end{pmatrix} \begin{pmatrix} j'_1 & j'_2 & J \\ -m'_1 & -m'_2 & M \end{pmatrix} \begin{pmatrix} \frac{1}{2} & \frac{1}{2} & \tau \\ \tau_1 & \tau_2 & -M \tau \end{pmatrix} \times \\
 & \quad \times \begin{pmatrix} \frac{1}{2} & \frac{1}{2} & \tau \\ \tau'_1 & \tau'_2 & -M \tau \end{pmatrix} \begin{pmatrix} L & l & \lambda \\ s & J & J' \end{pmatrix} \begin{pmatrix} L & l' & \lambda' \\ s & J & J' \end{pmatrix} \times \\
 & \quad \times \begin{pmatrix} l_1 & l_2 & \lambda \\ \frac{1}{2} & \frac{1}{2} & s \\ j_1 & j_2 & J \end{pmatrix} \begin{pmatrix} l'_1 & l'_2 & \lambda' \\ \frac{1}{2} & \frac{1}{2} & s \\ j'_1 & j'_2 & J \end{pmatrix} \times \\
 & \quad \times (1 - (-1)^{l+s+\tau}) F_{nn'l'l}^{J'\tau' s} , \tag{3.26}
 \end{aligned}$$

where

$$\begin{aligned}
 F_{nn'l'l'}^{J'\tau} S &= \langle n'lS: J'M, \tau M_{\tau} | V \nabla l' S: J'M, \tau M_{\tau} \rangle \\
 &= \frac{1}{2^{3/2}} \langle \tau M_{\tau} | \int \varphi_{n'lSJM}^* \left(\frac{\vec{r}}{\sqrt{2}} \right) V(\vec{r}) \varphi_{n'l'SJM} \left(\frac{\vec{r}}{\sqrt{2}} \right) d\vec{r} | M_{\tau} \rangle.
 \end{aligned} \tag{3.27}$$

In most of the situations, the interaction $V(\vec{r})$ conserves total angular momentum, parity and isospin. The 3-j, 6-j and 9-j symbols follow the notation of Edmonds (Eds 57). The normalization constant for the matrix elements is

$$\frac{1}{(1+\delta_{n_1 n_2} \delta_{l_1 l_2} \delta_{j_1 j_2})^{\frac{1}{2}}} \frac{1}{(1+\delta_{n'_1 n'_2} \delta_{l'_1 l'_2} \delta_{j'_1 j'_2})^{\frac{1}{2}}}.$$

Thus, apart from the geometrical factors occurring in the expression of equation (3.26), the two-body matrix elements can be obtained in a straightforward manner from the relative matrix elements of V in an oscillator basis.

III.3c Matrix-Elements of HF Single Particle Potential, $\langle \mu_1 | U | \mu'_1 \rangle$:

Since the summation in equation (3.20) is restricted to the radial quantum numbers, only the matrix elements of the form $\langle n_1 l_1 j_1 m_1 \tau_1, n_2 l_2 j_2 m_2 \tau_2 | V_{AN} | n'_1 l'_1 j'_1 m'_1 \tau'_1, n'_2 l'_2 j'_2 m'_2 \tau'_2 \rangle$ are required in the calculation of $\langle \mu_1 | U | \mu'_1 \rangle$. Writing explicitly,

$$\langle n_1 \ell_1 j_1 m_1 \tau_1 | U | n'_1 \ell'_1 j'_1 m'_1 \tau'_1 \rangle$$

$$= \sum_{n_2 n'_2=1}^N \sum_{\substack{\ell_2 j_2 m_2 \tau_2 \\ (\text{occ})}} \rho_{n_2 n'_2}(\ell_2 j_2) \times \\ \times \langle n_1 \ell_1 j_1 m_1 \tau_1, n_2 \ell_2 j_2 m_2 \tau_2 | V_{AN} | n'_1 \ell'_1 j'_1 m'_1 \tau'_1, n'_2 \ell'_2 j'_2 m'_2 \tau'_2 \rangle \quad (3.28)$$

with

$$\rho_{n_2 n'_2}(\ell_2 j_2) = \sum_{a(\text{occ})} c_{n_2}^a(\ell_2 j_2) c_{n'_2}^a(\ell'_2 j'_2) \quad (3.29)$$

In the case of a doubly closed shell nucleus all the occupied j_2 -subshells are completely filled, i.e., each one of them contains $2(2j_2+1)$ particles. Thus, the summation over m_2 and τ_2 in equation (3.28) can be carried out very easily and the orthogonality of the 3-j symbols leads to the result

$$\sum_{m_2 \tau_2} \langle n_1 \ell_1 j_1 m_1 \tau_1, n_2 \ell_2 j_2 m_2 \tau_2 | V_{AN} | n'_1 \ell'_1 j'_1 m'_1 \tau'_1, n'_2 \ell'_2 j'_2 m'_2 \tau'_2 \rangle \\ = \delta(\ell_1 \ell'_1) \delta(j_1 j'_1) \delta(m_1 m'_1) (2j_2+1) P(\ell_1 j_1 n_1 n'_1, \ell_2 j_2 n_2 n'_2) \quad (3.30)$$

$$P(\ell_1 j_1 n_1 n'_1, \ell_2 j_2 n_2 n'_2)$$

$$\begin{aligned}
 &= \sum_{\substack{\lambda \lambda' J J' \tau \\ nn' \ell' \ell' NL}} (-)^{\lambda + \lambda'} [J'] [\lambda] [\lambda'] [s] [J] [\tau] \langle n \ell NL \lambda | n_1 \ell_1 n_2 \ell_2 \rangle \times \\
 &\times \langle n' \ell' NL \lambda' | n'_1 \ell_1 n'_2 \ell_2 \lambda' \rangle \begin{Bmatrix} \ell_1 & \ell_2 & \lambda \\ \frac{1}{2} & \frac{1}{2} & s \\ j_1 & j_2 & J \end{Bmatrix} \begin{Bmatrix} \ell_1 & \ell_2 & \lambda' \\ \frac{1}{2} & \frac{1}{2} & s \\ j_1 & j_2 & J \end{Bmatrix} \times \\
 &\times (1 - (-1)^{\ell + s + \tau}) G_{nn' \ell \ell'}^{J' \tau} s
 \end{aligned} \tag{3.31}$$

with

$$\begin{aligned}
 G_{nn' \ell \ell'}^{J' \tau} s &= \sum_{\tau_2 M \tau} \begin{pmatrix} \frac{1}{2} & \frac{1}{2} & \tau \\ \tau_1 & \tau_2 & -M \tau \end{pmatrix} \begin{pmatrix} \frac{1}{2} & \frac{1}{2} & \tau \\ \tau'_1 & \tau'_2 & -M \tau \end{pmatrix} F_{nn' \ell \ell'}^{J' \tau} s \\
 &= \frac{1}{2} \delta(\tau_1 \tau'_1) F_{nn' \ell \ell'}^{J' \tau} s
 \end{aligned} \tag{3.32}$$

Thus,

$$\begin{aligned}
 \langle n_1 \ell_1 j_1 m_1 \tau_1 | U | n'_1 \ell'_1 j'_1 m'_1 \tau'_1 \rangle &= \delta(\ell_1 \ell'_1) \delta(m_1 m'_1) \delta(j_1 j'_1) \\
 &\quad \langle n_1 | U(\ell_1 j_1) | n'_1 \rangle
 \end{aligned} \tag{3.33}$$

where

$$\langle n_1 | U(\ell_1 j_1) | n'_1 \rangle = \sum_{n_2 n'_2=1}^N \sum_{\ell_2 j_2 (\text{occ})} \rho_{n_2 n'_2}(\ell_2 j_2) (2j_2 + 1) \\ P(\ell_1 j_1 n_1 n'_1, \ell_2 j_2 n_2 n'_2) . \quad (3.34)$$

For non-closed-shell nuclei, which contain partially filled j -subshells, following approximation is used for the density ρ of the occupied levels. It is assumed that the neutrons and protons are equivalent and averaging over the m -substates for a given j is done. The average density is given by

$$\rho_{n_2 n'_2}(\ell_2 j_2) = \sum_{a(\text{occ})} \frac{N_a(\ell_2 j_2)}{2(2j_2 + 1)} c_{n_2}^a(\ell_2 j_2) c_{n'_2}^a(\ell_2 j_2) , \quad (3.35)$$

where $N_a(\ell_2 j_2)$ = the number of nucleons in a given subshell $(\ell_2 j_2)$.

Equations (3.29) to (3.33) remain the same.

III.4 Iterative Solutions of HF Equations

With equations (3.21) and (3.33), equation (3.14) becomes

$$\begin{aligned}
& \sum_{n'_1=1}^N [\langle n_1 | T(\ell_1) | n'_1 \rangle + \langle n_1 | U(\ell_1 j_1) | n'_1 \rangle] c_{n'_1}^a(\ell_1 j_1) \\
& = \varepsilon_{a\ell_1 j_1} c_{n'_1}^a(\ell_1 j_1) , \quad (3.36)
\end{aligned}$$

where N is the number of terms included in expansion (3.20). There is one such equation for each $(\ell_1 j_1)$. The total ground state energy E_0 defined in equation (3.17) is

$$\begin{aligned}
E_0 = & \sum_{n_1 n'_1=1}^N \sum_{\ell_1 j_1 (\text{occ})} c_{n_1 n'_1}(\ell_1 j_1) 2(2j_1+1) \times \\
& \times [\langle n_1 | T(\ell_1) | n'_1 \rangle + \frac{1}{2} \langle n_1 | U(\ell_1 j_1) | n'_1 \rangle]
\end{aligned} \quad (3.37)$$

The factor $2(2j_1+1)$ comes from the sum on m_1 and τ_1 . The set of equations (3.36) is solved by the following iteration procedure:

- (i) An initial set of $c_{n_1}^a(\ell_1 j_1)$ is guessed and also which orbits are occupied. Usually, $c_{n_1}^a(\ell_1 j_1) = \delta_{na}$.
- (ii) With this set of coefficients the matrix elements of HF Hamiltonian occurring in equation (3.36) are calculated.
- (iii) Equation (3.36) is solved by diagonalizing a $N \times N$ Hamiltonian matrix. A new set of coefficients $c_{n_1}^a(\ell_1 j_1)$ is obtained. Total ground state energy E_0 is computed.

These new set of coefficients are recycled through the step (ii) for recalculating the matrix elements and another diagonalization of the matrix. This process is repeated until successive diagonalizations produce the same set of coefficients $C_{n_1}^a(l_1 j_1)$ and E_0 reaches a constant value. The final set of $C_{n_1}^a(l_1 j_1)$, are the correct expansion coefficients, E_0 is the total binding energy of the system and $\epsilon_{a l_1 j_1}$ are the single particle levels of the nucleus. The calculations are repeated for several values of oscillator range parameter $b = \sqrt{(\hbar/m_A \omega)}$, which enters in our expression through the expansion (3.20). The minimum in the E_0 vs. b curve is determined.

III.5 Coulomb and Centre-of-Mass Corrections

There are two important corrections to HF solutions arising due to the coulomb force between the protons and centre-of-mass motion of the nucleus. The effect of these corrections on the total binding energy can be estimated externally if one assumes some simple model for the nucleus. Thus, for example, if the nucleus is assumed to have a uniform spherical charge distribution, its coulomb energy would be given by

$$E_{\text{coul}} = \frac{3}{5} \frac{e^2}{R} Z(Z-1) \text{ with } R = 1.3A^{1/3} . \quad (3.38)$$

Similarly, if one assumes that the centre-of-mass of the nucleus is in the lowest 1s state of a harmonic oscillator

well, the kinetic energy of its motion is

$$E_{c.m.} = \frac{3}{4} \hbar \omega \text{ with } \hbar \omega = \frac{41.6}{b^2} \quad (3.39)$$

However, the effects of these corrections on various nuclear properties calculated in the framework of HF theory can be determined only if they are accounted for in a self-consistent manner, i.e., these corrections are included in the Hamiltonian h first and then the HF equations are solved. For this, the following procedure is used.

III.5a Coulomb Correction

The coulomb force between the nucleons can be written as

$$v_{12}^{\text{coul}} = \frac{e^2}{4r} (1+2\tau_1) (1+2\tau_2) , \quad (3.40)$$

v_{12}^{coul} acts only if both particles are protons. The Hamiltonian H with the coulomb correction is

$$\begin{aligned} H &= \sum_{i=1}^A T_i + \sum_{i < k}^A (v_{ik} + v_{ik}^{\text{coul}}) \\ &= \sum_{i=1}^A T_i + \sum_{i < k}^A v_{ik}^{\text{new}} , \end{aligned} \quad (3.41)$$

$$\text{where } v_{ik}^{\text{new}} = v_{ik} + v_{ik}^{\text{coul}} . \quad (3.42)$$

Thus, the only change which would occur in the HF equations is that the two-body matrix elements $\langle \mu_1 \mu_2 | V_{ik} | \mu'_1 \mu'_2 \rangle$ of V_{ik} will be replaced by those of V_{ik}^{new} . These matrix elements can still be given by expression (3.26), but $F_{nn' \ell \ell'}^{J' \tau S}$ now will consist of two terms,

$$F_{nn' \ell \ell'}^{J' \tau S} = F_{nn' \ell \ell'}^{J' \tau S} \text{ (nucleus)} + F_{nn' \ell \ell'}^{J' \tau S} \text{ (coulomb)} \quad (3.43)$$

with

$$\begin{aligned} F_{nn' \ell \ell'}^{J' \tau S} \text{ (coulomb)} &= \langle n \ell S J M, \tau M \tau | \frac{e^2}{r} | n' \ell' S' J' M', \tau M' \tau' \rangle \\ &= \delta(\tau_1) \delta(M_1) \delta(\ell \ell') \int_0^{\infty} R_{n \ell}^{J' \tau}(r) \frac{e^2}{r} R_{n' \ell'}^{J' \tau}(r) dr. \end{aligned} \quad (3.44)$$

Care should be exercised in carrying the summation over τ_2 in equation (3.30) since coulomb matrix elements depend upon the isospin quantum numbers. However, the sum over τ_2 can still be carried over explicitly if we make the time-saving, but non-essential approximation that in calculating $\langle \mu_1 | U | \mu'_1 \rangle$, $\rho_{n_2 n'_2}(\ell_2 j_2)$ is independent of τ_2 . Summation over m_2 is done as before. Thus, $G_{nn' \ell \ell'}^{J' \tau S}$ in equation (3.31) will now be replaced by

$$G_{nn' \ell \ell'}^{J' \tau S} = G_{nn' \ell \ell'}^{J' \tau S} \text{ (nucleus)} + G_{nn' \ell \ell'}^{J' \tau S} \text{ (coulomb)} \quad (3.45)$$

with

$$G_{nn'l'l'}^{J'\tau S} \text{ (coulomb)} = 2 \delta(\tau_1^{\frac{1}{2}}) \begin{pmatrix} \frac{1}{2} & \frac{1}{2} & 1 \\ \frac{1}{2} & \frac{1}{2} & -1 \end{pmatrix}^2 F_{nn'l'l'}^{J'\tau S}$$

$$= \frac{2}{3} \delta(\tau_1^{\frac{1}{2}}) F_{nn'l'l'}^{J'\tau S} \quad . \quad (3.46)$$

Subsequent changes will occur in the expressions that follow equation (3.30).

III.5b Centre-of-Mass Motion

Considering a nucleus with A particles, we use $3A$ coordinates for A orbitals. However, the centre-of-mass coordinates should be subtracted, so that we really have $3A-3$ independent coordinates. Thus, the Hamiltonian which describes the intrinsic state of the system is obtained by removing the centre-of-mass energy in equation (3.1). Thus, the intrinsic Hamiltonian is

$$H_I = H - \frac{\vec{P}^2}{2Am_A} \quad (3.47)$$

$$\text{with the total momentum } \vec{P} = \sum_i \vec{p}_i \quad . \quad (3.48)$$

The operator of the centre-of-mass kinetic energy can be written as a sum of one-body and two-body operators,

$$\frac{\vec{P}^2}{2m_A A} = \sum_{ik} \frac{\vec{p}_i \cdot \vec{p}_k}{2m_A A} \quad .$$

The square of the relative momentum is

$$\begin{aligned}
 (p_{ik})^2 &= \frac{1}{4} |\vec{p}_i - \vec{p}_k|^2 \\
 &= \frac{1}{4} ((\vec{p}_i)^2 + (\vec{p}_k)^2 - 2\vec{p}_i \cdot \vec{p}_k) \\
 \therefore \frac{1}{2}\vec{p}_i \cdot \vec{p}_k &= \frac{1}{4}(p_i^2 + p_k^2) - p_{ik}^2 \\
 \therefore \frac{p^2}{2m_A} &= \frac{1}{4m_A} \sum (p_i^2 + p_k^2) - \frac{p_{ik}^2}{m_A} . \quad (3.49)
 \end{aligned}$$

Equation (3.47) now becomes

$$H_I = \frac{1}{2} \sum_{i \neq k} v_{ik} + \frac{1}{2} \sum_{i \neq k} \frac{2p_{ik}^2}{Am_A} , \quad (3.50)$$

which is a pure two-body operator. The second term can be regarded as an additional potential $v_{12}^{c.m.} = \frac{2p_{12}^2}{Am_A}$ and can be treated as the nucleon-nucleon two-body interaction v_{12} . This adds an additional term to $F_{nn' \ell \ell}^{J' \tau' S}$ in equations (3.26) and (3.43), which is now given by

$$F_{nn' \ell \ell}^{J' \tau' S} \text{ (c.m.)} = \delta(\ell) \frac{2}{A} \langle n | T(\ell) | n' \rangle , \quad (3.51)$$

where $\langle n | T(\ell) | n' \rangle$ is defined in equation (3.21). The solution proceeds as before except that now in (3.36) and (3.37) one-body term $\langle n_1 | T(\ell_1) | n'_1 \rangle$ is missing.

III.6 Hartree-Fock Density Distribution and R.M.S. Radii

III.6a Density

The density of the particles inside the nucleus is

$$\rho_o(\vec{r}) = \sum_{\alpha=1}^A \left| \Psi_{\perp}(\vec{r}_1, \vec{r}_2 \dots \vec{r}_{\alpha-1}, \vec{r}, \vec{r}_{\alpha+1} \dots \vec{r}_A) \right|^2 \frac{d\vec{r}_1 \dots d\vec{r}_{\alpha-1} d\vec{r}_{\alpha+1} \dots d\vec{r}_A}{(3.52)}$$

Using expression (3.5) for Ψ_{\perp} and integrating over $(A-1)$ coordinates, one obtains

$$\begin{aligned} \rho_o(\vec{r}) &= \sum_{\alpha=1}^A \psi_{\alpha}^*(\vec{r}) \psi_{\alpha}(\vec{r}) \\ &= \sum_{\mu\mu'} \rho_{\mu\mu'} \varphi_{\mu}^*(\vec{r}) \varphi_{\mu'}(\vec{r}) . \end{aligned} \quad (3.53)$$

Writing $\rho_{\mu\mu'}$ and φ_{μ} 's explicitly from equations (3.16) and (3.18), and summing over m and τ we obtain

$$\rho_o(\vec{r}) = \frac{1}{2\pi} \sum_{nn'lj} (2j+1) \frac{R'_{nl}(\vec{r})}{r} \rho_{nn'}(lj) \frac{R'_{nl'}(\vec{r})}{r} . \quad (3.54)$$

This density is normalized so that $\int \rho_o(\vec{r}) d\vec{r} = A$. The proton

and neutron charge densities, $\rho_c(r)$ and $\rho_n(r)$, have the same form except that in equation (3.53) the summation is only over the proton or neutron orbits respectively, and the factor $\frac{1}{2\pi} \rho_{nn'}(\ell_j)$ in equation (3.54) is replaced by $\frac{1}{4\pi} \rho_{nn'}(\ell_j \tau)$. Finally, the three radial densities are related as

$$\rho_o(r) = \rho_c(r) + \rho_n(r) . \quad (3.55)$$

III.6b R.M.S. Radius

The mean square radius for the matter distribution is given by

$$\langle r^2 \rangle = \frac{\int \rho_o(r) r^2 dr}{\int \rho_o(r) dr} \quad (3.56)$$

$$= \frac{4\pi}{A} \int \rho_o(r) r^4 dr . \quad (3.57)$$

Using equation (3.54) this becomes

$$\langle r^2 \rangle = \frac{2}{A} \sum_{nn' \ell_j} (2j+1) \rho_{nn'}(\ell_j) \int_0^\infty R_n' \psi(r) R_{n'}' \psi(r) r^2 dr . \quad (3.58)$$

The integration can be carried over exactly and finally

$$\begin{aligned} \langle r^2 \rangle &= \frac{4b^2}{A} \sum_{n \ell_j} (2j+1) [\rho_{nn}(\ell_j) (2n + \ell - \frac{1}{2}) \\ &\quad - 2 \rho_{n+1}(\ell_j) \sqrt{n(n+\ell+\frac{1}{2})}] . \end{aligned} \quad (3.59)$$

The r.m.s. radius is $\sqrt{\langle r^2 \rangle}$. The mean square radius for charge distribution is given by expression similar to equation (3.59) except that A is replaced by Z and sum is only over the proton orbits.

III.7 HF Potential

The oscillator matrix elements of the HF single particle potential U are obtained from equation (3.34) after several iterations have determined a self-consistent density matrix $\rho_{nn'}(\ell_j)$. It is possible to express U in coordinate space by the equation,

$$U(\vec{r}|\vec{r}') = \sum_{n_1 n'_1=1}^N \sum_{\substack{\ell_1 j_1 m_1 \tau_1 \\ (\text{occ})}} \phi_{n_1 \ell_1 j_1 m_1 \tau_1}(\vec{r}) \langle n_1 | U(\ell_1 j_1) | n'_1 \rangle \phi_{n'_1 \ell_1 j_1 m_1 \tau_1}^*(\vec{r}'). \quad (3.60)$$

Using explicit forms for ϕ 's we have

$$U(\vec{r}|\vec{r}') = \sum_{\ell_1 j_1 m_1 \tau_1} \chi_{\frac{1}{2}}^{\tau_1} \psi_{\ell_1 \frac{1}{2} j_1}^{m_1}(\vec{r}) U_{\ell_1 j_1}(\vec{r}, \vec{r}')$$

$$\psi_{\ell_1 \frac{1}{2} j_1}^{m_1*}(\vec{r}') \chi_{\frac{1}{2}}^{\tau_1}, \quad (3.61)$$

where

$$U_{\ell_1 j_1}(\vec{r}, \vec{r}') = \sum_{n_1 n'_1} \frac{R_{n_1 \ell_1}(\vec{r})}{r} \langle n_1 | U(\ell_1 j_1) | n'_1 \rangle \frac{R_{n'_1 \ell_1}(\vec{r}')}{r'} \quad (3.62)$$

This is a non-local and state-dependent potential. A possible local equivalent to this potential can be obtained in the static approximation which consists of computing the velocity-dependent potential $U(\vec{r}|\vec{p})$ corresponding to non-local U at $\vec{p} = 0$. Thus,

$$\begin{aligned} U(\vec{r}|\vec{p}) &= \int U(\vec{r}|\vec{r}') d\vec{r}' \\ &= \sum_{n_1 n_1'} \frac{R_{n_1 0}'(r)}{r} \langle n_1 | U(0^{\frac{1}{2}}) | n_1' \rangle \int_0^\infty R_{n_1' 0}(r') r' dr', \end{aligned} \quad (3.63)$$

after doing the angular integrals. The integral on r' can be done by using the Laplace transform on page 30 of Magnus and Oberhettinger (Mas 49). The result is

$$\int_0^\infty R_{n_1 0}'(r) r dr = b^{3/2} \left(\frac{\pi}{2}\right)^{1/4} \frac{[\frac{1}{2}(2n-1)!]^{1/2}}{2^{n-3} (n-1)!} (-)^{n-1}. \quad (3.64)$$

The static potential becomes,

$$\begin{aligned} U(\vec{r}|\vec{p} = 0) &= - \sum_{n_1 n_1'} (-)^{n_1} \frac{R_{n_1 0}'(r)}{r} \langle n_1 | U(0^{\frac{1}{2}}) | n_1' \rangle b^{3/2} \left(\frac{\pi}{2}\right)^{1/4} \\ &\times \frac{[\frac{1}{2}(2n-1)!]^{1/2}}{2^{n_1-3} (n_1-1)!}. \end{aligned} \quad (3.65)$$

III.8 Choice of Nuclei for Spherical HF Calculations

The HF Hamiltonian h does not necessarily have the same symmetry property as the nuclear Hamiltonian H . The possible symmetries of the HF Hamiltonian are governed by the following theorem (Ria 68).

Theorem: Let R be an operator that commutes with H ,

$$R^{-1}HR = H. \quad (3.66)$$

Then, if R leaves the set of occupied orbitals invariant, it commutes with HF Hamiltonian h ,

$$R^{-1}hR = h. \quad (3.67)$$

The operator R will leave the set of occupied orbitals invariant if the states obtained by operating R on any occupied orbitals α may be expressed as a linear combination of occupied orbitals only. That is,

$$\Psi_{\bar{\alpha}} = R\Psi_{\alpha} = \sum_{\sigma=1}^A x_{\sigma}^{\alpha} \Psi_{\sigma} \quad \text{for } \alpha \leq A$$

and
$$\sum_{\alpha=1}^A x_{\mu}^{\alpha} x_{\mu'}^{\alpha} = \delta_{\mu\mu'}. \quad (3.68)$$

If the nuclear Hamiltonian H has spherical symmetry, it commutes with the three operators \mathcal{I}_x , \mathcal{I}_y and \mathcal{I}_z of the total angular momentum operator \mathcal{I} . We wish that HF Hamiltonian

should also have spherical symmetry in which case it should commute with \mathcal{T}_x , \mathcal{T}_y and \mathcal{T}_z . These operators will leave the set $\{\alpha = \text{aljm}\}$ of occupied orbitals invariant if for a particular j all m -substates are either filled or empty. Hence, spherical symmetry can exist only in nuclei that have right number of particles to form closed shells. Such nuclei in the range $A \leq 40$ are ^4He , ^{12}C , ^{16}O and ^{40}Ca and, thus, one would expect that results of spherical HF calculations would describe the ground state of these nuclei correctly. If the coulomb interaction is neglected and nuclear forces are assumed to be charge independent then the HF field is an isospin scalar, and neutron and proton orbits are degenerate.

III.9 Single Oscillator Approximation Limit to HF Solutions

In the limit when there is only one term in the expansion (3.20), the HF orbitals are represented by pure oscillator functions. In this case $\rho_{\mu_2 \mu_2'}$ will become

$$\begin{aligned}
 \rho_{\mu_2 \mu_2'} &= \sum_{\alpha(\text{occ})} c_{\mu_2}^\alpha c_{\mu_2'}^\alpha, \\
 &= \sum_{\alpha(\text{occ})} \delta_{\mu_2 \alpha} \delta_{\mu_2' \alpha} \\
 &= \sum_{\alpha(\text{occ})} \delta_{\alpha \mu_2} \delta_{\mu_2 \mu_2'}.
 \end{aligned} \tag{3.69}$$

Thus, the density $\rho_{\mu_2 \mu_2'}$ of the levels would be either one or

zero depending upon whether the state μ_2 is occupied or unoccupied in the ground state configuration. The single particle potential matrix elements are

$$\begin{aligned}
 \langle \mu_1 | U | \mu'_1 \rangle &= \sum_{\mu_2 \mu'_2} P_{\mu_2 \mu'_2} \langle \mu_1 \mu_2 | V_{AN} | \mu'_1 \mu'_2 \rangle \\
 &= \sum_{\mu_2 \mu'_2} \left(\sum_{\alpha(\text{occ})} \delta_{\mu_2 \mu'_2} \delta_{\alpha \mu_2} \right) \langle \mu_1 \mu_2 | V_{AN} | \mu'_1 \mu'_2 \rangle \\
 &= \sum_{\mu_2(\text{occ})} \langle \mu_1 \mu_2 | V_{AN} | \mu'_1 \mu_2 \rangle. \quad (3.70)
 \end{aligned}$$

The total energy E_0 is

$$\begin{aligned}
 E_0 &= \sum_{\mu_1 \mu'_1} P_{\mu_1 \mu'_1} [\langle \mu_1 | T | \mu'_1 \rangle + \frac{1}{2} \langle \mu_1 | U | \mu'_1 \rangle] \\
 &= \frac{1}{2} \sum_{\mu_1(\text{occ})} \delta_{\mu_1 \mu'_1} [\langle \mu_1 | T | \mu'_1 \rangle + \frac{1}{2} \langle \mu_1 | U | \mu'_1 \rangle], \quad (3.71)
 \end{aligned}$$

where the potential energy of the nucleus is,

$$P.E. = \frac{1}{2} \sum_{\mu_1 \mu_2(\text{occ})} \langle \mu_1 \mu_2 | V_{AN} | \mu_1 \mu_2 \rangle \quad (3.72)$$

For $N = Z$ nuclei with LS closed shells equation (3.72) reduces to a simple expression,

$$P.E. = \sum_{S \subset J} \omega_{n \ell NL}^{S \subset J} \langle n \ell S J | V | n \ell S J \rangle , \quad (3.73)$$

where the weight-factor $\omega_{n \ell NL}^{S \subset J}$ is given by

$$\begin{aligned} \omega_{n \ell NL}^{S \subset J} = & \left(\frac{1 - (-1)^{S + \subset + J}}{2} \right) [\subset] [J] \times \\ & \times \sum_{\substack{n_1 \ell_1 n_2 \ell_2 \lambda \\ (\text{occ})}} \sum_{\ell} \left[\frac{\lambda}{\ell} \right] \langle n \ell NL | n_1 \ell_1 n_2 \ell_2 \lambda \rangle^2 . \end{aligned} \quad (3.74)$$

The potential energy can also be written as

$$P.E. = \sum_{\mu(\text{occ})} W(\mu, \mu) + \frac{1}{2} \sum_{\substack{\mu \neq \mu' \\ (\text{occ})}} W(\mu, \mu') , \quad (3.75)$$

where $W(\mu, \mu')$ is the contribution to potential energy due to interaction of nucleons in the state μ, μ' and can be obtained with the help of equation (3.72). For doubly closed shell nuclei, the single particle potential U , defined in equation (3.70), can be written down explicitly as,

$$\begin{aligned} & \langle n_1 \ell_1 j_1 m_1 \tau_1 | U | n_2 \ell_2 j_2 m_2 \tau_2 \rangle \\ = & \sum_{\substack{n_2 \ell_2 j_2 \\ (\text{occ})}} \sum_{\subset} \left[\frac{J}{j_1} \right] \left[\frac{\subset}{j_2} \right] \langle n_1 \ell_1 j_1, n_2 \ell_2 j_2: JM, \subset M_{\subset} | V \right. \\ & \quad \left. [n_1 \ell_1 j_1, n_2 \ell_2 j_2: JM, \subset M_{\subset}] \right] \\ & \quad + (-1)^{j_1 + j_2 - J - \subset} [n_2 \ell_2 j_2, n_1 \ell_1 j_1: JM, \subset M_{\subset}] . \end{aligned} \quad (3.76)$$

Equation (3.76) defines the single particle potential for neutrons. For protons, additional coulomb term should be added and the result is that V in equation (3.76) is replaced by V^{new} , defined in equation (3.42). The kinetic energy T of a single nucleon in state T is given by

$$T = (2n_1 + \ell_1 - \frac{1}{2}) \hbar\omega, \quad \hbar\omega = \frac{41.6}{b^2} \cdot (3.77)$$

III.10 Validity of the HF Approximation

The determinantal wave function Ψ_{HF} constructed from the final self-consistent HF single particle orbitals φ_{α} 's cannot be the true many-body wave function and hence it is relevant to ask the question how good is Ψ_{HF} ? With the possible improvements to Ψ_{HF} , one can write an improved Ψ_I as

$$\Psi_I = A_0 \Psi_{\text{HF}} + A_1 \Psi_{\text{HF}}^{\text{1p-1h}} + A_2 \Psi_{\text{HF}}^{\text{2p-2h}} \dots \quad (3.78)$$

where

$$\Psi_{\text{HF}}^{\text{1p-1h}} = \sum_{\text{hp}} x_{\text{ph}} a_p^+ a_h^- \Psi_{\text{HF}} \quad (3.79)$$

$$\Psi_{\text{HF}}^{\text{2p-2h}} = \sum_{\substack{\text{p}_1 \text{p}_2 \\ \text{h}_1 \text{h}_2}} x_{\text{p}_1 \text{p}_2 : \text{h}_1 \text{h}_2} a_{\text{p}_1}^+ a_{\text{p}_2}^+ a_{\text{h}_1}^- a_{\text{h}_2}^- \Psi_{\text{HF}} \quad (3.80)$$

p and h refer to the HF unoccupied and occupied states respectively. The various amplitudes, i.e., A_0 , $A_1 x_{\text{ph}}$,

$A_2^X p_1 p_2$: $h_1 h_2$, etc. are in principle calculable. If A_0 is very large compared to the other amplitudes, Ψ_{HF} is close to Ψ_I . Making use of the fact that the HF Hamiltonian h does not have any matrix elements between the occupied and unoccupied states, it can be shown that the amplitudes for the 1p-1h excitations are identically zero and, thus, the corrections to Ψ_{HF} can come only from 2p - 2h and more complicated excitations. The admixture of 2p-2h excitations to Ψ_{HF} is measured by the ratio of some typical off-diagonal matrix elements of the Hamiltonian H , between the wave functions corresponding to these excitations and Ψ_{HF} , to the smallest amount of energy needed for two particle excitations. A small ratio results in small admixture. Same is true for higher excitations. This, then means, that the validity of the HF approximation is measured by the difference in the HF single particle energies of the unoccupied and occupied states. The lowest of these differences is the one between the uppermost occupied level and the lower most unoccupied level. If this is significantly large compared to the differences in the energy of the unoccupied states themselves or of the occupied states, we can speak of the existence of a gap of energy. The larger this gap is, the nearer is Ψ_{HF} to Ψ_I . Sometimes, a relaxation of the constraint imposed on single particle orbitals results in a considerable improvement in the approximation and is reflected in increase in the energy gap between occupied and unoccupied orbitals.

HF approximation is a variation procedure as described earlier in Section III.1 and provides an upper bound to the energy E_0 of the system. The possible corrections to E_0 arise from 2p-2h and higher excitations, and can be calculated by means of perturbation theory in Hartree-Fock basis. However, HF solutions have to be understood in a different way when one is dealing with the effective Hamiltonian of Shakin, Waghmare and co-workers. These authors obtain an effective Hamiltonian by using the theory of cluster expansion and higher-order terms in this expansion are dropped. HF method to such an effective Hamiltonian has not been applied as a variation procedure since we are not dealing with complete Hamiltonian. We, then, have used the HF method as an attempt to find orbitals in this harmonic oscillator basis that yield self-consistency so that 1p-1h corrections to the energy, calculated with this effective interaction are minimized.

CHAPTER IV

APPLICATIONS OF HARTREE-FOCK THEORY AND DISCUSSION

IV.1 Details of the Calculation

Spherical Hartree-Fock (HF) calculations have been carried out in considerable detail for the nuclei ^4He , ^8Be , ^{12}C and ^{16}O with effective Yale interaction. Less complete calculations have also been done for ^{10}Be and ^{18}O . In view of the fact that besides the properties such as binding energy, root-mean-square radius, spin-orbit splittings, etc., we are also interested in the distribution of protons inside a nucleus and that the motion of the centre-of-mass of the pair of particles contributes considerably to the binding energy, we add the coulomb and centre-of-mass correction terms to V while calculating the HF potential and wave functions (see Section III.5 for details). The effect of these two terms modifies the wave functions through the density matrix. These effects have not been included in a self-consistent way by Shakin et. al. (Shn 67b) while calculating the properties of ^{16}O and ^{40}Ca with effective Yale interaction. However, while they have included the second-order term in pseudopotential (VP) by adding a term $\frac{Q}{e} VP$ to H_{eff} , defined in equation (2.27), we have not included it in our calculation. HF calculations have also been done for the nuclei ^4He , ^{12}C , ^{16}O and ^{40}Ca with Sussex interaction. In these calculations also,

coulomb and centre-of-mass matrix elements are included in a self-consistent manner in all the cases, except in ^{40}Ca for which the effect of these terms is estimated externally. Two-body matrix elements are calculated using formula (3.26). Since the nuclear force has a short-range it is necessary to use only a few relative ℓ values in the calculation of two-body matrix elements of the nucleon-nucleon interaction. A maximum of relative $\ell=2$ states has been used in our calculation. Higher ℓ states are not expected to contribute significantly for light nuclei studied in the present work (Tan 68). The configuration space used in our HF calculations of $A \leq 16$ nuclei consists of $s_{1/2}$, $p_{3/2}$ and $p_{1/2}$ oscillator states of $n = 1, 2$ and 3 major shells for each of these states. In the calculation for ^{40}Ca and also for some of the lighter nuclei, a larger configuration space is employed which includes $d_{5/2}$ and $d_{3/2}$ oscillator states of $n = 1, 2$ and 3 major shells in addition to states described above. Thus, in all the HF calculations expansion (3.20) contains only three terms. Earlier HF calculations (Das 66: Sve 65: Shn 67b: Krr 66) provide some justification for such a truncation. However, this truncation makes our results depend on b ($= \sqrt{\frac{\hbar}{m\omega}}$), the oscillator range parameter and in the spirit of a proper variational calculation the criterion for the best choice of b is the one which minimizes binding energy. After a sufficient number of iterations have been performed, the computed

quantities converge to constant values and the number of iterations needed for such a convergence depend upon the initial C-coefficients. In all the calculations we start with initial $C_n^a(\ell j) = \delta_{na}$ and ten iterations have been found to give a satisfactory convergence of computed quantities which finally describe the properties of the nucleus. In order to study the nature of the HF wave functions and also the single particle potential, we have concentrated mainly on the results obtained for ^{16}O . The reason for this being, although there is quantitative disagreement between the HF wave functions of various nuclei studied here, the general nature of these wave functions remains the same for all the nuclei. The discrepancies wherever encountered have been pointed out. Single oscillator configuration approximation to the HF solutions has also been discussed. We present the results of our calculations in the following sections.

IV.2 Effective Yale Interaction Results

IV.2a Binding Energy, Single Particle Energies and Root-Mean-Square Radius

The ground state total energy E_0 of the nucleus is calculated as a function of oscillator range parameter b . The results of the binding energy as a function of b are shown in Figure IV.1 for the nuclei 4He , 8Be , ^{12}C and ^{16}O . Ideally, the HF results should be independent of b or basis chosen and E_0 vs. b curve should be a straight line. This would be true

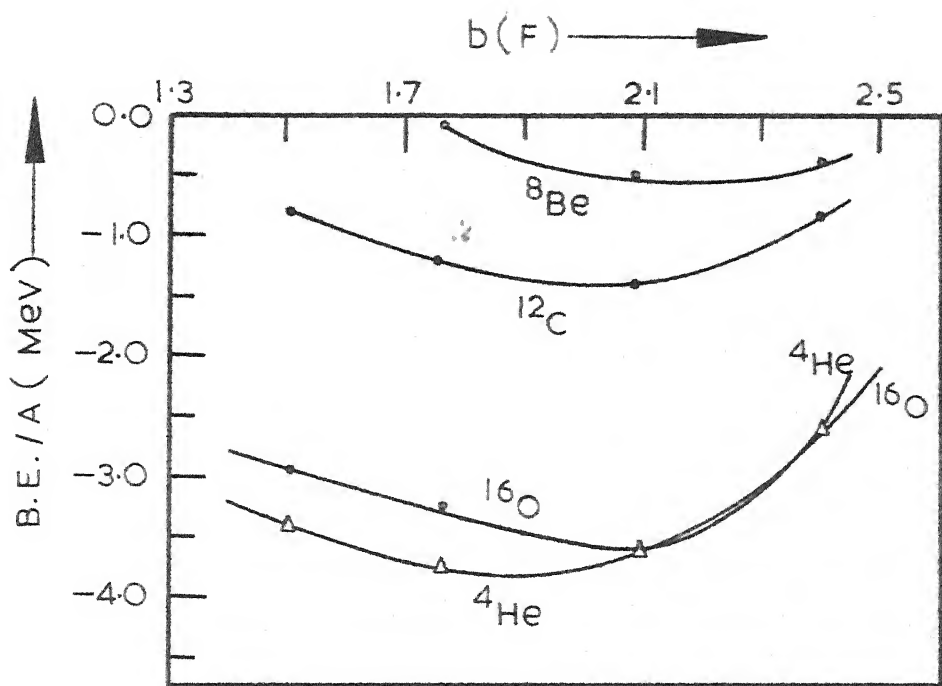


FIG. IV. HF binding energy per particle for various nuclei obtained with effective Yale interaction as a function of oscillator range parameter b .

only when the HF wave functions are expanded in a complete set. The larger the number of terms included in expansion (3.20), the weaker would be the dependence on b . However, from the figure we notice that the curves are reasonably flat near the values of b which give maximum binding. The two-body matrix elements needed for these calculations are evaluated using tables of relative matrix elements for the effective Yale potential given in reference (Shn 67b).

In Table IV.1, we list calculated HF properties of various nuclei for the values of b which give maximum binding ($b=1.76F$ for ^4He and $b=2.09F$ for ^8Be , ^{12}C and ^{16}O). These properties are the binding energy per particle (B.E./A), single particle energies, matter and charge root-mean-square (r.m.s.) radius, and spin-orbit splittings (l -s splittings). The corresponding experimental values wherever available are also given for the sake of comparison. Experimentally single particle neutron levels have been determined from the stripping process, as for example, the (d , p) reaction. Analysis of the experimental data on cross-sections for excitations of the various states of the final nucleus and angular distributions corresponding to these states gives information about the shell model single particle neutron states. Similarly, neutron hole states are located with (p , d) or (d , t) pick-up reactions while proton hole states are determined with the help of (p , $2p$) and (e , ep) knock-out

Table IV.1

Calculated HF properties with effective Yale interaction for various nuclei.

	$^4\text{He}_2$	$^8\text{Be}_4$	$^{12}\text{C}_6$	$^{16}\text{O}_8$	
Present work	Present work	Present work	Present work	Present work	Experiment
Single particle energies (MeV)					
neutron	-23.09	-23.86	-35.54	-45.60	-51 ^b
proton	-22.30	-20.4 ^{±0.3} ^f	-22.64	-33.23	-34.2 ^{±2} ^a
					-33 ^{±3} ^a
					-33 ^{±3.5}
neutron	3.66	0.96 ^f	-1.96	-9.61	-21.21
proton	4.42	1.97 ^f	-0.81	-7.44	-17.84
					-18 ^{±2.5}
neutron	4.82	4.36 ^f	-0.34	-8.60	-15.75
proton	5.51	5.37 ^f	0.79	-6.20	-12.45
					-13 ^{±2} ^a
					-12.4 ^{±1}
B.E./ A (MeV)	-3.77	-7.07 ^c	-0.50	-7.06 ^c	-1.42
				-7.68 ^c	-3.61
				-7.98 ^c	-7.98 ^c
1p _{3/2} - 1p _{1/2} splitting for neutron (MeV)	1.16	1.62	1.01	5.45	6.2 ^b
Matter r.m.s. radius (F)	1.7750	3.4283	2.8158	2.5486	
Charge r.m.s. radius (F)	1.7783	1.67 ^d	3.4735	2.8571	2.54 ^e
					2.5699
					2.71 ^d
					2.47 ^d
a.	Riou (Riu 65)	d.	Hofstadter (Hor 57)		
b.	Cohen (Coh 63a, 63b)	e.	Ulrich et. al. (Ul 58)		
c.	Mattauch et. al (Mah 65)	f.	Vashakidze et. al. (Vae 68)		

reactions. From the Table IV.1 we see that binding energy results are in poor agreement with the experimental values. The reason for the discrepancy in the binding energies stems from the fact that we have not taken into account the second-order term in VP. Calculations of Shakin et. al. (Shn 67b) show clearly that this term is important as far as the binding energies of nuclei are concerned. In fact this term alone gives a binding of about 3 - 4 MeV per particle. In view of this, the theoretical results are in satisfactory agreement for ^4He and ^{16}O but still somewhat poor for ^8Be and ^{12}C . This is, however, not surprising. From the experimental information on transition rates and quadrupole moments these nuclei are known to be deformed. This conclusion is also reached from the calculations of Bassichis et. al. (Bas 67). In fact, these authors have made deformed HF calculations (mixing different orbital angular momentum states) and obtain binding energies for ^8Be and ^{12}C which are lower than spherical HF estimates. Their results are in satisfactory agreement with the experiment. Pal et. al. (Pal 67) have also recently performed similar calculations for the $8 \leq A \leq 40$ nuclei and obtain satisfactory agreement for the deformed nuclei in this region. However, these authors have not included coulomb and centre-of-mass corrections in a self-consistent manner. On the other hand, if we include more orbitals in the expansion of basis states our results would be somewhat improved.

The calculated $1p_{3/2} - 1p_{1/2}$ splitting in ^{16}O is about 10 percent smaller than the result obtained from quasi (pp') scattering (Tyn 66). The agreement would be still better if second-order terms in VP are included (Shn 67b). The HF single particle levels are in satisfactory agreement with the experimental values. There is a large gap between the occupied and the unoccupied levels in the case of ^4He and ^{16}O and is a characteristic of HF approximation. The calculated charge and matter r.m.s. radii are in fair agreement with the experimental data. When the second-order term in VP is taken into account the particles interact more strongly and it is expected that this would result in an increase in the binding of HF single particle levels and decrease in the values of charge and matter r.m.s. radii.

In order to estimate the effects of coulomb (coul) and centre-of-mass (c.m.) corrections on various nuclear properties we have repeated the HF calculations for the following cases.

- Case A: Without coulomb and centre-of-mass corrections.
- Case B: With centre-of-mass and without coulomb corrections.
- Case C: With coulomb and without centre-of-mass corrections.
- Case D: With both the corrections included.

Table IV.2 shows the total ground state energy E_0 obtained in different cases for $b=2.09F$. The kinetic energy of the centre-of-mass motion is determined from the difference

Table IV.2

Effect of coulomb and centre-of-mass corrections on total ground state energy of various nuclei obtained with effective Yale interaction, $b = 2.09F$. All energies are in MeV.

	Case A	Case B	Case C	Case D	E_{coul}	$E_{\text{c.m.}}$	$E^{(1)}_{\text{coul}} + E_{\text{c.m.}}$	$E^{(1)}_{\text{coul}} + E_{\text{c.m.}}^{(2)}$
$^4\text{He}_2$	-3.166	-15.16	-2.516	-14.41	0.752	11.89	0.857	7.139
$^8\text{Be}_4$	2.025	-6.678	4.072	-4.009	2.669	8.881	3.939	7.139
$^{12}\text{C}_6$	-13.19	-24.30	-6.025	-17.03	7.266	11.00	8.703	7.139
$^{16}\text{O}_8$	-59.96	-72.18	-45.84	-57.34	14.34	12.00	14.77	7.139
								$+ E_{\text{coul}}^{(1)} = \frac{2}{5} \frac{e^2}{R} Z(Z-1), \quad E_{\text{c.m.}}^{(1)} = \frac{3}{4} \mathcal{K}(41.6/b^2)$

between E_0 obtained in cases D and C. Similarly, the coulomb energy of the nucleus is obtained from the difference of total energies in cases D and B. From the table, we see that centre-of-mass correction is very important for the nuclei ^4He , ^8Be while coulomb correction is not so important. For ^{16}O , coulomb and centre-of-mass effects tend to cancel each other. These corrections to the binding energies have also been estimated externally by assuming that the charge distribution of the nucleus is that of a uniformly charged sphere and centre-of-mass moves in 1s state of a harmonic oscillator well (see expressions 3.38 and 3.39) and compared with the values obtained self-consistently. It is seen that in all the cases the spherical model overestimates the coulomb energy.

The effect of these corrections on the HF single particle energies is shown in Table IV.3 for $b=2.09\text{F}$. The energy of the $1s_{1/2}$ occupied state for ^4He becomes almost double when the centre-of-mass correction is included. This correction is also very important to reproduce the correct ordering of $1p_{3/2}$ and $1p_{1/2}$ single particle levels in ^{12}C . In Table IV.4, we give the matter r.m.s. (r_0) and charge r.m.s. (r_c) radii obtained in different cases for $b=2.09\text{F}$. The coulomb correction increases r_0 in all the nuclei, whereas the centre-of-mass correction reduces r_0 in the case of ^4He and ^{16}O by approximately 20 percent and 8 percent respectively. Besides, charge r.m.s. radius is larger than matter

Effect of coulomb and centre-of-mass corrections on HF single particle energies of various nuclei obtained with effective Yale interaction, $b = 2.09 \text{ fm}$.
All energies are in MeV.

Nucleus	State	Case A	Case B	Case C	Case D
		Neutron	Proton	Neutron	Proton
$^4\text{He}_2$	$1s_{1/2}$	-11.56	-21.28	-11.41	-10.80
	$1p_{3/2}$	2.95	1.26	2.95	3.68
	$1p_{1/2}$	3.99	1.75	3.98	4.65
	$2s_{1/2}$	6.71	4.71	6.73	7.36
$^8\text{Be}_4$	$1s_{1/2}$	-18.96	-24.23	-18.35	-17.02
	$1p_{3/2}$	-0.70	-2.08	-0.58	0.73
	$1p_{1/2}$	-0.21	-0.44	-0.10	1.32
	$2s_{1/2}$	4.82	2.81	4.82	6.05
$^{12}\text{C}_6$	$1s_{1/2}$	-33.20	-36.48	-32.17	-29.79
	$1p_{3/2}$	-7.38	-9.97	-7.09	-4.93
	$1p_{1/2}$	-9.11	9.05	-8.73	-6.18
	$2s_{1/2}$	3.02	1.21	2.98	4.94
$^{16}\text{O}_8$	$1s_{1/2}$	-44.85	-46.50	-43.92	-40.43
	$1p_{3/2}$	-18.95	-21.65	-18.56	-15.22
	$1p_{1/2}$	-13.78	-15.99	-13.52	-10.32
	$2s_{1/2}$	1.59	-0.66	1.53	4.28

Table IV.4

Effect of coulomb and centre-of-mass corrections on charge (r_c) and mass (r_o) r.m.s. radius of various nuclei obtained with effective Yale interaction, $b = 2.09F$.

Nucleus	Case A r_o (F)	Case B r_o (F)	Case C r_o (F)	Case C r_c (F)	Case D r_o (F)	Case D r_c (F)
$^4\text{He}_2$	2.2229	1.9013	2.2382	2.2438	1.9066	1.9096
$^8\text{Be}_4$	3.0335	3.3531	3.0873	3.1113	3.4283	3.4735
$^{12}\text{C}_6$	2.7403	2.7526	2.7926	2.8144	2.8158	2.8571
$^{16}\text{O}_8$	2.5420	2.5150	2.5734	2.5876	2.5486	2.5699

centre-of-mass corrections on HF calculations has also been recently studied by Gunye (Gue 68a) for several nuclei in the 2s-1d shell.

HF calculations for ^{10}Be and ^{18}O have been carried out for only one value of $b=2.09\text{F}$. The calculated binding energies per particle for ^{10}Be and ^{18}O are -0.77 MeV and -5.33 MeV compared to the experimental values of -6.5 MeV and -7.5 MeV respectively. Thus, ^{10}Be is considerably under-bound under the assumption of a spherically symmetric HF field. Our interest in doing the HF calculations for these nuclei is not only to study their ground state static properties but also to employ the HF single particle energies and wave functions obtained in these calculations in a configuration mixing calculation described in a later Chapter. In view of this, we shall only present the results of single particle energies and expansion coefficients for these nuclei. The neutron single particle HF levels are given in Table IV.5.

In the case of ^{10}Be , $1p_{1/2}$ level lies below the $1p_{3/2}$ level in absence of centre-of-mass correction, an effect similar to that encountered in ^{12}C . Figure IV.2 shows the variation of neutron single particle HF levels with the nucleon number A . Proton energies would show similar variation. As seen from the figure, the levels become more and more bound as the nucleon number increases and the effect is largest for the lowest $1s_{1/2}$ level.

Table IV.5

HF single particle energies of various nuclei for effective Yale interaction obtained without coulomb and centre-of-mass corrections.

Nucleus States	$^{10}\text{Be}_4$ (MeV)	$^{18}\text{O}_8$ (MeV)	$^{16}\text{O}_8$ (MeV)
$^1\text{s}_{1/2}$	-26.99	-47.10	-44.85
$^1\text{p}_{3/2}$	- 4.91	-20.99	-18.95
$^1\text{p}_{1/2}$	- 2.56	-16.94	-13.78
$^1\text{d}_{5/2}$	- 1.38	- 0.66	0.67
$^2\text{s}_{1/2}$	2.50	0.48	1.59
$^1\text{d}_{3/2}$	-	3.10	4.70

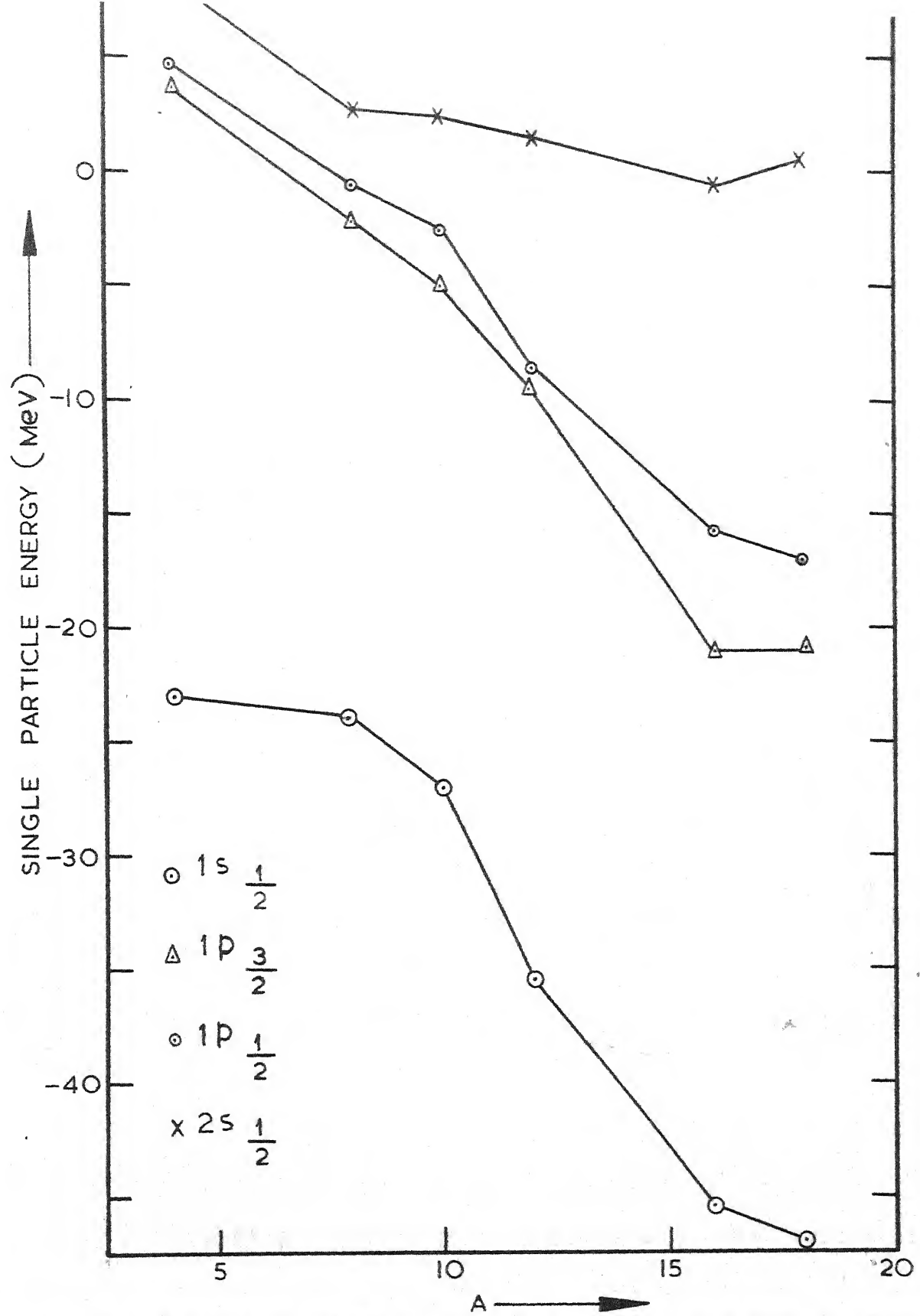


FIG. IV.2 Variation of HF neutron single particle energy obtained with effective Yale interaction with the nucleon number A.

The single particle energies can also be obtained directly by computing the self-consistent total energy E_{ex} of the A+l (for unoccupied states) or A-l (for occupied states) system and taking the difference of E_{ex} and E_0 (the ground state energy of the nucleus with A nucleons). Such a calculation has been carried out for ^{16}O where a single particle was removed from the states $1s_{1/2}$, $1p_{3/2}$ and $1p_{1/2}$ or added to $2s_{1/2}$ state in turn and it is assumed that resulting states of ^{15}O and ^{17}O still remain spherical. Thus, for the occupied levels of ^{16}O , the energy of the i^{th} level is given by

$$\varepsilon_i = E(^{16}O) - E^i(^{15}O), \quad (4.1)$$

where i indicates a hole in the i^{th} level. The unoccupied levels are similarly given by

$$\varepsilon_i = E^i(^{17}O) - E(^{16}O). \quad (4.2)$$

The difference between the single particle energies obtained in this way and the corresponding energies obtained in the HF calculation is the rearrangement energy of the system. The results are presented in Table IV.6.

In a similar manner, particle-hole excited states of ^{16}O are calculated assuming that they are still spherical. Some such states are given in Table IV.7. The first excited 0^+ state of ^{16}O is experimentally observed at 6.05 MeV and is expected to arise from two particle-two hole (2p-2h), four particle-four hole (4p-4h) excitations whereas the

Table IV.6

Comparison of single particle neutron energies obtained directly with eigenvalues of ^{160}O for effective Yale interaction, $b=2.09\text{F}$.

$E_{\text{ex}} = \pm (E_0(\text{Lj}) - E_0(\text{GS}))$, the plus being for particle states and minus for hole states.

State	Total energy of the state $E_0(\text{MeV})$	Excitation energy E_{ex} (MeV)	Eigenvalue ε_{alj} (MeV)	Rearrangement energy $ \varepsilon_{\text{alj}} - E_{\text{ex}} $ (MeV)
G.S.	-57.835	0.000		
$(1s_{1/2})^{-1}$	-17.061	-40.773	-45.596	4.822
$(1p_{3/2})^{-1}$	-38.734	-19.101	-21.208	2.107
$(1p_{1/2})^{-1}$	-43.572	-14.263	-15.753	1.490
$(2s_{1/2})$	-57.921	- 0.086	- 0.528	0.442

Table IV.7

Particle-hole states in $^{16}_0$ for effective Yale interaction, $b=2.09F$. E_{ex} is determined from the difference of total energies of excited state and ground state.

State	Total energy E_0 (MeV)	Excitation energy E_{ex} (MeV)
Ground State	-57.835	0.000
$(1p_{1/2})^{-1} (1d_{5/2})$	-50.436	7.399
$(1p_{1/2})^{-1} (2s_{1/2})$	-43.380	13.455
$(1p_{1/2})^{-2} (1d_{5/2})^2$	-42.180	15.655
$(1p_{1/2})^{-2} (2s_{1/2})^2$	-30.651	27.184
$(1s_{1/2})^{-2} (2p_{3/2})^2$	13.669	71.504
$(1s_{1/2})^{-2} (2p_{1/2})^2$	13.894	71.729

lowest calculated 0^+ state comes at 15.65 MeV. Thus, it is necessary to introduce departure from spherical symmetry or residual interaction to describe this state. In fact, it is an experimental fact that all nuclei which are spherical in ground state, such as ^{16}O , exhibit deformation in their excited states and vice versa. Thus, the excited states of ^{16}O would not be described well under the assumption of a zero order spherical field. Kelson (Ken 65) and Bassichis and Ripka (Bas 65) have satisfactorily reproduced the excited states of ^{16}O by carrying out deformed HF calculations for the excited particle hole states and using projection of angular momentum technique. They have obtained lowest 0^+ state very near the experimental value.

IV.2b Hartree-Fock Wave Functions and Density

After a sufficient number of iterations have been performed the single particle wave functions Ψ_α are determined from a final set of coefficients C_μ^α by substituting them into equation 3.20. These expansion coefficients are given in Tables (IV.8 - IV.13) for the nuclei ^4He , ^8Be , ^{12}C , ^{16}O , ^{10}Be and ^{18}O respectively. The results are presented for the values of b which give maximum binding ($b=1.76\text{F}$ for ^4He , $b=2.09\text{F}$ for all other nuclei). We shall discuss here the nature of the wave functions for ^{16}O alone and only make remarks on the structure of wave functions for other nuclei. The radial HF wave function $R_{\alpha\ell}^j$ (see equation 3.19 for detailed expression) for the $s_{1/2}$, $p_{3/2}$ and $p_{1/2}$ (neutron)

Table IV.8

Expansion coefficients $c_n^a(lj)$ for ${}^4\text{He}_2$, $b = 1.76\text{F}$
 obtained with effective Yale interaction.

tes	n	neutron			proton		
		1	2	3	1	2	3
1	1	0.9684	0.2224	0.1129	-0.9694	-0.2185	-0.1123
2	2	-0.1573	0.8959	-0.4156	0.1527	-0.8940	0.4213
3	3	0.1936	-0.3847	-0.9025	0.1924	-0.3912	-0.8999
1	1	0.8055	-0.4828	0.3435	0.7939	-0.4966	0.3510
2	2	0.5920	0.6800	-0.4325	0.6078	0.6658	-0.4327
3	3	0.0247	-0.5518	-0.8336	0.0188	-0.5569	-0.8304
1	1	0.7137	-0.5986	0.3636	0.7042	-0.6060	0.3700
2	2	-0.6931	-0.5286	0.4901	-0.7020	-0.5164	0.4905
3	3	0.1012	0.6018	0.7922	0.1062	0.6051	0.7890

Table IV.9

Expansion coefficients $C_n^a(\ell j)$ for ${}^8\text{Be}_4$, $b = 2.09\text{F}$.
obtained with effective Yale interaction.

states			neutron			proton			
ℓ	j	a	n	1	2	3	1	2	3
0	1		1	0.9191	0.3255	0.2220	0.9204	0.3220	0.2219
	$\frac{1}{2}$	2	2	-0.2294	0.9003	-0.3701	-0.2216	0.8970	-0.3825
		3	3	0.3204	-0.2893	-0.9021	0.5222	-0.3028	-0.8969
1	$\frac{3}{2}$	2	1	0.8930	-0.2663	0.3629	0.8740	-0.3059	0.3775
	$\frac{3}{2}$	2	2	0.3953	0.8494	-0.3497	0.4401	0.8277	-0.3482
		3	3	0.2151	-0.4557	-0.8637	0.2060	-0.4705	-0.8580
1	$\frac{1}{2}$	2	1	0.8025	-0.4665	0.3721	0.7816	-0.4898	0.3862
	$\frac{1}{2}$	2	2	0.5921	0.6990	0.3997	0.6203	0.6750	-0.3994
		3	3	0.0739	-0.5410	-0.8373	0.0651	-0.5518	-0.8314

Table IV.10

Expansion coefficients $c_n^a(\ell j)$ for $^{12}\text{C}_6$, $b = 2.09\text{F}$
obtained with effective Yale interaction.

states			neutron			proton			
ℓ	j	a	n	1	2	3	1	2	3
0	1		1	0.9357	0.3140	0.1608	0.9379	0.3083	0.1594
	$\frac{1}{2}$		2	-0.2430	0.9041	-0.3516	-0.2294	0.8952	-0.3820
			3	0.2557	-0.2899	-0.9223	0.2604	-0.3217	-0.9103
1	1		1	0.9672	0.1215	0.2233	0.9685	0.0844	0.2344
	$\frac{3}{2}$		2	-0.0115	0.8983	-0.4392	0.0317	0.8915	-0.4518
			3	0.2539	-0.4222	-0.8702	0.2471	-0.4450	-0.8608
1	1		1	0.9667	0.0854	0.2414	0.9655	0.0453	0.2563
	$\frac{1}{2}$		2	0.0296	0.8991	-0.4367	0.0768	0.8912	-0.4471
			3	0.2543	-0.4293	-0.8666	0.2487	-0.4513	-0.8570

Table IV.11(a)

Expansion coefficients $C_n^a(Lj)$ for $^{16}\text{O}_8$, $b = 2.09\text{F}$
obtained with effective Yale interaction.

states			neutron			proton		
L	j	$a \backslash n$	1	2	3	1	2	3
0	1	1	0.9472	0.3033	0.1058	0.9497	0.2965	0.1006
	$\frac{1}{2}$	2	-0.2532	0.9065	-0.3380	-0.2361	0.8892	-0.3919
	3		0.1966	-0.2939	-0.0354	0.2056	-0.3484	-0.9145
1	1	1	0.9282	0.3214	0.1876	0.9341	0.3034	0.1880
	$\frac{3}{2}$	2	-0.2118	0.8706	-0.4441	-0.1857	0.8629	-0.4700
	3		0.3060	-0.3725	-0.8761	0.3048	-0.4042	-0.8624
1	1	1	0.9491	0.2434	0.1998	0.9555	0.2102	0.2068
	$\frac{1}{2}$	2	-0.1294	0.8799	-0.4573	-0.0889	0.8741	-0.4775
	3		0.2872	-0.4081	-0.8666	0.2811	-0.4379	-0.8540
2	1	1	0.9486	0.0570	0.3143	0.9460	0.0082	0.3240
	$\frac{5}{2}$	2	0.0931	0.9165	-0.3890	0.1242	0.9142	-0.3858
	3		0.3024	-0.5983	-0.8660	0.2994	-0.4052	-0.8638

Table IV.11(b)

Expansion coefficients $\beta_n^a(\ell_j)$ for $^{16}\text{O}_8$, $b = 2.09\text{F}$
 obtained in the HF calculation with effective
 Yale interaction without coulomb and
 centre-of-mass corrections.

ℓ	j	a	n	1	2	3
0	$\frac{1}{2}$	1		0.9475	0.3047	0.0969
		2		-0.3008	0.9522	-0.0529
		3		0.1084	-0.0210	-0.9939
1	$\frac{3}{2}$	1		0.9414	0.3032	0.1476
		2		-0.2547	0.9261	-0.2782
		3		0.2210	-0.2243	-0.9491
1	$\frac{1}{2}$	1		0.9570	0.2498	0.1476
		2		-0.1953	0.9309	-0.3088
		3		0.2146	-0.2666	-0.9396
2	$\frac{5}{2}$	1		0.9789	0.0328	0.2017
		2		0.0407	0.9360	-0.3496
		3		0.2002	-0.3504	-0.9150
2	$\frac{3}{2}$	1		0.9390	-0.2555	0.2301
		2		0.3302	0.8569	-0.3958
		3		0.0960	-0.4476	-0.8891

Table IV.12

Expansion coefficients $C_n^a(\ell j)$ for $^{10}\text{Be}_4$, $b = 2.09 \text{ F}$
obtained with effective Yale interaction.

states		neutron			proton			
ℓ	j	$a \backslash n$	2	3	1	2	3	
0	1	1	0.9339	0.3023	0.1909	0.9363	-0.3044	0.1751
	$\frac{1}{2}$	2	-0.2150	0.9014	-0.3758	-0.2277	0.9059	0.3570
	3	3	0.2857	-0.3099	-0.9068	0.2673	-0.2944	-0.9175
1	1	1	0.9548	-0.0711	0.2887	0.9601	-0.0621	0.2725
	$\frac{3}{2}$	2	0.1908	0.8911	-0.4118	0.1760	0.8917	-0.4169
	3	3	0.2280	-0.4483	-0.3643	0.2171	-0.4483	-0.8671
1	1	1	0.9133	-0.2546	0.3178	0.9472	-0.1594	0.2780
	$\frac{1}{2}$	2	0.3759	0.8272	-0.4177	-0.2708	0.8621	-0.4283
	3	3	0.1566	-0.5010	-0.3512	0.1714	-0.4810	-0.8598
2	1	1	0.7076	-0.5740	0.4121	-0.7288	-0.5548	0.4013
	$\frac{5}{2}$	2	-0.7066	-0.5660	0.4247	0.6847	0.5988	-0.4155
	3	3	0.0105	0.5917	0.8061	0.0097	-0.5776	-0.8163

Table IV.13(a)

Expansion coefficients $C_n^a(\ell, j)$ for $^{18}\text{O}_8$, $b = 2.09\text{F}$
obtained with effective Yale interaction.

states			neutron			proton			
ℓ	j	a	n	1	2	3	1	2	3
0	1		1	0.9420	0.3185	0.1062	0.9482	0.3035	0.0942
	$\frac{1}{2}$	2	2	-0.2715	0.9088	-0.3169	-0.2525	0.8996	-0.3564
		3	3	0.1975	-0.2697	-0.9425	0.1929	-0.3124	-0.9296
1	1		1	0.9133	0.3552	0.1990	0.9199	0.3446	0.1872
	$\frac{3}{2}$	2	2	-0.2368	0.8610	-0.4502	-0.2256	0.8555	-0.4662
		3	3	0.3313	-0.3640	-0.8705	0.3208	-0.3866	-0.8647
1	1		1	0.9268	0.3091	0.2133	0.9361	0.2916	0.1966
	$\frac{1}{2}$	2	2	-0.1850	0.8700	-0.4571	-0.1693	0.8637	-0.4748
		3	3	0.3269	-0.3842	-0.8635	0.3083	-0.4112	-0.8579
2	1		1	0.9392	0.1429	0.5121	0.9411	0.1614	0.2972
	$\frac{5}{2}$	2	2	-0.0052	0.9151	-0.4030	-0.0277	0.9127	-0.4078
		3	3	0.3432	-0.3770	-0.3603	0.3371	-0.3755	-0.8633

Table IV.13(b)

Expansion coefficients $c_n^a(\ell j)$ for $^{18}\text{O}_8$, $b = 2.09\text{F}$
 obtained in the HF calculation with effective
 Yale interaction without coulomb and
 centre-of-mass corrections.

ℓ	j	a	n	1	2	3
0	$\frac{1}{2}$	1		0.9499	0.2991	0.0903
		2		-0.2990	0.9541	-0.0152
		3		0.0907	0.0126	-0.9958
1	$\frac{3}{2}$	1		0.9405	0.3083	0.1429
		2		-0.2651	0.9287	-0.2593
		3		0.2126	-0.2026	-0.9552
1	$\frac{1}{2}$	1		0.9520	0.2701	0.1442
		2		-0.2212	0.9324	-0.2856
		3		0.2116	-0.2400	-0.9474
2	$\frac{5}{2}$	1		0.9792	0.0727	0.1894
		2		-0.0028	0.9382	-0.3460
		3		0.2028	-0.3383	-0.9189
2	$\frac{3}{2}$	1		0.9658	-0.1589	0.2050
		2		0.2291	0.8931	-0.3872
		3		0.1216	-0.4209	-0.8989

states are plotted in Figures (IV.3 - IV.5). The proton wave functions are only slightly different from these as can be noticed from the expansion coefficients for the neutron and protons. Pure harmonic oscillator wave functions have also been calculated for a value of the parameter b which gives the same r.m.s. radius as obtained from HF calculations, and these are plotted in Figures (IV.3 - IV.5). From these figures we notice that the occupied orbitals for ^{16}O can be well approximated by the harmonic oscillator functions while the structure of the unoccupied orbitals is quite different. The unoccupied orbitals are damped inside and have large amplitudes at large distances. This is true for all the three states. Similar effects are observed for the wave functions of other nuclei. The reason for a value of b different for HF and harmonic oscillator wave functions for the same value of the r.m.s. radius is obvious from Tables (IV.8 - IV.13). In other words, strong mixing of various orbitals is responsible for this difference as well as the nature of the unoccupied orbitals. From Figures (IV.3 - IV.5), we also see that there is an overall shift of the peaks of the HF wave functions with respect to the harmonic oscillator ones to larger values of r . In the spherical HF calculations one mixes different orbitals corresponding to the far-lying states (n mixing). These states have weaker binding and are associated with larger separation from the centre of potential. The range in which nucleons move is considerably large compared to pure states. Therefore, the average separation of the

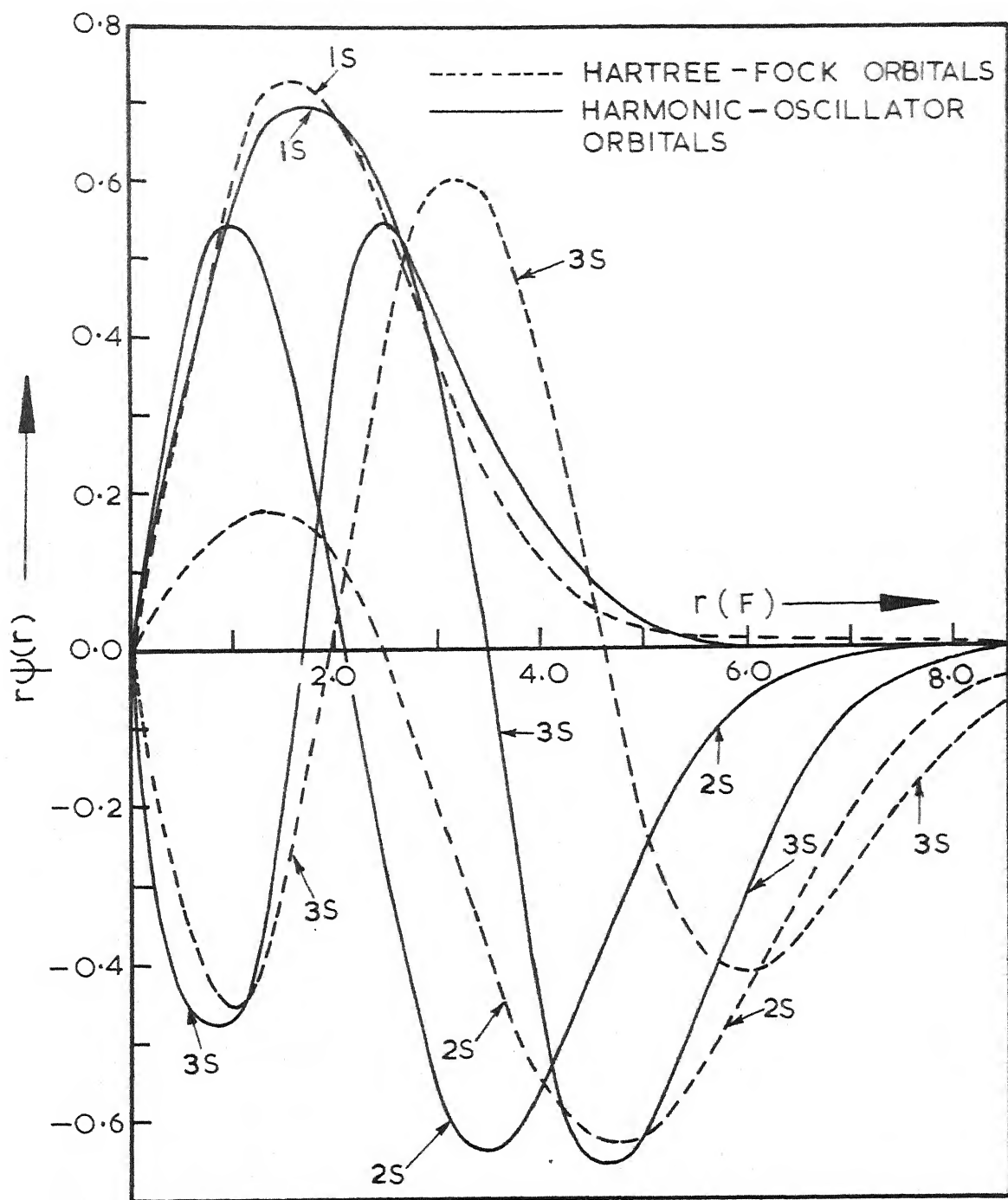


FIG. IV.3 $s_{1/2}$ HF orbitals for ^{16}O obtained with effective Yale interaction. The harmonic oscillator orbitals shown here are obtained for a value of b which gives same r.m.s. radius as obtained from HF calculations.

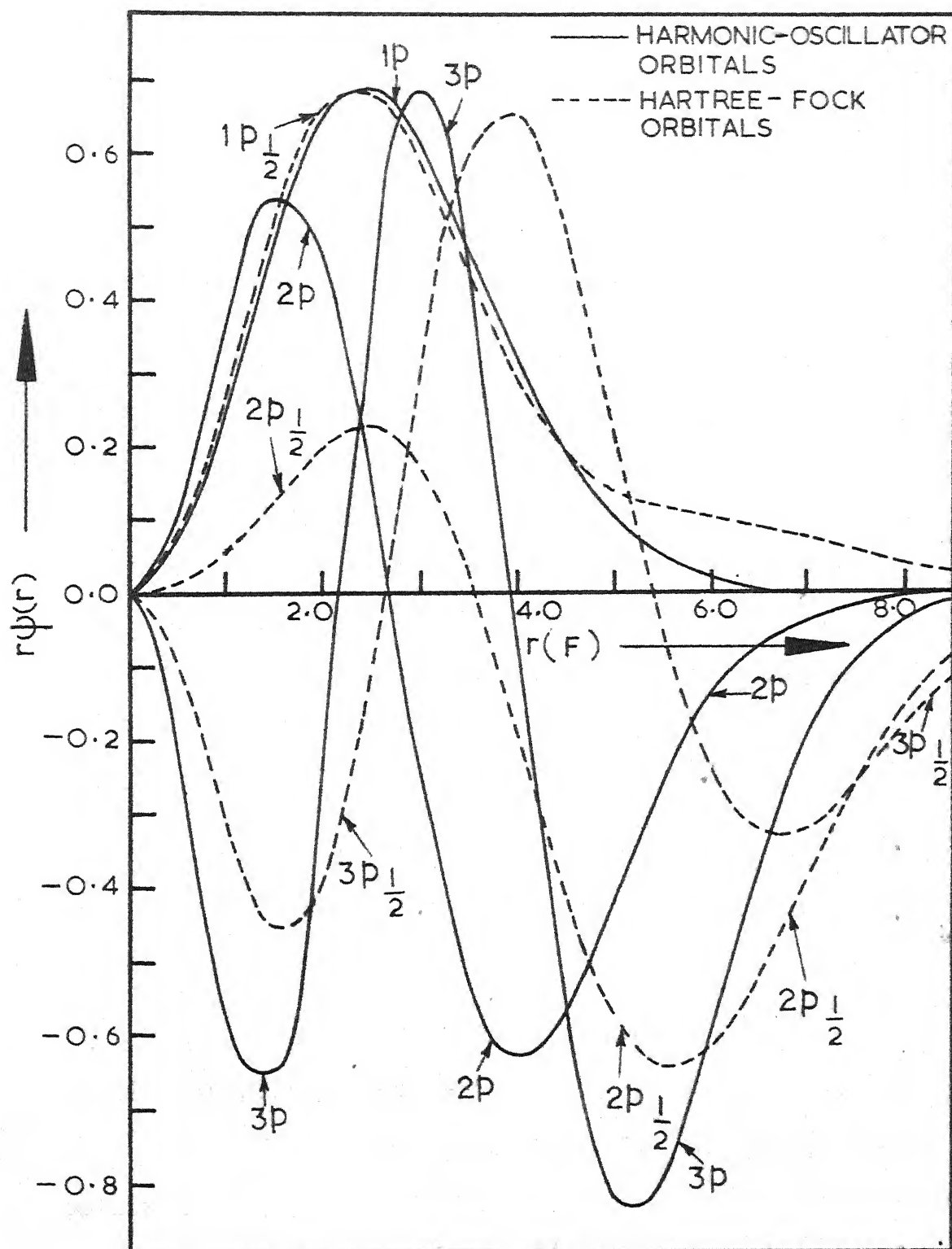


FIG. IV.5 $p_{1/2}$ HF and harmonic oscillator orbitals for ^{16}O .
Other details are same as in Fig. IV.3.

nucleons from the centre of the potential is increased, resulting in the shift of peaks. For ^{16}O , using the HF values of r.m.s. radius the calculated value of b for the oscillator functions turns out to be 1.699F . However, for this value of b the two wave functions do not overlap exactly. Best overlap is obtained for the tabulated b values (Table IV.14). For ^8Be nucleus, the calculated value of b is 2.424F . This large b indicates weak binding as can be verified from Table IV.1.

HF single particle proton orbitals with and without the correction terms have been plotted in Figures (IV.6 - IV.8) for some of the single particle states in ^{16}O and ^4He . As seen from the Figures (IV.6 - IV.7), the correction terms have very little effect on occupied orbitals in ^{16}O but the unoccupied orbitals have been significantly affected and the centre-of-mass correction is much more important than the coulomb correction. Figure IV.8 shows the proton orbital in ^4He with and without the centre-of-mass correction.

HF matter and charge densities for light nuclei (^4He , ^8Be , ^{12}C , ^{16}O) are shown in Figures (IV.9 - IV.10). Both the matter and charge densities of ^{16}O show a dip at the centre. Such a dip is predicted from electron scattering experiments.

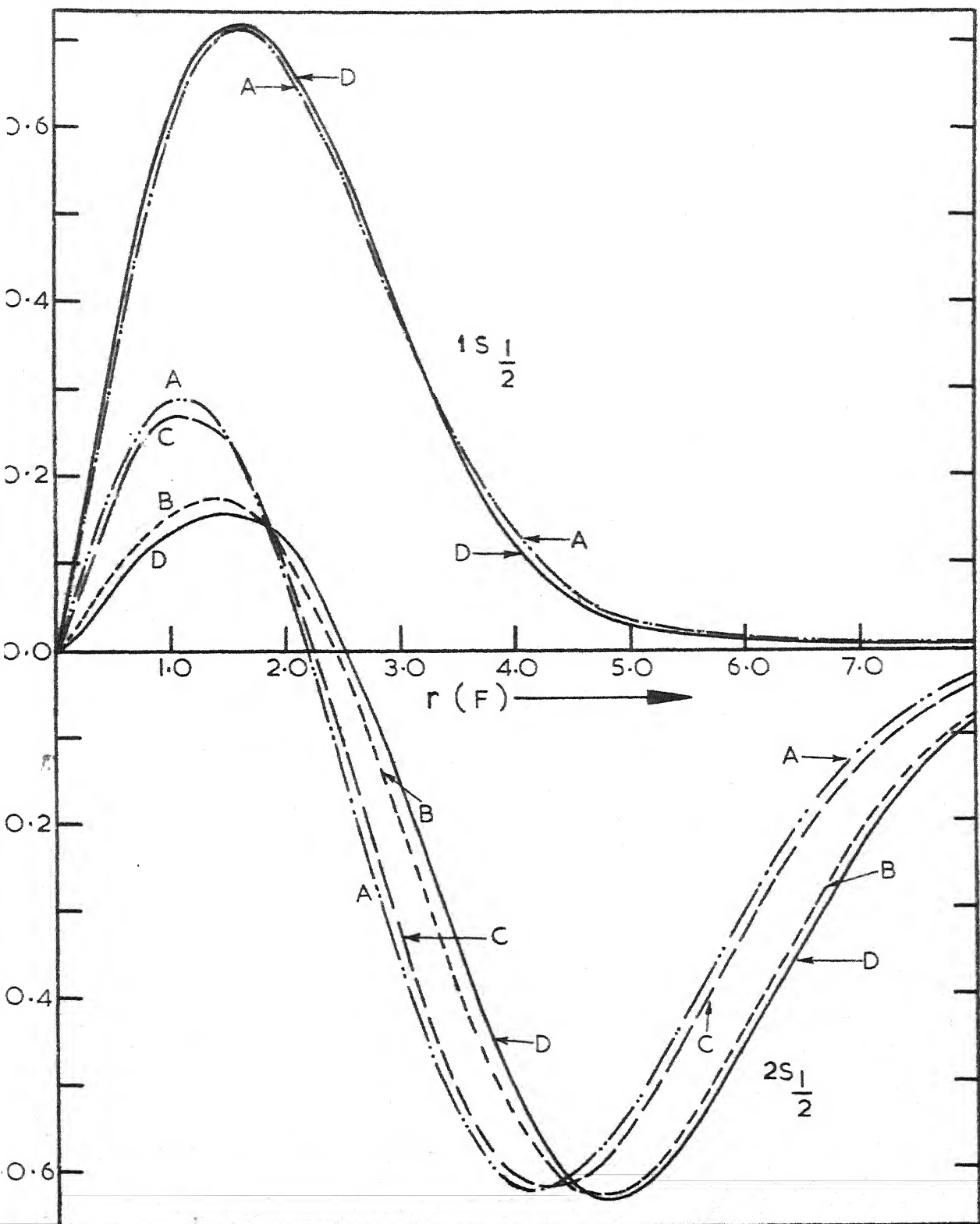
IV.2c Hartree-Fock Potential

The matrix elements $\langle n|U|n' \rangle$ of the HF single particle potential U are given in Table IV.15 for ^{16}O neutron states for $b=2.09\text{F}$. Since $\langle n|U|n' \rangle = \langle n'|U|n \rangle$, only $n \leq n'$ values are

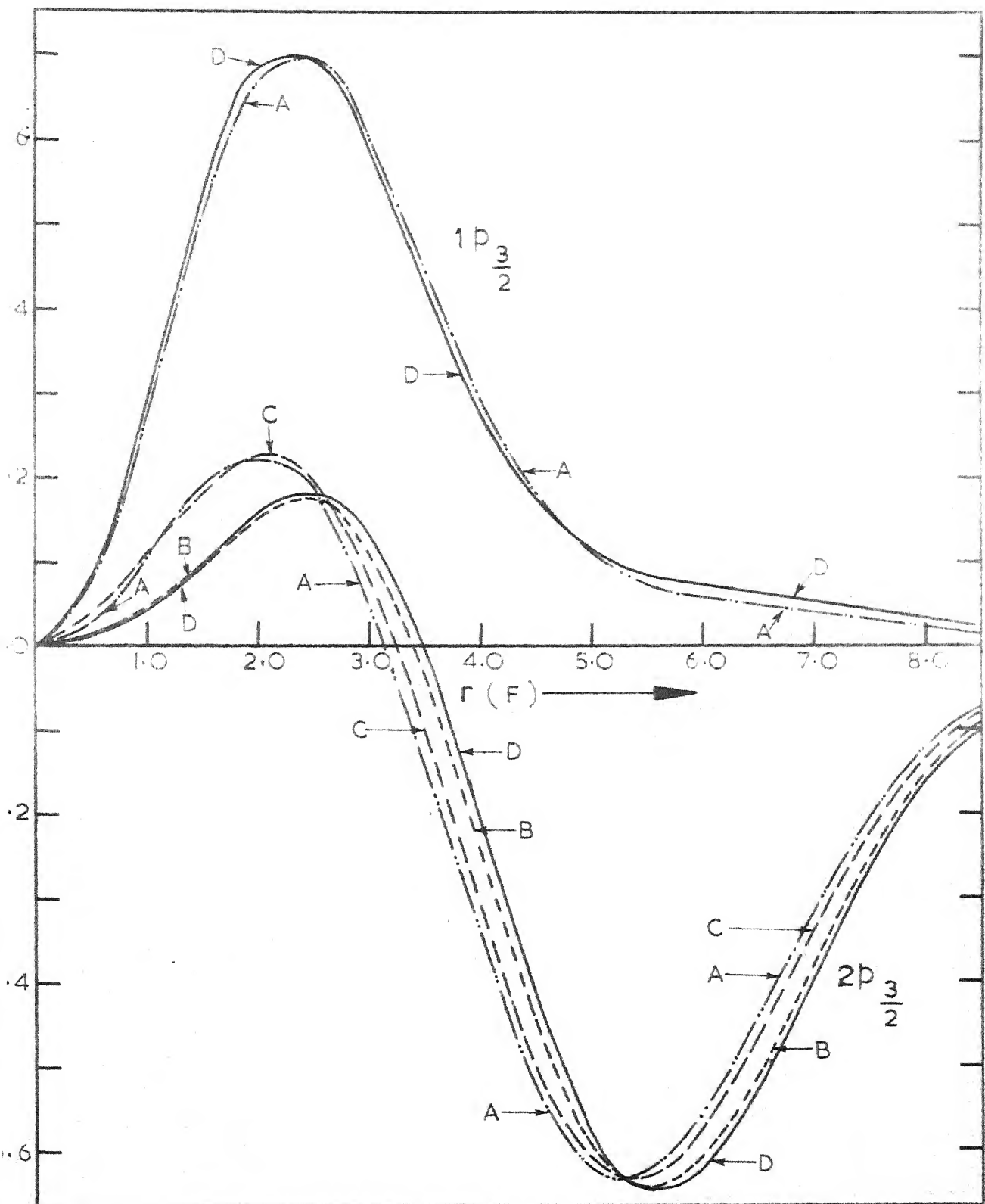
Table IV.14

Values of the oscillator parameter (b) giving the best overlap of the HF orbital for $^{16}\text{O}_8$ obtained with effective Yale interaction and harmonic oscillator wave functions.

Orbital	b(F)
$^1\text{s}_{1/2}$	1.612
$^1\text{p}_{3/2}$	1.625
$^1\text{p}_{1/2}$	1.667



G. IV.6. $s_{1/2}$ state HF proton wave functions for ^{16}O obtained with effective Yale interaction. Curve A corresponds to wave functions without coulomb and centre-of-mass corrections. Curves B and C are obtained in absence of coulomb and centre-of-mass corrections respectively. Curve D is obtained when both the corrections are taken into account.



IV.7. $p_{3/2}$ state HF proton wave functions for ^{16}O obtained with effective Yale interaction. Other details are same as in Fig. IV.6.

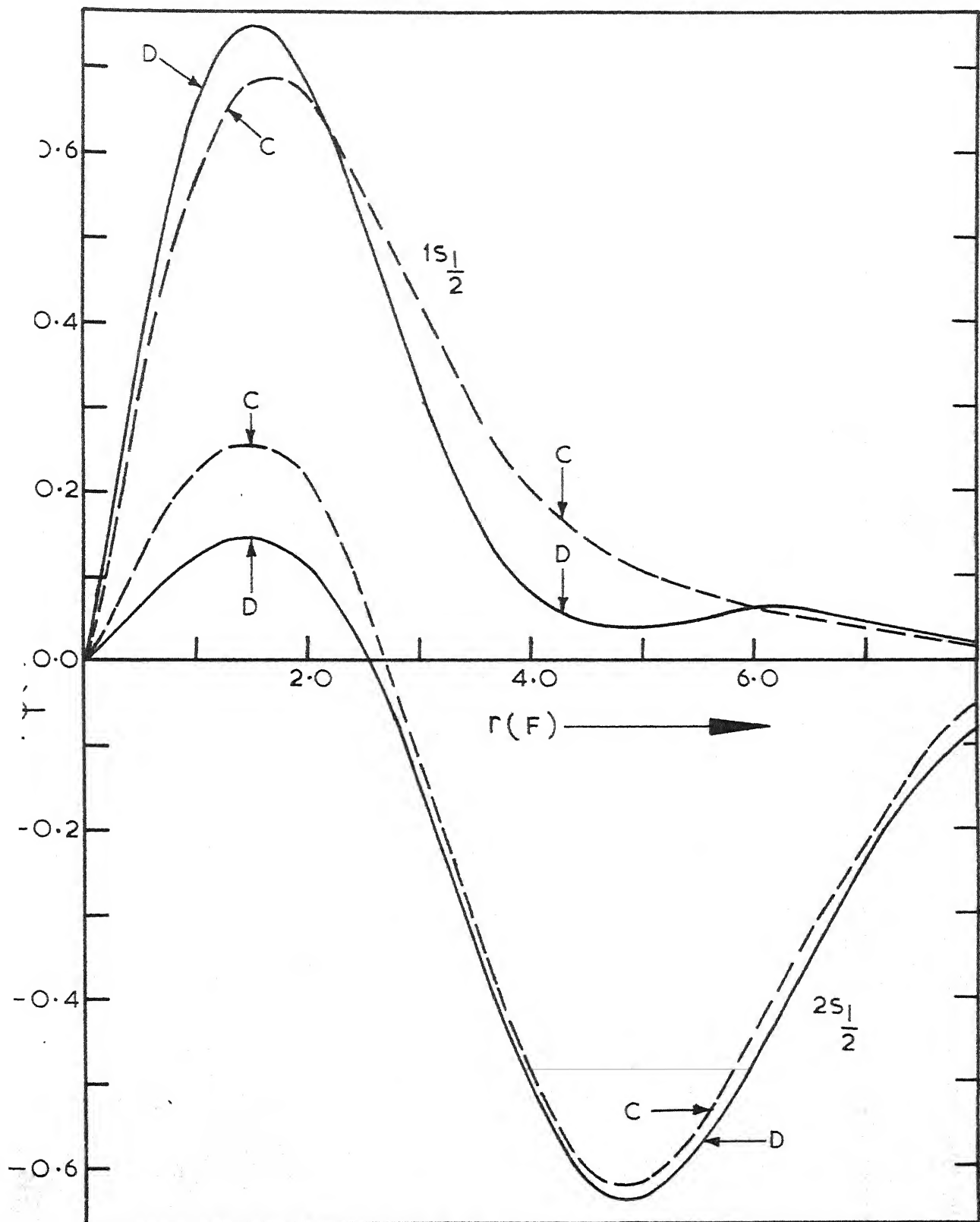


FIG. IV.8 $s_{1/2}$ state HF proton wave functions for ${}^4\text{He}$ obtained with effective Yale interaction. Other details are same as in Fig. IV.6.

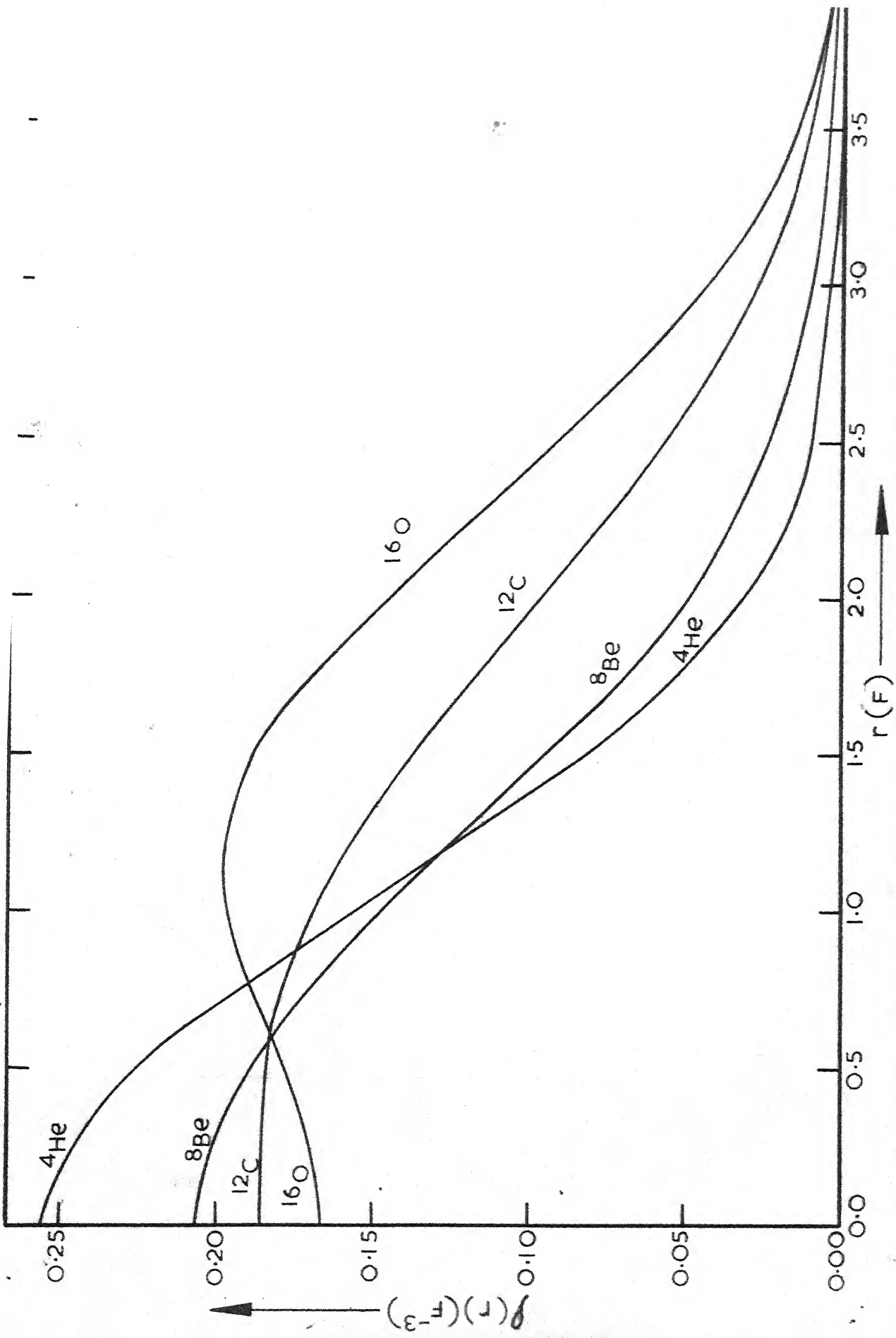


FIG. IV.9 HF matter density for light nuclei obtained with effective Yale interaction.

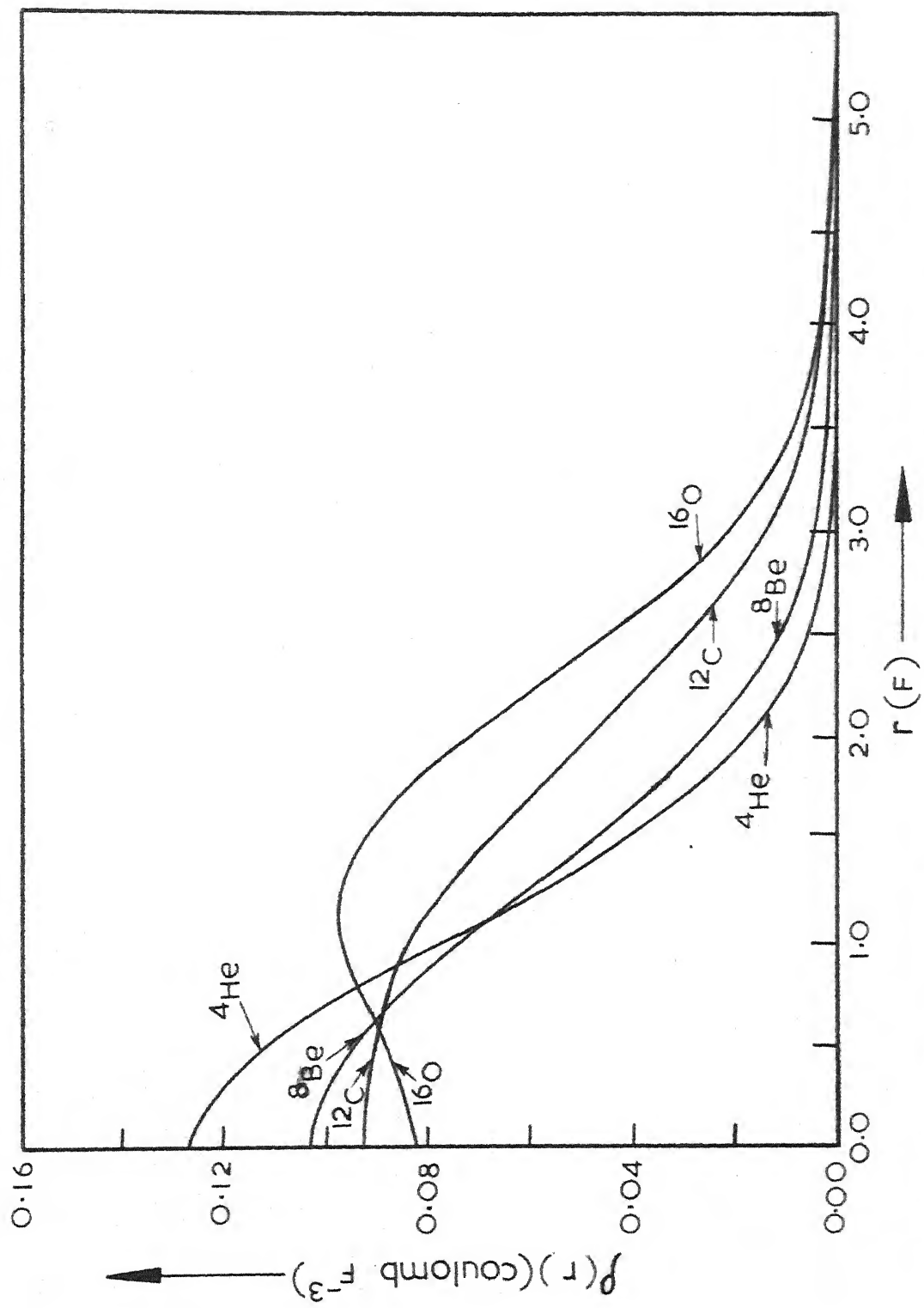


FIG. IV.10 HF charge density for light nuclei obtained with effective
Yale interaction.

Table IV.15

Matrix elements $\langle n | U(\theta, j) | n' \rangle$ of the HF potential for $^{16}\text{O}_8$, $b = 2.09\text{F}$ obtained with effective Yale interaction for neutron states.

l	j	n'	n	1	2	3
0 1/2	1			-23.5188		
	2			-13.6123	13.3058	
	3			- 6.4951	1.6423	25.7619
1 3/2	1			- 0.1265		
	2			- 7.5401	15.6957	
	3			- 7.1378	3.2100	25.5869
1 1/2	1			3.9921		
	2			- 5.2032	17.8884	
	3			- 6.5334	4.4390	26.8043
2 5/2	1			10.0815		
	2			- 1.8058	16.9826	
	3			- 5.4234	4.4253	24.0448

given. The potentials $U_{lj}(r, r')$ have also been evaluated using expression (3.62) for different single particle neutron states (lj) of ^{16}O for $b=2.09F$. These potentials have been plotted in Figures (IV.11 - IV.13) for the $s_{1/2}$, $p_{3/2}$ and $p_{1/2}$ neutron states respectively in ^{16}O . The fact that HF potential is non-local and state-dependent is obvious from the plots. A local potential would give a delta function at $r = r'$. Potentials for $p_{3/2}$ and $p_{1/2}$ states are very similar. The HF single particle potentials for other nuclei are expected to show similar behaviour.

The static limit of the HF potential has been calculated using equation (3.65). As seen from Figure IV.14, this potential does not resemble any of the standard local potential forms such as harmonic oscillator, Woods-Saxon, etc. The static limit of the potential is most attractive at about $r = 1.8F$ and becomes repulsive beyond $r = 3.6F$. It is not clear what meaning this local potential can have.

We have also attempted to find out the parameters of a local potential which would give the same single particle energies as obtained in the HF calculation. The local potential employed is of Woods-Saxon form with spin-orbit and coulomb terms added to it. The detailed shape of the potential is given in Appendix A. Calculations have been carried out for ^{16}O . The range parameters r_N and r_s of the potential were kept fixed at a value of $1.25F$, appropriate for ^{16}O and the strengths V_N and V_{SO} of the central and spin-orbit parts of the potential are

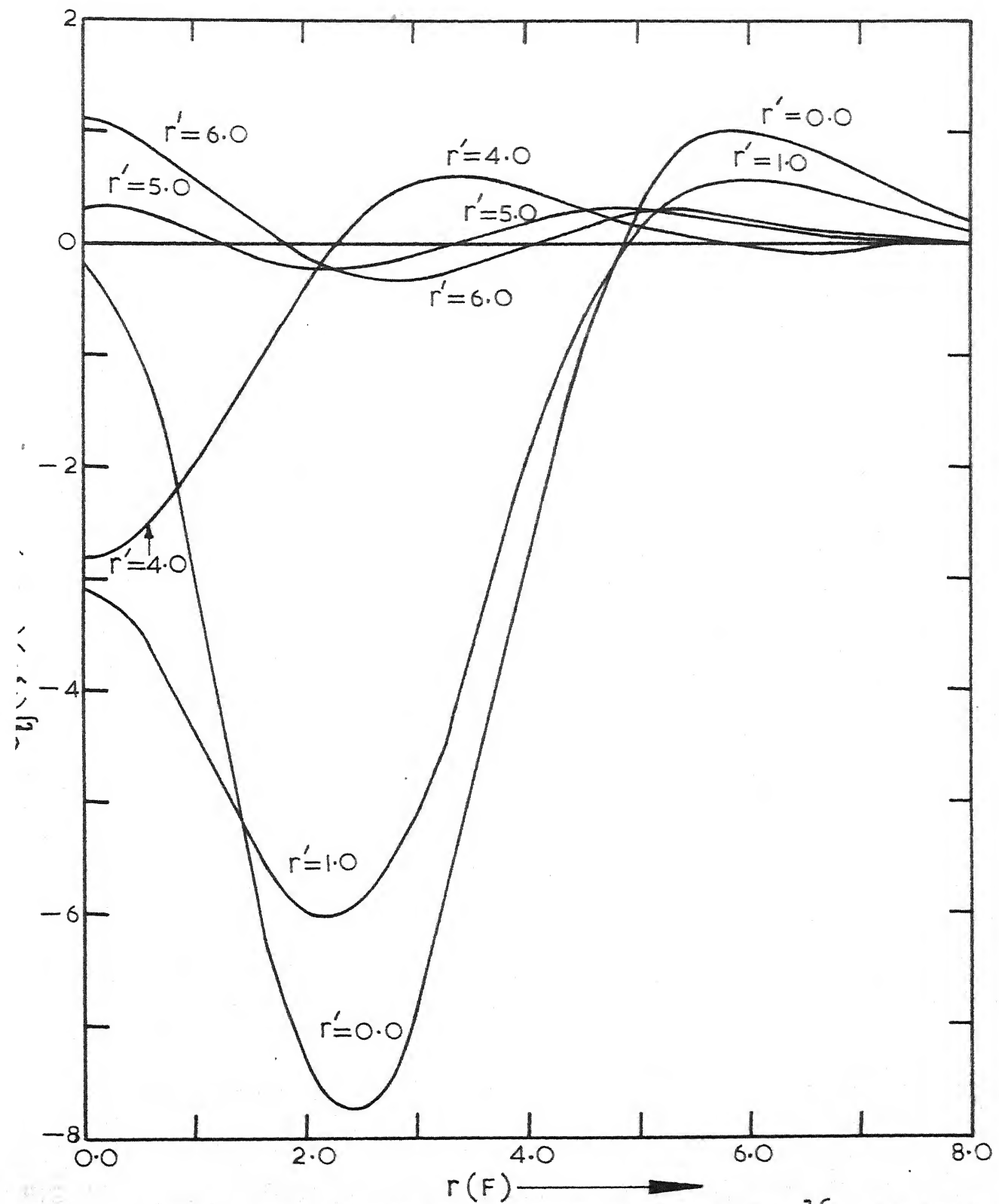


FIG. IV.11 $s_{1/2}$ state HF single particle potential for ^{16}O obtained with effective Yale interaction.

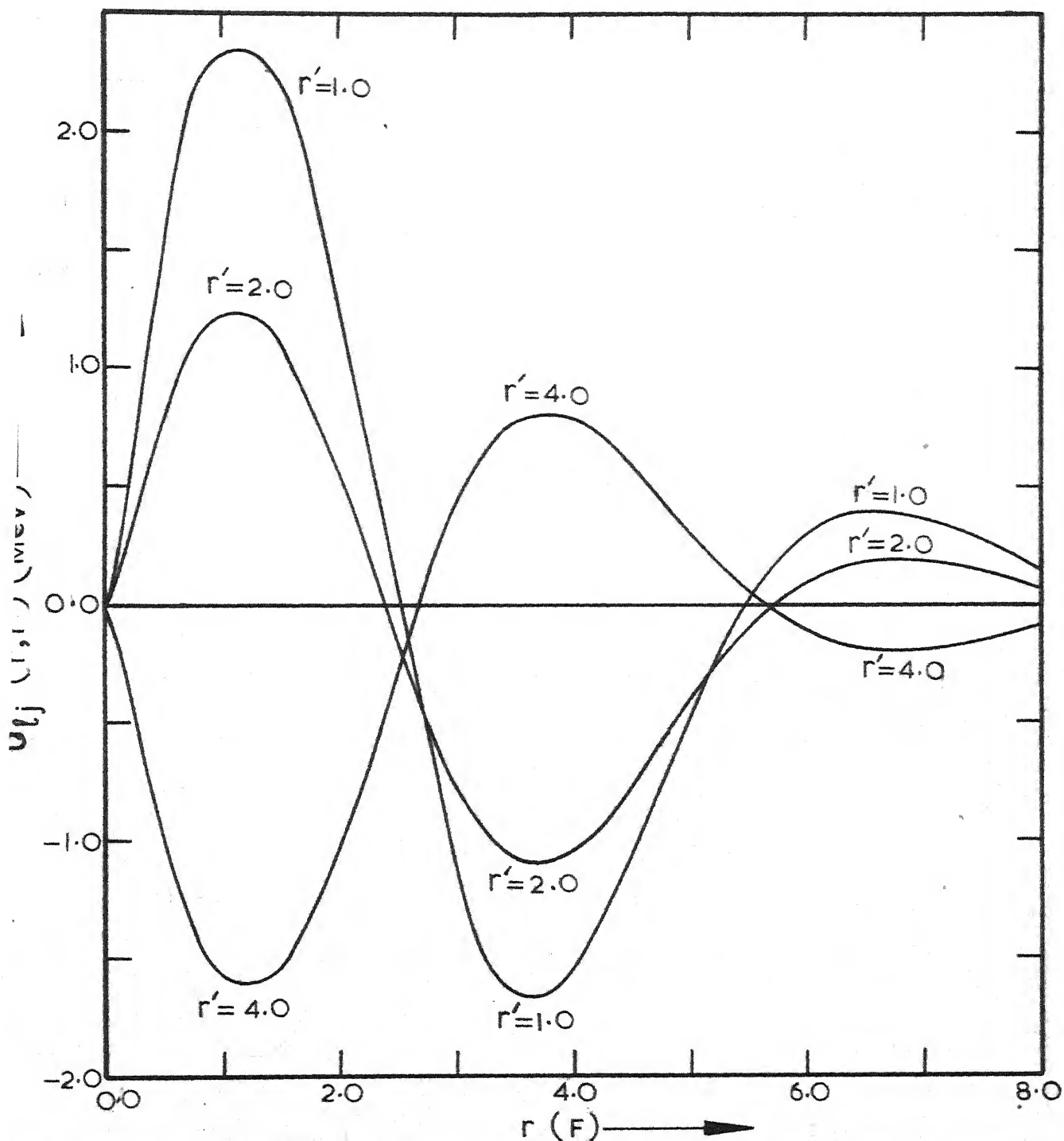


FIG. IV.12 $p_{3/2}$ state HF single particle potential for ^{16}O obtained with effective Yale interaction.

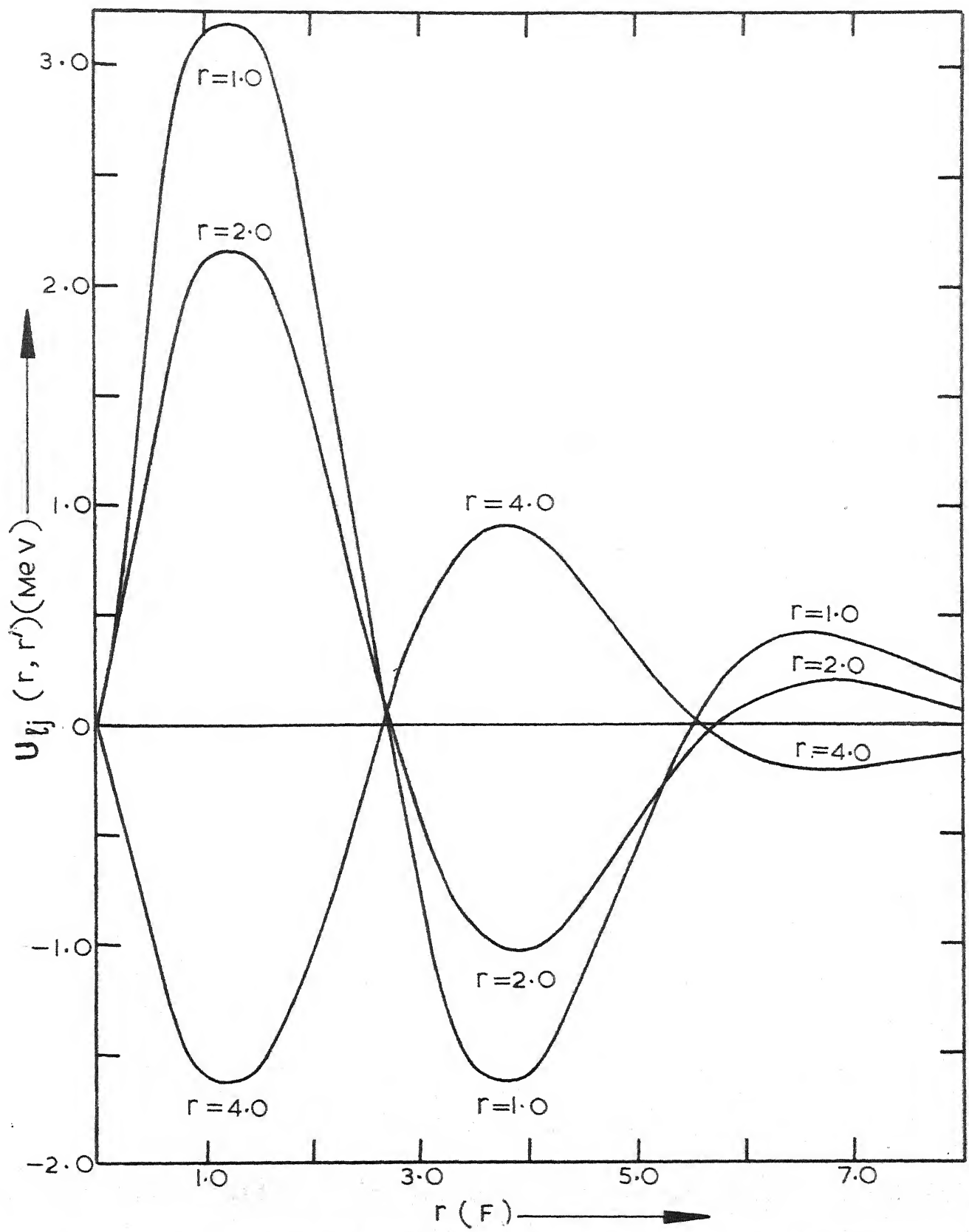


FIG. IV.13 $p_{1/2}$ state HF single particle potential for ^{16}O obtained with effective Yale interaction.

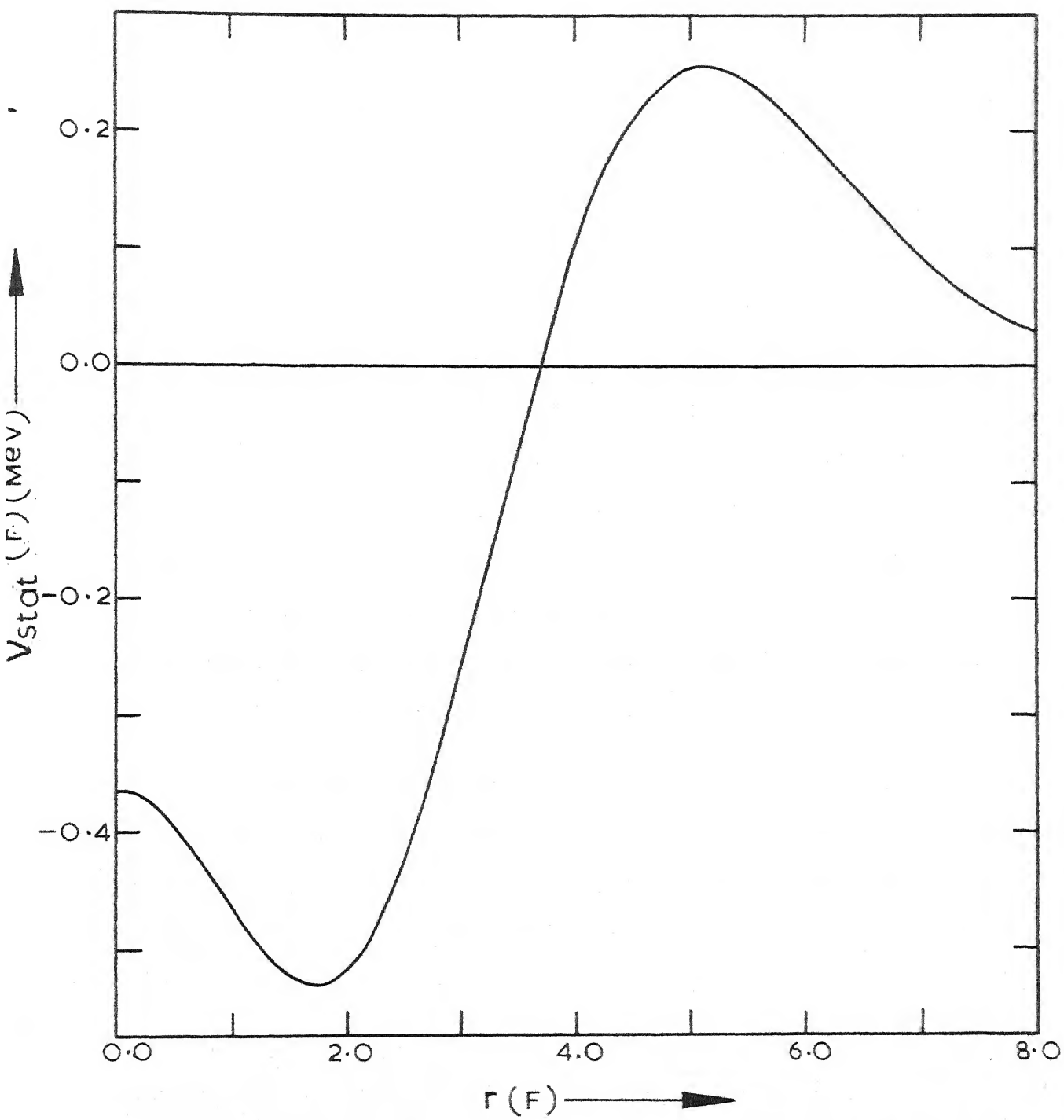


FIG. IV.14 Static limit of the non-local HF potential for ^{16}O obtained with effective Yale interaction.

varied so as to reproduce the HF single particle levels. For the $1p_{3/2}$ (21.21 MeV) and $1p_{1/2}$ (15.75 MeV) neutron levels of ^{16}O , the strengths are found to be $V_N = 58.206$ MeV and $V_{so} = 8.834$ MeV. The corresponding single particle wave functions are plotted in Figures (IV.15 - IV.16) and also compared with the HF wave functions. It is seen that the two wave functions (HF and equivalent local potential) agree pretty closely in the region $r \leq 3.5E$, but the HF wave function has a much longer tail. Non-local correction to the wave function (see Appendix A) has also been applied. The $1p_{3/2}$ wave functions for different values of the non-locality range parameter a_{nl} are shown in Figure IV.16. As the parameter a_{nl} is increased the tail of the wave function approaches the HF wave function, but the disagreement in the inner region increases.

It should be mentioned that the two-body coulomb and centre-of-mass matrix elements, used in the calculations reported in this section, have been calculated with a maximum relative $l = 2$. This has caused some error in our calculations since coulomb force is a long-range force and there would be significant contributions coming from larger l values. Later on, coulomb and centre-of-mass matrix elements were calculated with a maximum relative $l = 10$ (maximum allowed l in the smaller configuration space) and some of the HF calculations for effective Yale interaction were repeated with these new coulomb and centre-of-mass matrix elements. A few revised HF results have been added to Appendix B. It is seen that static properties of

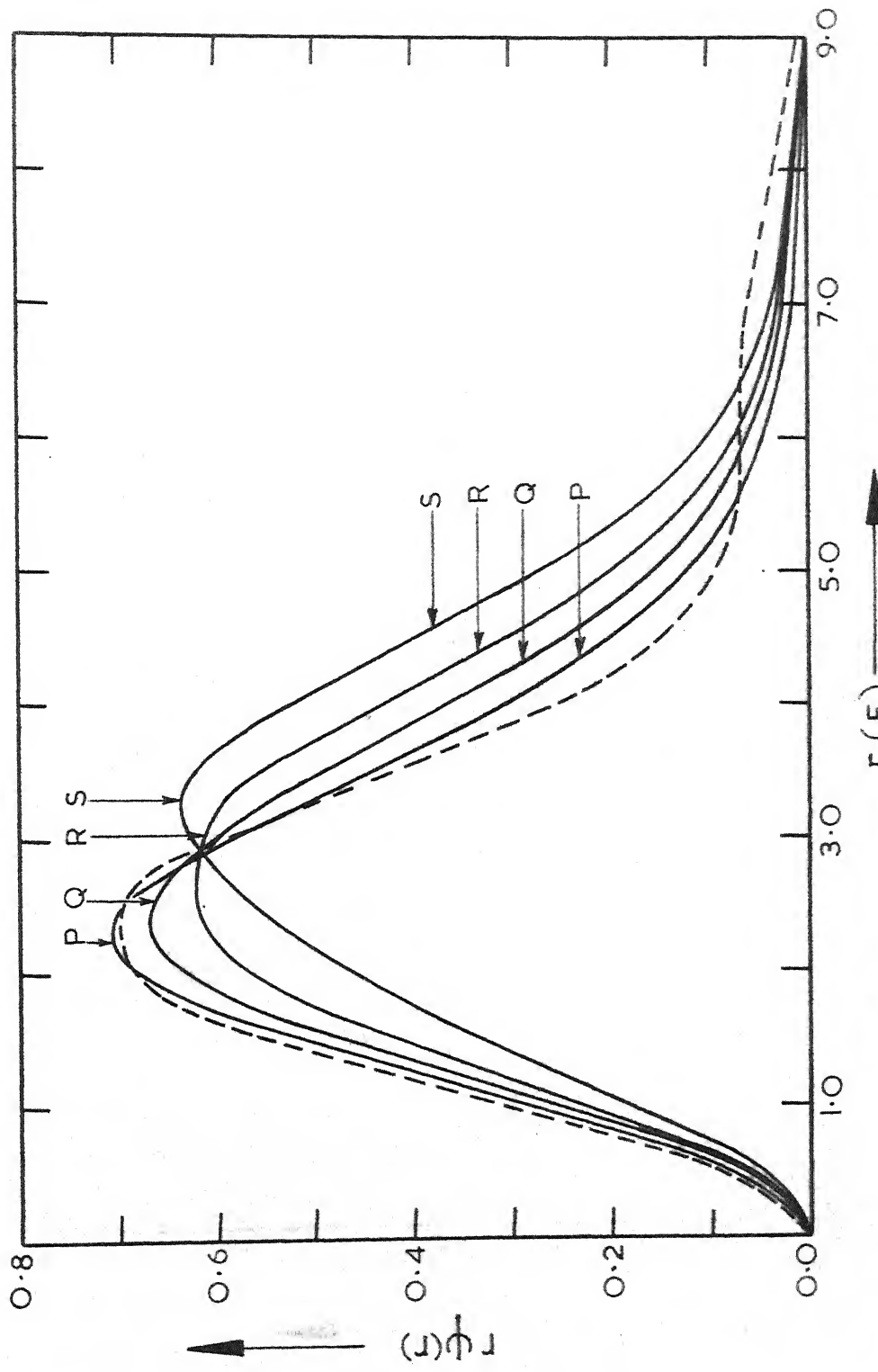


FIG. IV.15 $1P_{3/2}$ state wave functions of a local potential which gives same energies for $1P_{3/2}$ and $1P_{1/2}$ states as obtained in HF calculations with effective Yale interaction for 160 . Dashed curve represents the HF wave function and solid curves represent the wave functions of equivalent local potential. Curve P is obtained in absence of non-local correction while curves Q, R and S are obtained with the non-locality range parameter taken as 1.0F, 1.5F and 2.0F respectively. 129

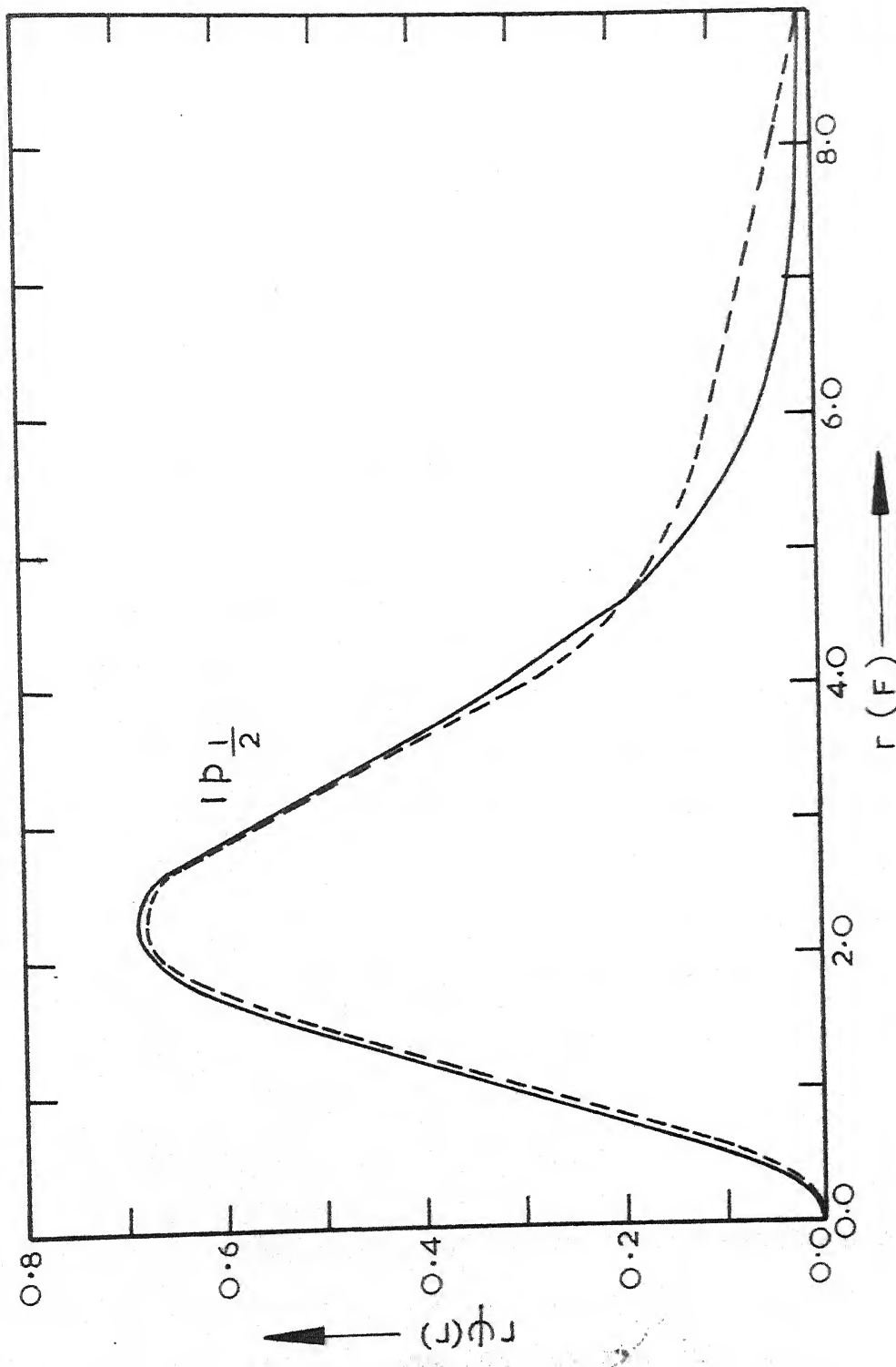


FIG. IV.16 $1p_{1/2}$ state wave function of a local potential which gives the same energies for $1p_{3/2}$ and $1p_{1/2}$ states as obtained in HF calculations with effective Yale interaction for $^{16}_O$. Dashed curve represents the HF wave function and solid curve is the wave function of equivalent local potential.

nuclei are not very much affected. These new coulomb and centre-of-mass matrix elements have been used in the HF calculations with Sussex interaction reported in next section.

IV.3 Sussex Interaction Results

HF calculations with Sussex relative matrix elements have been done for the nuclei ^4He , ^{12}C , ^{16}O and ^{40}Ca . Two-body matrix elements occurring in the HF equations are calculated using tables of relative matrix elements given in reference (Elt 68a). The tables given in reference (Elt 68a) are not complete since only the matrix elements between the states whose oscillator energies [i.e. $(2n+\ell-\frac{1}{2})\hbar\omega$] differ by not more than $2\hbar\omega$ are tabulated. Some other matrix elements, such as off-diagonal matrix elements of the type $\langle n' | v | n \rangle$ when the radial quantum numbers differ by more than one, i.e. $(n' - n) \geq 2$, are also needed in the present work and have been calculated using a simple recurrence formula (Elt 68a) from the tables given by Elliott et. al. (see Appendix C). The complete set of matrix elements used in our calculation is given in Tables IV.16 for some of the relative states. The specific form of the two-body Sussex interaction is not known but is not needed in any part of the calculation.

Results of HF calculations obtained with Sussex interaction are tabulated in Tables (IV.17 - IV.19) for the nuclei ^4He , ^{12}C and ^{16}O and for several values of b . We have not

Table IV.16(a)

Sussex relative matrix elements for 3S_1 channel,
 $b = 2.0F$. Only $n' \leq n$ values are given since
 $\langle n' | ^3S_1 | V | n | ^3S_1 \rangle = \langle n | ^3S_1 | V | n' | ^3S_1 \rangle$

n	n'	1	2	3	4	5	6	7
1		-5.58						
2		-5.22	-5.11					
3		-4.41	-4.24	-3.76				
4		-3.45	-3.35	-2.93	-2.53			
5		-2.47	-2.46	-2.21	-1.89	-1.61		
6		-1.56	-1.62	-1.53	-1.34	-1.13	-0.89	
7		-0.74	-0.87	-0.89	-0.83	-0.67	-0.43	-0.07

Table IV.16(b)

Sussex relative matrix elements for 3P_1 channel,
 $b = 2.0F$. Only $n' \leq n$ values are given since
 $\langle n' | ^3P_1 | V | n | ^3P_1 \rangle = \langle n | ^3P_1 | V | n' | ^3P_1 \rangle$.

n	n'	1	2	3	4	5	6	7
1		1.20						
2		1.34	1.85					
3		1.40	1.97	2.48				
4		1.41	2.13	2.70	3.14			
5		1.42	2.27	2.87	3.26	3.39		
6		1.47	2.36	2.95	3.20	3.22	3.21	
7		1.53	2.40	2.88	3.00	3.04	0.00	0.00

Table IV.16(c)Sussex relative matrix elements for 1P_1 channel, $b = 2.0F$. Only $n' \leq n$ values are given since

$$\langle n' ^1P_1 | V | n ^1P_1 \rangle = \langle n ^1P_1 | V | n' ^1P_1 \rangle.$$

n	n'	1	2	3	4	5	6	7
1		0.86						
2		1.21	1.78					
3		1.46	2.17	2.71				
4		1.66	2.48	3.09	3.54			
5		1.81	2.72	3.37	3.84	4.14		
6		1.93	2.88	3.56	4.01	4.30	4.50	
7		2.02	2.99	3.65	4.08	4.39	4.63	0.00

Table IV.16(d)Sussex relative matrix elements for 3D_2 channel, $b = 2.0F$. Only $n' \leq n$ values are given since

$$\langle n' ^3D_2 | V | n ^3D_2 \rangle = \langle n ^3D_2 | V | n' ^3D_2 \rangle.$$

n	n'	1	2	3	4	5	6	7
1		-1.63						
2		-1.43	-2.01					
3		-1.19	-2.11	-2.46				
4		-1.09	-1.92	-2.33	-2.60			
5		-1.04	-1.59	-2.15	-2.44	-2.74		
6		-0.93	-1.34	-1.87	-2.34	-2.62	-2.86	
7		-0.77	-1.16	-1.62	-2.15	-2.51	-0.00	-0.00

Table IV.17

Calculated HF properties for ${}^4\text{He}_2$ obtained with Sussex interaction.

$b(F)$	1.5	1.8	2.0	2.2	Experi- mental
B.E./A (MeV)	- 3.602	- 3.263	- 3.134	- 2.947	- 7.07 ^a
Matter r.m.s. radius (F)	1.695	1.827	1.898	1.999	
Charge r.m.s. radius (F)	1.699	1.831	1.901	2.002	1.67 ^b
Single particle energies (MeV)					
$1s_{\frac{1}{2}}$	neutron -24.05	-21.24	-20.15	-18.75	
	proton -23.21	-20.47	-19.41	-18.04	-20.4 \pm 0.3 ^c
$1p_{\frac{3}{2}}$	neutron 6.38	4.62	3.94	3.42	0.96 ^d
	proton 7.36	5.46	4.72	4.12	1.97 ^d
$1p_{\frac{1}{2}}$	neutron 8.86	6.05	4.99	4.18	4.36 ^d
	proton 9.76	6.83	5.70	4.81	5.37 ^d
$2s_{\frac{1}{2}}$	neutron 13.58	8.65	6.83	5.57	
	proton 14.47	9.40	7.50	6.18	
$1p_{\frac{3}{2}}-1p_{\frac{1}{2}}$ splitting (MeV)	neutron 2.49	1.43	1.05	0.76	
	proton 2.41	1.36	0.98	0.68	

a. Mattauch et. al. (Mah 65)

b. Hofstadter et. al. (Hor 67)

c. Riou (Riu 65)

d. Vashakidze et. al. (Vae 68)

Table IV.18

Calculated HF properties for $^{12}\text{C}_6$ obtained with Sussex interaction.

b(F)	1.5	1.8	2.0	2.2	Experi- mental
B.E./A (MeV)	- 2.309	- 2.107	- 1.992	- 1.828	- 7.68 ^a
Matter r.m.s. radius (F)	2.227	2.404	2.489	2.609	
Charge r.m.s. radius (F)	2.238	2.419	2.504	2.625	2.47 ^b
Single particle energies (MeV)					
$1s_{\frac{1}{2}}$	neutron	-47.73	-42.03	-39.67	-36.51
	proton	-44.67	-39.25	-36.99	-33.94 -33.0 ± 3.5 ^c
$1p_{\frac{3}{2}}$	neutron	-15.34	-13.43	-12.79	-11.90
	proton	-12.54	-10.92	-10.30	-9.52
$1p_{\frac{1}{2}}$	neutron	-11.98	-11.78	-11.77	-11.47
	proton	- 8.84	- 8.85	- 8.91	- 9.23
$2s_{\frac{1}{2}}$	neutron	5.04	2.76	2.34	2.18
	proton	7.71	5.03	4.49	4.17
$1p_{\frac{3}{2}} - 1p_{\frac{1}{2}}$	neutron	3.36	1.72	1.02	0.43
splitting (MeV)	proton	3.70	2.07	1.39	0.29

a. Mattauch et. al. (Mah 65)

b. Hofstadter et. al. (Hor 67)

c. Riou (Riu 65)

Table IV.19

Calculated HF properties for $^{16}\text{O}_8$ obtained with Sussex interaction.

b(F)	1.5	1.8	2.0	2.2	Experi- mental
B.E./A (MeV)	- 5.111	- 4.910	- 4.850	- 4.772	- 7.98 ^a
Matter r.m.s. radius $r_o(F)$	2.217	2.325	2.380	2.478	
Charge r.m.s. radius $r_c(F)$	2.227	2.337	2.391	2.479	2.71 ^b
$r_o \times B.E./A$ (MeV-F)	11.231	11.416	11.543	11.825	$\sim 11^c$
Single particle energies (MeV)					
$1s_{\frac{1}{2}}$	neutron	-57.16	-53.05	-51.33	-48.43 ~ -51
	proton	-53.04	-49.16	-47.51	-44.65 $-34+3.5^e$ $-44+2$
$1p_{\frac{3}{2}}$	neutron	-28.82	-26.57	-25.77	-24.44 -21.81^d
	proton	-24.86	-22.82	-22.11	-21.17 $-18+2.5^e$ $-19+1$
$1p_{\frac{1}{2}}$	neutron	-19.90	-19.18	-19.20	-18.90 -15.65^d
	proton	-16.06	-15.53	-15.61	-16.44 $-13+2^e$ $-12.4+1$
$2s_{\frac{1}{2}}$	neutron	2.12	0.15	0.10	0.31 $- 4.15^d$
	proton	5.76	3.38	3.15	3.12
$1p_{\frac{3}{2}} - 1p_{\frac{1}{2}}$ splitting (MeV)	neutron	8.92	7.39	6.57	5.54 6.16^d
	proton	8.80	7.29	6.50	4.73

a. Mattauch et. al. (Mah 65)

b. Hofstadter et. al. (Hor 67)

c. Angeli et. al. (Ani 69)

d. Cohen et. al. (Con 63a, 63b)

e. Riou (Riu 65)

presented the results for $b = 1.4F$ and $b = 1.6F$, since they are close to $b = 1.5F$ results. Binding energy per particle vs. b curves (Figure IV.17) are very nearly straight lines for all these nuclei (^4He , ^{12}C and ^{16}O). We find that the calculated binding energies for ^{16}O is about (30 - 40 percent) less than the corresponding experimental value and still poorer agreement with the experimental data has been obtained in the case of ^4He and ^{12}C . As described in Section IV.2a, binding energy result for ^{12}C will improve if the constraint of spherical symmetry is relaxed. Moreover, since minimas in the binding energy vs. b curves could not be obtained till $b = 1.5F$, the calculations should have been extended to lower values of b in order to know how much maximum binding one can obtain in such a calculation. The matrix elements in reference (Elt 68a) have been calculated only up to $b = 1.4F$ since lack of experimental phase shift data above energies > 300 MeV imposes a lower limit on the value of b up to which matrix elements can be determined accurately (see Section II.3). However, as pointed out by Elliott et. al, the matrix elements for lower b values can be obtained by a polynomial fit to the matrix element vs. b curve in the known region and extrapolation of the fitted polynomial to smaller b values, but the reliability of the matrix elements so obtained can be questioned. Moreover, even for the smaller configuration space included in the present calculation and for $b < 1.4F$, the relative matrix elements of V involving energies $E > 300$ MeV will also enter. The second and higher-order terms (see expansion 2.56) for such matrix elements are quite important since the

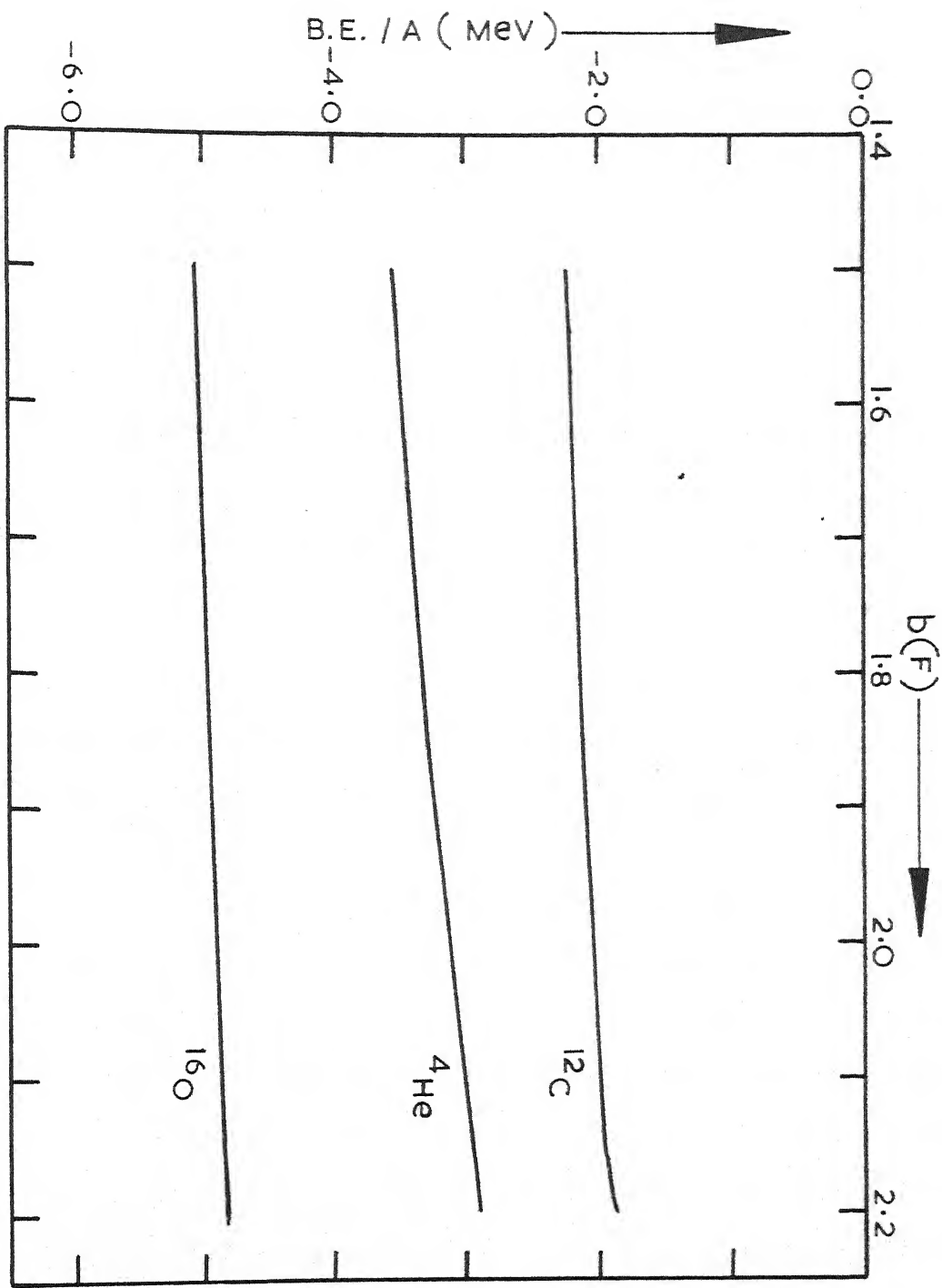


FIG. IV. 17 HF binding energy per particle for various nuclei obtained with Sussex interaction as a function of oscillator range parameter b .

auxiliary potential can be chosen to approximate the true potential only below 300 MeV. In view of this, the calculations have not been carried out for smaller values of b .

As seen from Table IV.19, the single particle energy levels in ^{16}O are overbound compared to experimental data. The coulomb correction shifts the proton levels relative to neutron levels but the relative separation between any two proton levels is very nearly the same as the corresponding separation between the neutron levels. Angeli et. al. (Ani 68), on the basis of experimentally measured cross-sections, have suggested the following relationship between the binding energy per particle and matter r.m.s. radius for ^{16}O ,

$$\text{B.E./A (MeV)} \propto r_0(\text{F}) \approx 11. \quad (4.3)$$

Our HF calculations for ^{16}O agree with this.

Assuming that the Sussex interaction V can be broken up into central, spin-orbit and tensor parts, the matrix elements of any particular component can be expressed in terms of the matrix elements of the full potential as described in Appendix C. Such a calculation has been carried out and the results are presented in Table IV.20 for some of the relative states of nucleon-nucleon pair. In order to test the effects of each of these parts on various ground state properties HF calculations have been repeated with the contributions of

- (i) only the central part,

Table IV.20(a)

Central, spin-orbit and tensor components of Sussex relative matrix elements $\langle n|V|n \rangle$, diagonal in oscillator radial quantum number n for $b = 2.0F$.

Radial Quantum Number	Channel	Central	Spin-orbit	Tensor	Total
n=1	3P_0	-0.15	0.60	-2.05	-1.58
	3P_1	-0.13	0.30	1.03	1.20
	3P_2	-0.13	-0.30	-0.21	-0.64
n=2	3P_0	-0.15	1.34	-2.67	-1.48
	3P_1	-0.15	0.67	1.33	1.85
	3P_2	-0.15	-0.67	-0.27	-1.09
n=3	3P_0	-0.03	2.11	-2.92	-0.84
	3P_1	-0.03	1.06	1.46	2.49
	3P_2	-0.03	-1.06	-0.29	-1.38
n=1	3D_1	-0.39	0.10	1.27	0.98
	3D_2	-0.39	0.03	-1.27	-1.63
	3D_3	-0.39	-0.07	0.36	-0.10

Contd..

Table IV.20(a) (Contd.)

Radial Quantum Number	Channel	Central	Spin-orbit	Tensor	Total
n=2	3D_1	-0.46	0.28	1.65	1.47
	3D_2	-0.46	0.09	-1.65	-2.02
	3D_3	-0.46	-0.19	0.47	-0.18
n=3	3D_1	-0.56	0.43	2.05	1.92
	3D_2	-0.56	0.14	-2.05	-2.47
	3D_3	-0.56	-0.29	0.58	-0.27

Table IV.20(b)

Central, spin-orbit and tensor components of Sussex relative matrix elements $\langle n|V|n' \rangle$, off-diagonal in oscillator radial quantum number ($n \neq n'$)
for $b = 2.0F$.

Radial Quantum Number	Channel	Central	Spin-orbit	Tensor	Total
	3P_0	-0.15	0.88	-2.1	-1.37
$n = 1$	3P_1	-0.15	0.44	1.05	1.34
$n' = 2$	3P_2	-0.15	-0.44	-0.21	-0.80
	3P_0	-0.10	1.68	-2.46	-0.88
$n = 2$	3P_1	-0.10	0.84	1.23	1.97
$n' = 3$	3P_2	-0.10	-0.84	-0.25	-1.19
	3P_0	-0.13	1.11	-1.95	-0.97
$n = 1$	3P_1	-0.13	0.55	0.98	1.40
$n' = 3$	3P_2	-0.13	-0.55	-0.20	-0.88
	3D_1	-0.31	0.22	1.19	1.10
$n = 1$	3D_2	-0.31	0.07	-1.19	-1.43
$n' = 2$	3D_3	-0.31	-0.15	0.34	-0.12

Contd..

Table IV.20(b) (Contd.)

Radial Quantum Number	Channel	Central	Spin-orbit	Tensor	Total
n = 2 n' = 3	3D_1	-0.48	0.32	1.73	1.57
	3D_2	-0.48	0.11	-1.73	-2.11
	3D_3	-0.48	-0.21	0.50	-0.19
n = 1 n' = 3	3D_1	-0.25	0.25	1.03	1.03
	3D_2	-0.25	0.08	-1.03	-1.20
	3D_3	-0.25	-0.17	0.29	-0.13

- (ii) central and spin-orbit part,
- (iii) central and tensor parts of the interaction.

We present the results in Tables (IV.21 - IV.22) for the nuclei ^{16}O and ^{12}C respectively and for $b = 2.0\text{F}$. This is also the value of b for which spin-orbit splitting for ^{16}O is closest to experimental value (see Table IV.19). As seen from the tables, major portion of the binding energy comes from central part of the interaction while the tensor force leads to saturation. In the case of ^{16}O almost all of the spin-orbit splitting comes from the spin-orbit part of the force. In ^{12}C , tensor force also produces large splitting but of wrong sign. This is consistent with the findings of Wong (Wog 63) and Tarbutton (Tan 68). The contribution to the splittings from the spin-saturated shells (in spin-saturated shells both the members of the doublet $j = l \pm \frac{1}{2}$ are completely filled), such as in ^{16}O , is positive and comes mainly from the spin-orbit part of the two-body potential. In the nuclei with spin unsaturated shells, such as in ^{12}C , there is significant contribution to the splitting from the tensor forces, but it always has the wrong sign. Thus, the effect of only partially filling up a $j = l \pm \frac{1}{2}$ doublet is to decrease the splitting. The spin-orbit splitting is a sensitive function of b and increases rapidly with decreasing b . This is expected since the spin-orbit force dominates at high-energy.

HF calculations have also been carried out for ^{40}Ca and also for ^{16}O in the larger configuration space which

Table IV.21

Effect of central, spin-orbit and tensor parts of Sussex interaction on calculated HF properties of $^{16}\text{O}_3$ for $b = 2.0\text{F}$.

	Only Central	No Tensor		No Spin-orbit	
B.E./ A (MeV)	-4.828		-4.924		-4.917
Matter r.m.s. radius (F)	2.376		2.365		2.362
Charge r.m.s. radius (F)	2.387		2.367		2.365
Single particle energies (MeV)	Neutron Proton Neutron Proton Neutron Proton				
$1s_{\frac{1}{2}}$	-51.11	-47.29	-51.78	-47.82	-51.61 -47.70
$1p_{\frac{3}{2}}$	-23.60	-19.96	-26.13	-22.63	-23.86 -20.40
$1p_{\frac{1}{2}}$	-23.60	-19.96	-19.15	-16.25	-23.73 -20.93
$2s_{\frac{1}{2}}$	0.15	3.20	0.14	3.18	0.20 3.21
$1p_{\frac{3}{2}} - 1p_{\frac{1}{2}}$ splitting (MeV)	0.00	0.00	6.98	6.38	0.13 -0.53

Table IV.22

Effect of central, spin-orbit and tensor parts of Sussex interaction on calculated HF properties of $^{12}\text{C}_6$ for $b = 2.0\text{F}$.

	Only Central	No Tensor	No Spin-orbit
B.E./ A (MeV)	-1.506	-2.627	-1.007
Matter r.m.s. radius (F)	2.594	2.403	2.712
Charge r.m.s. radius (F)	2.610	2.415	2.731
Single particle energies (MeV)	Neutron Proton Neutron Proton Neutron Proton		
$1s_{\frac{1}{2}}$	-34.25 -31.72 -41.49 -38.71 -32.32 -29.90		
$1p_{\frac{3}{2}}$	-11.67 -9.30 -15.51 -12.93 -9.34 -7.07		
$1p_{\frac{1}{2}}$	-10.49 -7.72 -8.74 -6.13 -12.54 -10.09		
$2s_{\frac{1}{2}}$	2.63 4.73 2.45 4.62 2.51 4.58		
$1p_{\frac{3}{2}} - 1p_{\frac{1}{2}}$ splitting (MeV)	1.18 1.58 6.77 6.80 -3.20 -3.02		

includes $d_{5/2}$ and $d_{3/2}$ oscillator states of $n = 1 - 3$ major shells as well. In these calculations, coulomb and centre-of-mass corrections were not included in a self-consistent manner. Results are presented in Tables (IV.23 - IV.24) for ^{40}Ca and ^{16}O respectively and for $b = 2.0\text{F}$. In the case of ^{40}Ca the calculated binding energy is close to experimental value, but the single particle levels are somewhat overbound compared to experimental data. Expansion coefficients are given in Tables (IV.25 - IV.28) for the nuclei ^4He , ^{12}C , ^{16}O and ^{40}Ca respectively. Table IV.29 shows variation of expansion coefficients for ^{16}O with b .

IV.4 Discussion

In our calculations with effective Yale interaction we find that binding energies for ^4He and ^{16}O are in fair agreement with the experimental data when the second-order term in VP is taken into account. Reasonable values for the binding energies of ^8Be and ^{12}C can only be obtained if the HF field is permitted to be deformed. An important correction to the binding energy arises because of the approximate treatment of the energy denominator e in the evaluation of second-order terms in expression (2.27). The energy denominator e is defined as the difference in the energy between the excited intermediate state and the occupied initial state. In reference (Shn 67a), the intermediate states were taken to be plane waves and the energy of the interacting pair was

Table IV.23

Calculated HF properties for $^{40}\text{Ca}_{20}$, obtained with Sussex interaction without coulomb and centre-of-mass corrections, $b = 2.0\text{F}$.

	Sussex	Experimental
Single particle energies (MeV)		
$1s_{1/2}$	-93.04	
$1p_{3/2}$	-61.70	
$1p_{1/2}$	-55.03	
$1d_{5/2}$	-33.17	-21.9 ^a
$2s_{1/2}$	-25.88	-18.2 ^a
$1d_{3/2}$	-22.20	-15.6 ^a
B.E./A (MeV)	- 9.84	
$E_{\text{coul.}}/A$ (MeV)	1.85	
$E_{\text{c.m.}}/A$ (MeV)	- 0.20	
B.E./A (MeV) including c.m. and coul. corrections	- 8.19	- 8.55 ^b
$1p_{3/2}$ - $1p_{1/2}$ splitting (MeV)	6.67	
$1d_{5/2}$ - $1d_{3/2}$ splitting (MeV)	10.97	7.0 ^c
ℓ -splitting in the same major shell, $2s$ - $1d$ (MeV)	- 2.90	- 1.1 ^d
r.m.s. radius (F)	2.789	3.50 ^e

a. Elton et. al. (El 67)

b. Mattauch et. al. (Mah 65)

c. Cohen et. al. (Con 63a)

d. Dey et. al. (Dey-Preprint)

e. Hofstadter et. al. (Hor 67)

Table IV.24

Single particle energies of $^{16}_0S$, $b = 2.0F$ obtained in the HF calculation with Sussex interaction without coulomb and centre-of-mass corrections.

State	Single particle energy (MeV)
$1s_{\frac{1}{2}}$	-51.08
$1p_{\frac{3}{2}}$	-23.41
$1p_{\frac{1}{2}}$	-17.13
$1d_{\frac{5}{2}}$	- 1.87
$2s_{\frac{1}{2}}$	- 0.68
$1d_{\frac{3}{2}}$	3.40

Table IV.25

Expansion coefficients $c_n^a(lj)$ for ${}^4\text{He}_2$ obtained
with Sussex interaction, $b = 1.8F$.

states			neutron			proton			
ℓ	j	a	n	1	2	3	1	2	3
0	$\frac{1}{2}$	1	1	0.9700	0.2152	0.1128	0.9711	0.2108	0.1121
		2	2	-0.1599	0.9150	-0.3704	-0.1547	0.9131	-0.3773
		3	3	0.1829	-0.3413	-0.9220	0.1818	-0.3490	-0.9193
1	$\frac{3}{2}$	1	1	0.9020	-0.3627	0.2341	0.8939	-0.3785	0.2401
		2	2	0.4301	0.8018	-0.4150	0.4472	0.7907	-0.4182
		3	3	0.0371	-0.4750	-0.8792	0.0316	-0.4812	-0.8761
1	$\frac{1}{2}$	1	1	0.8323	-0.4949	0.2495	0.8239	-0.5057	0.2558
		2	2	-0.5502	-0.6833	0.4800	-0.5621	-0.6718	0.4823
		3	3	-0.0671	0.5360	0.8410	0.0721	0.5412	0.8378

Table IV.26

Expansion coefficients $c_n^a(lj)$ for $^{12}C_6$ obtained
with Sussex interaction, $b = 2.0F$.

states			neutron			proton		
l	j	$a \backslash n$	1	2	3	1	2	3
0	$\frac{1}{2}$	1	0.9397	0.3139	0.1359	0.9422	0.3075	0.1330
		2	-0.3004	0.9473	-0.1109	-0.2888	0.9467	-0.1427
		3	0.1635	-0.0634	-0.9845	0.1698	-0.0960	-0.9808
1	$\frac{3}{2}$	1	0.9647	0.2140	0.1532	0.9688	0.1954	0.1525
		2	-0.1582	0.9366	-0.3126	-0.1360	0.9335	-0.3318
		3	0.2104	-0.2773	-0.9374	0.2072	-0.3007	-0.9309
1	$\frac{1}{2}$	1	0.9675	0.1999	0.1547	0.9714	0.1801	0.1546
		2	-0.1451	0.9404	-0.3074	-0.1220	0.9376	-0.3258
		3	0.2069	-0.2750	-0.9389	0.2036	-0.2976	-0.9327

Table IV.27(a)

Expansion coefficients $C_n^a(lj)$ for $^{16}\text{O}_8$ obtained
with Sussex interaction, $b = 2.0\text{F}$.

states			neutron			proton			
l	j	a	n	1	2	3	1	2	3
0	$\frac{1}{2}$	1		0.9433	0.3140	0.1079	0.9461	0.3069	0.1038
		2		0.3163	-0.9487	-0.0040	-0.3040	0.0517	-0.0433
		3		-0.1011	-0.0379	0.9942	0.1121	-0.0094	-0.9937
1	$\frac{3}{2}$	1		0.9236	0.3447	0.1677	0.9286	0.3328	0.1639
		2		-0.3026	0.9242	-0.2331	-0.2837	0.9218	-0.2643
		3		0.2353	-0.1645	-0.9579	0.2391	-0.1989	-0.9504
1	$\frac{1}{2}$	1		0.9445	0.2882	0.1577	0.9500	0.2712	0.1549
		2		-0.2380	0.9311	-0.2765	-0.2153	0.9279	-0.3043
		3		0.2265	-0.2236	-0.9480	0.2262	-0.2557	-0.9399

Table IV.27(b)

Expansion coefficients $c_n^a(\ell_j)$ for $^{16}\text{O}_8$ obtained in the HF calculation with Sussex interaction without coulomb and centre-of-mass correction, $b = 2.0\text{F}$.

state	ℓ	j	a	n	1	2	3
0	$\frac{1}{2}$	1			0.9398	0.3224	0.1132
		2			0.3275	-0.9444	-0.0287
		3			-0.0976	-0.0640	0.9932
1	$\frac{3}{2}$	1			0.9336	0.3216	0.1582
		2			-0.2817	0.9314	-0.2305
		3			0.2215	-0.1706	-0.9601
1	$\frac{1}{2}$	1			0.9539	0.2609	0.1483
		2			-0.2136	0.9374	-0.2749
		3			0.2107	-0.2306	-0.9500
2	$\frac{5}{2}$	1			0.9750	0.1027	0.1971
		2			-0.0323	0.9428	-0.3318
		3			0.2199	-0.3172	-0.9225
2	$\frac{3}{2}$	1			0.9592	-0.1930	0.2065
		2			0.2618	0.8821	-0.3917
		3			0.1066	-0.4298	-0.8966

Table IV.28

Expansion coefficients $C_n^a(l_j)$ for $^{40}\text{Ca}_{20}$ obtained in the HF calculation with Sussex interaction without coulomb and centre-of-mass correction, $b = 2.0\text{F}$.

states		l	j	a	n	1	2	3
l	j					1	2	3
0	$\frac{1}{2}$	0	1		1	0.9455	0.3139	0.0870
			2		2	0.3211	-0.8533	-0.4108
			3		3	-0.0547	-0.4163	0.9076
1	$\frac{3}{2}$	1	1		1	0.9163	0.3781	0.1320
			2		2	0.3995	-0.8859	-0.2357
			3		3	-0.0278	-0.2687	0.9628
1	$\frac{1}{2}$	1	1		1	0.9167	0.3740	0.1407
			2		2	0.3927	-0.9082	-0.1445
			3		3	-0.0738	-0.1878	0.9794
2	$\frac{5}{2}$	2	1		1	0.9058	0.3886	0.1687
			2		2	-0.3779	0.9212	-0.0926
			3		3	0.1914	-0.0201	-0.9813
2	$\frac{3}{2}$	1	1		1	0.9316	0.3266	0.1595
			2		2	-0.2938	0.9350	-0.1986
			3		3	0.2140	-0.1381	-0.9670

Table IV.29

Expansion coefficients for $^{16}\text{O}_8$ obtained with Sussex interaction. Only $c_n^a(\ell j) = \delta_{n\alpha} c_n^a(\ell j)$ coefficients are given.

ℓ	j	$b(F) \rightarrow$	1.5	1.8	2.0	2.2
		coefficient				
0	$\frac{1}{2}$	c_1^1	-0.9934	0.9729	0.9433	0.9162
	$\frac{3}{2}$	c_2^2	-0.9658	0.9703	-0.9487	-0.9199
	$\frac{5}{2}$	c_3^3	-0.9674	-0.9936	0.9942	0.9855
1	$\frac{3}{2}$	c_1^1	-0.9935	0.9659	0.9236	0.8827
	$\frac{5}{2}$	c_2^2	-0.9243	0.9373	0.9242	0.9063
	$\frac{7}{2}$	c_3^3	-0.9247	-0.9544	-0.9579	-0.9510
1	$\frac{1}{2}$	c_1^1	0.9935	-0.9809	0.9445	0.9043
	$\frac{3}{2}$	c_2^2	0.9042	-0.9357	0.9311	0.9170
	$\frac{5}{2}$	c_3^3	-0.9079	-0.9395	-0.9480	-0.9452

replaced by a constant average value Δ . Thus, e was taken as

$$-e = \frac{e^2}{2m_A} (k_1^2 + k_2^2) + \Delta \quad (4.4)$$

with $\Delta = 20$ MeV. However, Δ is actually state-dependent and generally larger than 20 MeV. The approximate treatment of Δ causes an uncertainty of about 20 percent in the 3S_1 matrix elements which are the most important ones in the binding energy calculation. Actually, the energy denominator should be

$$-e_{HF} = \frac{e^2}{2m_A} (k_1^2 + k_2^2) + \epsilon_{1HF} + \epsilon_{2HF} , \quad (4.5)$$

where ϵ_{1HF} and ϵ_{2HF} refer to the HF single particle energies of the initial state of the nucleon pair. This would mean that the second-order terms occurring in the effective interaction depend upon the HF solutions, which in turn cannot be obtained without a pre-knowledge of the effective interaction. Thus, there is a double self-consistency problem involved. Shakin et. al. (Shn 67b) have solved this problem by approximating $\epsilon_{1HF} + \epsilon_{2HF}$ with Δ . With an intelligent choice of Δ , $e(\Delta)$ can be made close to e_{HF} and the difference $V(\frac{Q}{e_{HF}} - \frac{Q}{e})V$ can be evaluated by perturbation theory in HF basis. These corrections are referred to as spectral corrections and are expected to add roughly ~ 1 MeV per particle to the binding energies (Shn 67b). Thus, binding energy results would further improve when these corrections are taken into account.

It is expected that the results would improve if more terms are included in the expansion (3.20) of HF wave functions. However, the situation is somewhat ambiguous due to the following reason. It has been pointed out by Pal and Stamp (Pal 67) that there is a possibility of double counting of the contribution of high-energy states when HF wave functions are expanded in terms of oscillator states with large number of nodes and singular interactions are used. The strongly repulsive short-range part of these interactions gives rise to excitations to high-lying intermediate states. The contributions of these states are included in the calculation of reaction matrix. Now, when the HF wave functions are expanded in terms of harmonic oscillator states of $n = 1, 2, 3$ and still higher major shells, which are quite high-lying in energy, there is a possibility of double counting. Thus, one is left with two alternatives. First is, if one wishes to avoid the double counting only low-lying oscillator states should be included in the expansion of HF orbitals and one has to be satisfied with almost pure oscillator states. This would not determine the tail of the wave function correctly. On the other hand, if more terms are used in the expansion (3.20), the HF wave functions are determined more accurately but there is always a danger of double counting. Since inclusion of oscillator states of $n = 1, 2$ and 3 major shells appears to be a reasonable compromise between these two alternatives, we expect that such a double counting would not cause any serious error in our calculations with effective Yale interaction.

In the calculation of Sussex matrix elements (Elt 68a), as pointed out by Mavromatis (Mas 69), the higher-order terms in the auxiliary potential are left out (see expansion 2.56). The most important of these are the second-order Born term $V \frac{Q}{e} V$ and the dispersion term $t_A \left(\frac{Q}{e_n} - \frac{Q}{e_A} \right) t_A$. In the calculation of reaction matrix elements with Hamada-Johnston (HJ) potential Kuo and Brown (Kuo 66) have observed that exclusion principle plays an important role in reducing the size of the Born term for singlet states. However, they have also observed that there is a large contribution to this term from the tensor part of the force for triplet states. The studies of Dahlblom (Dan 64) and Levinger et. al. (Ler 60) also show that tensor forces give large contributions to binding energy when calculated to second-order in perturbation theory: their contribution being typically ten times larger than the corresponding contribution for the pure central forces. Thus, there would be considerable improvement in the binding energy results when this term is accounted for. Dispersion corrections are also expected to contribute significantly.

In Tables (IV.30 - IV.33) ^{16}O and ^{40}Ca results of present calculation are compared with those of various other spherical HF and Brueckner-Hartree-Fock (BHF) calculations. Different types of nucleon-nucleon interactions used in these calculations are also specified. It is seen that Yale and HJ potentials give very similar results when the second-order term in VP is not taken into account in the former. This is hardly

Table IV.30

Comparison of our results for the HF binding energy and r.m.s. radius of ^{16}O and $^{40}\text{Ca}_{20}$ with other calculations. Numbers marked with \checkmark are taken from reference (Shn 67b) and are the results obtained when second-order term in VP was included.

References	Present Work	(Ken 66)	(Das 69)	(Brr 61)	(Tan 68)	(Das 66)
Interaction Properties ↓	Yale Sussex	Tabakin Hamada -Johnston	Gammel -Thaler	Effective potential derived from t-matrix of Kuo	Velocity -dependent effective potential	
^{16}O	$\text{B.E.}/\text{A}$ (MeV)	-3.61 -5.12 \checkmark	-4.85 -2.41	-3.84 -4.41	-4.81 -4.81	-4.883
	Matter r.m.s. radius (F)	2.549	2.380	2.46	2.40	2.539
	Charge r.m.s. radius (F)	2.570	2.391	2.420	2.61	2.673
$^{40}\text{Ca}_{20}$	$\text{B.E.}/\text{A}$ (MeV)	-7.93 \checkmark	-8.19 -3.74	-4.20 -6.12	-5.64 -7.297	
	Matter r.m.s. radius (F)	2.84 \checkmark	2.789	2.963 2.97	2.88 3.186	3.47

Table IV.31

Comparison of our results for the HF single particle neutron energies of ^{160}O with other calculations. Numbers enclosed in square brackets are the results obtained without coulomb and centre-of-mass corrections. Numbers inside rounded brackets are the results obtained when second-order term in pseudopotential was included but correction terms were not taken into account and have been taken from reference (Shn 67b). All numbers are in MeV.

Reference	Present work	(Swe 65)	(Das 69)	(Brr 61)	(Das 66)	(Tan 68)
Interaction	Yale	Sussex	Tabakin	Hamada -Johnston -Thaler	Gammel	Velocity- dependent effective potential
State						derived from t- matrix of Kuo
1s _{1/2}	-45.60 (-51.9)	-51.33 [-51.08]	-46.62	-43.8	-44.3	-40.6
1p _{3/2}	-21.21 (-23.2)	-25.77 [-23.41]	-17.85	-20.3	-19.0	-16.2
1p _{1/2}	-15.75 (-17.8)	-19.20 [-17.13]	-6.38	-15.9	-14.9	-16.2
1d _{5/2}		-1.87		0.43		
2s _{1/2}	-0.53	0.10 [- 0.68]	10.35	0.95		1.9
1d _{3/2}		3.40		4.6		0.90
1p _{3/2} -1p _{1/2} splitting	5.45	6.57	11.47	4.4	4.1	0.0
						5.8

Table IV.32

Comparison of our results for the HF proton single particle energies of $^{16}\text{O}_8$, with other calculations. All numbers are in Mev.

Reference	Present work	(Sve 65)	(Das 69)	(Brr 61)	(Tan 68)
Interaction	Yale	Sussex	Tabakin	Hanada -Johnston -Thaler	Gammel -Thaler Effective po- tential deri- ved from t- matrix of Kuo
State					
$1s_1/2$	-42.10	-47.51	-40.73	-40.4	-39.6
$1p_3/2$	-17.84	-22.11	-13.53	-17.0	-14.6
$1p_1/2$	-12.45	-15.61	-3.40	-12.6	-10.7
$2s_1/2$	1.58	3.15	12.95	3.8	3.8
$1p_3/2$ - $1p_1/2$	4.39	6.50	10.13	4.4	3.9
					5.7

Table IV.33

Comparison of our results for the HF single particle energies in $^{40}\text{Ca}_{20}$ with other calculations. Numbers inside rounded brackets are the results obtained when second-order term in pseudopotential was included in effective Yale interaction. Proton energies are marked with V . All numbers are in MeV.

Reference	Present work	(Shn 67b)	(Swe 65)	(Das 69)	(Brr 61)	(Das 66)	(Tan 68)
Interaction	Sussex	Yale	Tabakin	Hamada -Johnston -Thaler	Gammel	Velocity-dependent potential derived from t-potential	Effective matrix of Kuo
State							
1s _{1/2}	-93.04	-74.8 (-90.0)	-71.53	-66.1 -58.2V	-70.1 -60.0V	-67.8	-73.0V
1p _{3/2}	-61.70	-48.4 (-59.8)	-45.12	-44.7 -37.0V	-44.7 -35.1V	-41.0	-46.5V
1p _{1/2}	-55.03	-43.5 (-54.9)	-35.16	-41.1 -35.5V	-38.6 -24.2V	-41.0	-38.9V
1d _{5/2}	-33.17	-22.8 (-31.3)	-21.22	-23.7 -16.2V	-20.6 -11.6V	-18.6	-42.3V
2s _{1/2}	-25.88	-17.6 (-23.7)	-13.22	-20.5 -13.1V	-16.0 -7.3V	-17.7	-23.4V
1d _{3/2}	-22.20	-15.9 (-22.6)	-7.82	-17.7 -10.5V	-13.4 -4.9V	-18.6	-16.1V
1d _{5/2} -1d _{3/2} splittings	10.97	7.9 (8.7)	13.40	6.0 5.7V	7.2 6.7V	0.0	-17.5V -10.3V -16.8V -9.6V 6.6V 6.5V

surprising because of the similar nature of these two potentials and also for the fact that they give same quantitative fit to the two-body data. Besides, in the calculations referred in the table, reaction matrix elements from both these potentials were obtained using similar techniques. For example, effective interaction from Yale potential was derived using Moszkowski-Scott separation technique and an attractive pseudopotential was added for those states where the potential is repulsive. Reaction matrix elements from HJ potential were also calculated using separation technique and the reference-spectrum method was used for the repulsive part of the potential. It is of some interest to compare the Sussex interaction results with those of potentials obtained from a fit to the phase shift data such as HJ, Yale, and Tabakin. It is found that Sussex interaction results for the binding energy are better than any other realistic interaction results at least in first-order. Strikingly close similarity can be seen in the Sussex and effective Yale results when the second-order term in VP is included in latter. Very few spherical HF and BHF calculations have been carried out for ^{12}C and ^4He . In the spherical HF calculations of Davies et. al. (Das 66) using a very simple velocity-dependent potential the calculated B.E./A is -2.40 MeV, which is larger than the values obtained with Yale (-1.42 MeV) and Sussex (-1.99 MeV) interactions (see Tables IV.1 and IV.18). Recently, Krieger (Krr-Preprint) has reported HF calculations in a basis of cartesian harmonic oscillator wave functions using a velocity-dependent interaction especially derived for use in HF

calculations. For ^4He , he obtains, $\text{B.E.}/A = -0.825 \text{ MeV}$ compared to our calculated values of -3.77 MeV and -3.60 MeV with effective Yale and Sussex interactions respectively. Thus, it appears that realistic interactions which fit the two-body data give more binding in ^4He than the effective interaction of Krieger which fits the nuclear matter data.

We have found that the binding of the lowest $1s_{1/2}$ state increases very rapidly as the nucleon number changes. A local potential with reasonable strength would not give such deeply bound $1s_{1/2}$ states and thus, this phenomenon is attributed to the non-locality of the HF potential. There is some experimental evidence from $(e, e'\gamma)$ experiments (Ami 64) that the binding energy of this level really changes from ≈ 35 to 60 MeV as one goes from $A = 12$ to 28 . However, the interpretation of the data is not unambiguous in view of the very wide peak corresponding to $1s_{1/2}$ level. More experimental evidence to settle this point conclusively seems to be necessary.

HF is the first term in Brueckner-Goldstone perturbation expansion and second and higher-order corrections to it will arise from $2p-2h$ (two particle-two hole), $4p-4h$, and higher excitations. The large gap between the occupied and the unoccupied levels indicates that these corrections would be small so that HF solutions would be close to the actual solutions. However, in order to obtain good wave functions and also improved binding energy, one must introduce $2p-2h$ type

correlations in the framework of the theory. The error introduced in choosing the harmonic oscillator wave functions as a basis set can be considerably reduced by improving the wave functions at large distances to give proper tails. The results of our analyses also indicate that our approximation of assuming an average value of the oscillator parameter b (same for all states) may not be good for making detailed calculations with HF wave functions. However, the basic characteristics indicate that care must be exercised while treating the particle-hole types of problems.

IV.5 Results for Single Oscillator Configuration Approximation

In this approximation, we have calculated the binding energies of ^4He , ^{12}C , ^{16}O and ^{40}Ca . In the case when HF wave functions are replaced by pure oscillator wave functions, the binding energies of doubly closed LS-shell nuclei (^4He , ^{16}O , ^{40}Ca) are calculated using expression (5.73). Weight-factors for ^{16}O and ^{40}Ca are given in Tables (IV.34 - IV.35). ^{12}C has a partially filled p-shell and we have used the following approximation to calculate its potential energy.

$$\text{P.E.}({}^{12}\text{C}) = W(1s, 1s) + \frac{2}{3} [W(1s, 1p) + W(1p, 1p)] , \quad (4.6)$$

where $W(\alpha, \beta)$ gives the contribution to potential energy arising from interaction of nucleons in the states α and β . Binding energy results for these nuclei are presented in Table IV.36

Table IV.34

Weight-factors for $^{16}\text{O}_8$. We have used the notation $2T+1, 2S+1 \ \ell_j(n\ell NL)$ for relative states.

State	Weight-factor
$^{13}\text{S}_1(0000)$	3
$^{31}\text{S}_0(0000)$	3
$^{13}\text{S}_1(0001)$	9
$^{31}\text{S}_0(0001)$	9
$^{13}\text{S}_1(0010)$	9
$^{13}\text{S}_1(0002)$	9
$^{31}\text{S}_0(0010)$	9
$^{31}\text{S}_0(0002)$	9
$^{11}\text{P}_1(010L)$	6
$^{33}\text{P}_0(010L)$	6
$^{33}\text{P}_1(010L)$	18
$^{33}\text{P}_2(010L)$	30
$^{13}\text{D}_1(0200)$	1.5
$^{13}\text{D}_2(0200)$	2.5
$^{13}\text{D}_3(0200)$	3.5
$^{31}\text{D}_2(0200)$	7.5
$^{13}\text{S}_1(1000)$	1.5
$^{31}\text{S}_0(1000)$	1.5

Table IV.35

Weight-factors for $^{40}\text{Ca}_{20}$. Notation used is same as in Table IV.34. Weight-factors for $^{31}\text{S}_0$ states are same as those for $^{13}\text{S}_1$ states.

State	Weight-factor	State	Weight-factor
$^{13}\text{S}_1(0000)$	3	$^{33}\text{P}_1(0101)$	27
$^{13}\text{S}_1(0001)$	9	$^{33}\text{P}_2(0101)$	45
$^{13}\text{S}_1(0002)$	15	$^{11}\text{P}_1(0102)$	7.75
$^{13}\text{S}_1(0010)$	3.0	$^{33}\text{P}_0(0102)$	7.75
$^{13}\text{S}_1(0011)$	6.75	$^{33}\text{P}_1(0102)$	26.25
$^{13}\text{S}_1(0003)$	15.75	$^{33}\text{P}_2(0102)$	43.75
$^{13}\text{S}_1(0020)$	1.125	$^{11}\text{P}_1(0110)$	1.75
$^{13}\text{S}_1(0012)$	5.62	$^{33}\text{P}_0(0110)$	1.75
$^{13}\text{S}_1(0004)$	10.13	$^{33}\text{P}_1(0110)$	5.25
$^{13}\text{S}_1(1000)$	3.0	$^{33}\text{P}_2(0110)$	8.75
$^{13}\text{S}_1(1001)$	5.25	$^{11}\text{P}_1(0111)$	2.25
$^{13}\text{S}_1(1010)$	1.75	$^{33}\text{P}_0(0111)$	2.25
$^{13}\text{S}_1(1002)$	3.13	$^{33}\text{P}_1(0111)$	6.75
$^{13}\text{S}_1(2000)$	11.12	$^{33}\text{P}_2(0111)$	11.25
$^{11}\text{P}_1(0100)$	3	$^{11}\text{P}_1(0103)$	5.25
$^{33}\text{P}_0(0100)$	3	$^{33}\text{P}_0(0103)$	5.25
$^{33}\text{P}_1(0100)$	9	$^{33}\text{P}_1(0103)$	10.75
$^{33}\text{P}_2(0100)$	15	$^{33}\text{P}_2(0103)$	26.25
$^{11}\text{P}_1(0101)$	9	$^{11}\text{P}_1(1100)$	2.25
$^{33}\text{P}_0(0101)$	9	$^{33}\text{P}_0(1100)$	12.25

Contd.

Table IV.35 (Contd.)

State	Weight-factor	State	Weight-factor
$^3\text{P}_1(1100)$	6.75	$^1\text{D}_3(0210)$	1.46
$^3\text{P}_2(1100)$	11.25	$^3\text{D}_2(0210)$	3.13
$^1\text{P}_1(1101)$	2.25	$^1\text{D}_1(1200)$	1.12
$^3\text{P}_1(1101)$	2.25	$^1\text{D}_2(1200)$	1.38
$^3\text{P}_1(1101)$	6.75	$^1\text{D}_3(1200)$	2.62
$^3\text{P}_2(1101)$	11.25	$^3\text{D}_2(1200)$	5.62
$^1\text{D}_1(0200)$	5	$^1\text{P}_3(0300)$	5.25
$^1\text{D}_2(0200)$	5	$^3\text{P}_2(0300)$	11.25
$^1\text{D}_3(0200)$	7	$^3\text{P}_3(0300)$	15.75
$^3\text{D}_2(0200)$	15	$^3\text{P}_4(0300)$	20.25
$^1\text{D}_1(0201)$	5.25	$^1\text{P}_3(0301)$	5.25
$^1\text{D}_2(0201)$	8.75	$^3\text{D}_2(0301)$	11.25
$^1\text{D}_3(0201)$	12.24	$^3\text{P}_3(0301)$	15.75
$^3\text{D}_2(0201)$	26.24	$^3\text{D}_4(0301)$	20.25
$^1\text{D}_1(0202)$	5.08	$^1\text{D}_3(0400)$	2.63
$^1\text{D}_2(0202)$	5.13	$^1\text{D}_4(0400)$	3.32
$^1\text{D}_3(0202)$	7.20	$^1\text{G}_5(0400)$	4.13
$^3\text{D}_2(0202)$	15.42	$^3\text{D}_4(0400)$	10.13
$^1\text{D}_1(0210)$	0.62		
$^1\text{D}_2(0210)$	1.04		

Table IV.36

Binding energy per particle of various nuclei
 obtained in the single oscillator
 configuration approximation.

Interaction	Sussex			Yale
Nucleus	${}^4\text{He}_2$	${}^{12}\text{C}_6$	${}^{16}\text{O}_8$	${}^{40}\text{Ca}$
b(F)	1.4	1.8	1.8	2.0
B.E./A (MeV)	0.33	-3.72	-4.17	-7.30
				-3.14

for the values of b which give r.m.s. radius close to experimental values. Results obtained with effective Yale interaction are also given in this table. In the binding energy calculation of ^{40}Ca with Sussex interaction and for $b = 2.0\text{F}$ we find that contributions to potential energy of S, P, D and F states are 93.4%, 0.69%, 5.3% and 0.55% respectively. The G-state contributes almost negligibly. P-state matrix elements are large but they tend to cancel each others contribution to potential energy. On the other hand, although F-state relative matrix elements are relatively smaller, they occur with large weight-factors and make a net contribution to potential energy comparable to that of P states. Thus, in any precise calculations F-state should be included while G-state can be neglected.

Single particle neutron and proton energies of ^{16}O obtained with Sussex and Yale interaction are given in Table IV.37 (see Section III.9 for formulae used). It is seen that Sussex levels are more spread out for smaller values of b . Single particle neutron energies for ^{40}Ca are given in Table IV.38 along with the experimental values. On comparing these energies with self-consistent HF single particles energies (see Table IV.23), it is seen that the effect of self-consistency on the single particle levels is to increase the binding of the occupied states. Same conclusion can be drawn on comparing the ^{16}O levels given in Table IV.37 with those given earlier (see Tables IV.1 and IV.19).

Table IV.37
Single particle energy levels of $^{16}\text{O}_8$

Single particle state energies (MeV)	SUSSEX			YALE			Experimental proton ^a neutron ^b
	b = 1.8 F	b = 1.5 F	b = 1.76 F	proton	neutron	proton	
1s _{1/2}	-34.09	-39.36	-48.42	-54.74	-33.87	-39.26	-34 ± 3.5 -44 ± 2 -33-51
1p _{3/2}	-13.58	-18.45	-19.91	-25.76	-11.84	-16.82	-13 ± 2.5 -19 ± 1 -21.81
0p _{1/2}	-10.00	-14.87	-11.63	-17.47	-7.56	-12.54	-13 ± 2 -12.4 ± 1.0 -15.65
1d _{5/2}	4.31	-0.66	-15.29	9.33	8.12	3.04	
2s _{1/2} -1d _{5/2}	0.90	0.67	-5.29	-5.57	2.58	2.34	0.87
1d _{3/2} -1d _{5/2}	4.78	4.79	0.33	0.34	5.73	5.74	5.08

a. Liou et. al. (Riu 65)

b. Cohen et. al. (Coh 63a, 63b)

Table IV.38

Neutron single particle energy levels of $^{40}\text{Ca}_{20}$
for $b = 2.0$ F.

single particle state	SUSSEX (MeV)	Experimental ^a
$1d_{\frac{5}{2}}$	-21.8	-21.9
$2s_{\frac{1}{2}}$	-21.0	-18.2
$1d_{\frac{3}{2}}$	-16.85	-15.6
$1f_{\frac{7}{2}}$	- 5.06	- 8.4
$2p_{\frac{3}{2}}$	- 6.03	- 6.3
$1f_{\frac{5}{2}}$	- 6.99	- 4.3
$2p_{\frac{1}{2}}$	- 3.87	- 2.9

a. Elton et. al. (Eln. 67)

On comparing the single oscillator configuration approximation results with those obtained in HF calculations, we find that the approximation of using pure oscillator wave functions is not too bad as far as the estimation of binding energies and single particle energies are concerned.

CHAPTER V

CONFIGURATION MIXING CALCULATIONS WITH
HARTREE-FOCK WAVE FUNCTIONSV.1 Details of the Calculations

In this Chapter we shall describe the results of configuration mixing calculations, with Hartree-Fock (HF) wave functions, carried out in the spirit of a standard shell model spectroscopy calculation for the nuclei ^{18}O , ^{18}F and ^{10}Be . The main assumption of the shell model is that the nucleons move independently of each other in an average potential well, commonly taken to be of harmonic oscillator or Woods-Saxon type. The more fundamental way of obtaining the average potential field of the shell model, starting from free nucleon-nucleon interaction, is the HF method. We have seen in Chapter IV that the HF orbitals for the occupied levels of low-mass nuclei can be well approximated by pure oscillator wave functions but the two differ appreciably for the unoccupied levels. Since the HF orbitals are obtained in a more fundamental way, one would be tempted to believe that they should be closer to the true single nucleon wave functions compared to the pure oscillator wave functions. The single particle wave functions and energies used in our calculations have been obtained by solving the HF equations self-consistently as described in Chapters III and IV. Each unknown HF single particle orbital Ψ_α is expanded in terms of pure oscillator wave functions

$$\Psi_\alpha = \sum_\mu c_\mu^\alpha \varphi_\mu . \quad (5.1)$$

Here α and μ specify the angular and isospin quantum numbers of the Hartree-Fock (HF) and harmonic oscillator (HO) single particle states: $\alpha = (aljm\tau)$, $\mu = (nljm\tau)$, where a and n are radial quantum numbers. The HF field is constrained to be spherically symmetric (see Chapter III), and also the forces are assumed to be charge independent so that the summation in equation (5.1) is restricted only to the radial quantum number n . Three oscillator states of $n = 1, 2$ and 3 major shells are used in each expansion. Thus, equation (5.1) becomes,

$$\Psi_\alpha = \sum_{n=1}^N c_\alpha^\mu \varphi_\mu$$

or $\Psi_{aljm\tau} = \sum_{n=1}^3 c_n^a(lj) \varphi_{nljm\tau}$ (5.2)

In a spherical field the angular parts of the single particle wave functions are the vector spherical harmonics $Y_{l\frac{1}{2}j}^m$, defined in equation (2.14) and thus, more explicitly, the wave functions Ψ and φ can be written as

$$\Psi_{aljm\tau} = R_{alj}^{\text{HF}}(r) Y_{l\frac{1}{2}j}^m(\hat{r}) \chi_{\frac{1}{2}}^\tau$$

$$\text{and } \varphi_{nljm\tau} = R_{nlj}^{\text{HO}}(r) Y_{l\frac{1}{2}j}^m(\hat{r}) \chi_{\frac{1}{2}}^\tau, \quad (5.3)$$

where R and χ specify the radial (see expression 3.19) and isospin parts of the wave functions respectively. Using

expressions (5.3), equation (5.2) can be rewritten as,

$$R_{a\ell j}^{\text{HF}} = \sum_{n=1}^3 c_n^a(\ell j) R_{n\ell j}^{\text{HO}}. \quad (5.4)$$

The low-lying excited states of ^{18}O , ^{18}F and ^{10}Be are obtained under the assumption that the last two nucleons move in a HF field and interact with each other through some residual interaction. The remaining ($A-2$) nucleons take part only in producing the average field. The energy levels are obtained by constructing and diagonalizing a Hamiltonian matrix, including all the degenerate configurations having the lowest possible energies. The matrix elements are $\langle \alpha\beta J\tau | V | \gamma\delta J\tau \rangle$, where $\alpha, \beta, \gamma, \delta$ specify the HF single particle states. These matrix elements are evaluated analytically using expansion (5.2),

$$\langle \alpha\beta J\tau | V | \gamma\delta J\tau \rangle_{\text{HF}} = \sum_{\mu_1 \mu_2 \mu'_1 \mu'_2} c_{\alpha}^{\mu_1} c_{\beta}^{\mu_2} c_{\gamma}^{\mu'_1} c_{\delta}^{\mu'_2} \langle \mu_1 \mu_2 J\tau | V | \mu'_1 \mu'_2 J\tau \rangle_{\text{HO}}. \quad (5.5)$$

Writing explicitly,

$$\begin{aligned} & \langle a_1 \ell_1 j_1, a_2 \ell_2 j_2: J\tau | V | a'_1 \ell'_1 j'_1, a'_2 \ell'_2 j'_2: J\tau \rangle_{\text{HF}} \\ &= \sum_{n_1 n_2 n'_1 n'_2} c_{a_1}^{n_1}(\ell_1 j_1) c_{a_2}^{n_2}(\ell_2 j_2) c_{a'_1}^{n'_1}(\ell'_1 j'_1) c_{a'_2}^{n'_2}(\ell'_2 j'_2) \times \\ & \times \langle n_1 \ell_1 j_1, n_2 \ell_2 j_2: J\tau | V | n'_1 \ell'_1 j'_1, n'_2 \ell'_2 j'_2: J\tau \rangle_{\text{HO}}. \quad (5.6) \end{aligned}$$

Thus, each of the HF matrix element is expressed as a sum of several two-body matrix elements in harmonic oscillator basis with proper weight-factors (products of different C-coefficients). There are eighty-one terms to be summed in equation (5.6) when 3 states are used in expansion (5.2). The expansion coefficients are obtained self-consistently and the results have already been presented in Chapter IV. The two-body matrix elements of the interaction in harmonic oscillator basis have been calculated using equation (3.26). A maximum of relative $\ell = 2$ states has been used in our calculations. Single particle energies are added to the diagonal terms. We have carried out the calculations with both the HF single particle energies calculated in Chapter IV, and the experimental single particle energies. The latter approach has been followed by most of the authors (Kuo 66; Clt 68). It has got the advantage that it takes into account the interaction of the last two neutrons with the closed core to all orders, but the disadvantage is that it may obscure the shortcomings of our calculations which might be obvious otherwise.

The following two nucleon-nucleon interactions have been used in our calculation:

- (i) Effective Yale interaction (see Section II.2)
- (ii) Sussex interaction (see Section II.3)

The prescription used to obtain the effective Yale interaction from the Yale potential (Shn 67a), and the matrix elements of the Sussex interaction (Elt 68a) in an oscillator basis

directly from experimental phase shift data has been described in Chapter II.

In an ideal case, the shell model calculations should be carried out in an infinite dimensional configuration space when the free nucleon-nucleon interaction is used as residual interaction. This is, however, not practicable and the shell model calculations can only be carried out in a limited configuration space. The neglected shells renormalize the interaction in the space of the shells considered in one's calculation. The problem is then to find out an effective interaction which would give the same results, when used in a limited configuration space, as the true interaction would give in an infinite dimensional configuration space. Several authors have worked in this direction of establishing a relationship between free nucleon-nucleon interaction and effective interaction. We mention here the work of Kuo and Brown (Kuo 66, 67) dealing with Hamada-Johnston (HJ) potential, and of Clement and Baranger (Clt 68) dealing with Tabakin potential. In their calculations of ^{18}F and ^{18}O , these authors find that there are two important corrections arising from neglected configurations to the free nucleon-nucleon interaction. First is the second Born correction in the matrix elements of triplet even tensor force. These are the corrections arising from the excitation of two valence nucleons to intermediate states of very high-energy. These corrections mainly affect the $\tau = 0$ matrix elements. In deriving the effective Yale interaction from the Yale potential,

Shakin et. al. (Shm 67a) have calculated the second-order Born corrections by combining Moszkowski-Scott separation technique and Kuo and Brown method (Kuo 66) of taking intermediate states as plane waves and angle averaged Pauli operator. No such corrections are included in Sussex interaction.

The second important correction arises due to the excitation of the particles from ^{16}O core to the intermediate states, which lie close in energy to those included explicitly in the diagonalization. Such corrections are known as core-polarization effects. Kuo and Brown, and Clement and Baranger have calculated the admixture of 3p-1h (three particle-one hole) states to the usual 2p state by using second-order perturbation theory in harmonic oscillator basis. They find that these corrections, although relatively smaller than the Born correction, are quite important for $\mathcal{T} = 1$ states particularly for $J = 0^+$ states. $\mathcal{T} = 0$ states are, however, almost unaffected. No such corrections have been included in our calculations for either of the two interactions used.

The configuration space used in our calculations for $A = 18$ nuclei consists of $(1d_{5/2} 2s_{1/2})$ shell model states.

The ground state configuration for both these nuclei is $(1d_{5/2})^2$. The level spectrum that one would observe in ^{18}O is,

$$(1d_{5/2})^2 : J = 0^+, 2^+, 4^+$$

$$(2s_{1/2})^2 : J = 0^+$$

$$(1d_{5/2} 2s_{1/2}) : J = 2^+, 3^+ .$$

All these states have total isospin $\mathcal{T} = 1$. The following $\mathcal{T} = 0$ levels (besides the $\mathcal{T} = 1$ levels mentioned above) would be observed in the case of ^{18}F ,

$$(1d_{5/2})^2 : J = 1^+, 3^+, 5^+$$

$$(2s_{1/2})^2 : J = 1^+$$

$$(1d_{5/2} 2s_{1/2}) : J = 2^+, 3^+ .$$

The $1d_{3/2}$ state, which lies at $\sim 5\text{MeV}$ in ^{17}O , has not been included in our calculations mainly because of computational difficulties. The HF single particle parameters used in our calculations of ^{18}O should have been obtained from self-consistent HF calculations for ^{17}O . The observed ground state spin of ^{17}O is $J = \frac{5}{2}^+$. The HF method described in Chapter III would only describe an intrinsic state of ^{17}O and the ground state with spin $J = \frac{5}{2}^+$ can be obtained by projecting out good angular momentum states. To avoid such complexities, we decided to take single particle parameters from self-consistent HF calculations for ^{16}O or ^{18}O . The spherical HF calculations give the $J = 0^+$ ground state of these nuclei. In taking the single particle parameters from ^{16}O HF calculations the contributions of the interaction of outer two neutrons with the closed core to the self-consistent average field and wave functions are missed. In ^{18}O HF calculations, part of the interaction between the last two neutrons is already included in the calculation of self-consistent field and thus, the residual interaction left over is not just the free nucleon-nucleon interaction but gets modified. However, we think that these

101

corrections would be small and average self-consistent field would not be very different for ^{16}O , ^{17}O and ^{18}O . In all our calculations the last two neutrons in ^{18}O , and one neutron and one proton in ^{18}F have been treated on equal footing. It is assumed that the self-consistent field is the same for neutron and proton so that same wave functions (neutron wave functions) describe the motion of both the particles outside the closed core. This is, however, not a very serious restriction as we have seen in Chapter IV that coulomb force has little effects on the single particle HF wave functions of light nuclei.

The configuration space used for the calculations of ^{10}Be levels consists of $1p_{3/2}$ and $1p_{1/2}$ shell model states. The ground state configuration for this nucleus is $(1p_{3/2})^2$. All low-lying levels of ^{10}Be would have $\tau = 1$ and the following spectrum would be observed,

$$(1p_{3/2})^2 : J = 0^+, 2^+$$

$$(1p_{3/2} 1p_{1/2}) : J = 1^+, 2^+$$

$$(1p_{1/2})^2 : J = 0^+.$$

V.2 Results and Discussion

Results of our calculations obtained with effective Yale interaction are shown in Figures (V.1 - V.2) for ^{18}O and ^{18}F respectively. In these figures, YA and YB refer to calculations done with single particle wave functions obtained from HF calculations for ^{16}O without coulomb and centre-of-mass

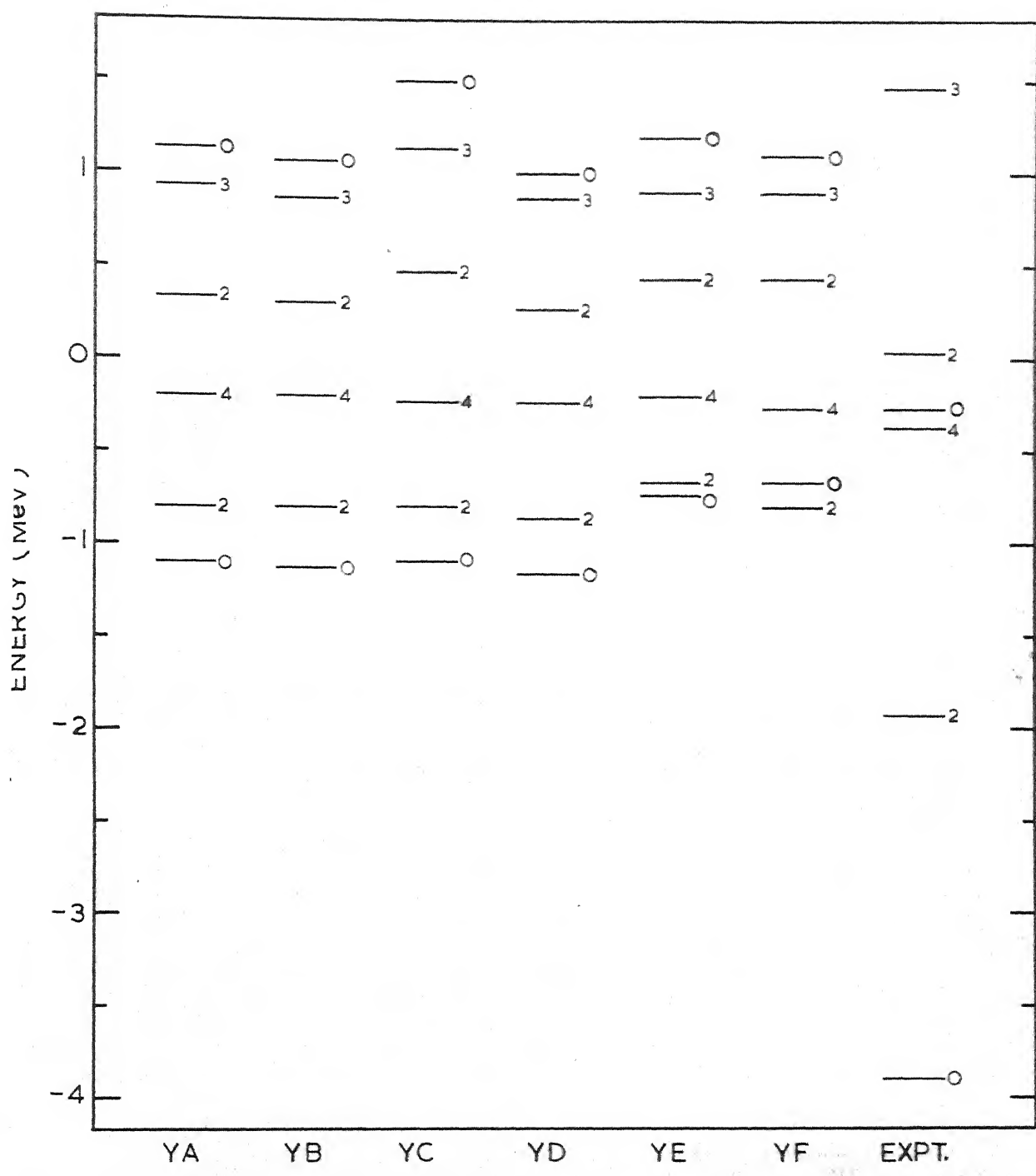


FIG. V.1 Positive parity states of ^{18}O obtained with effective Yale interaction and HF wave functions. All states have $\tau = 1$.

ENERGY (MeV)

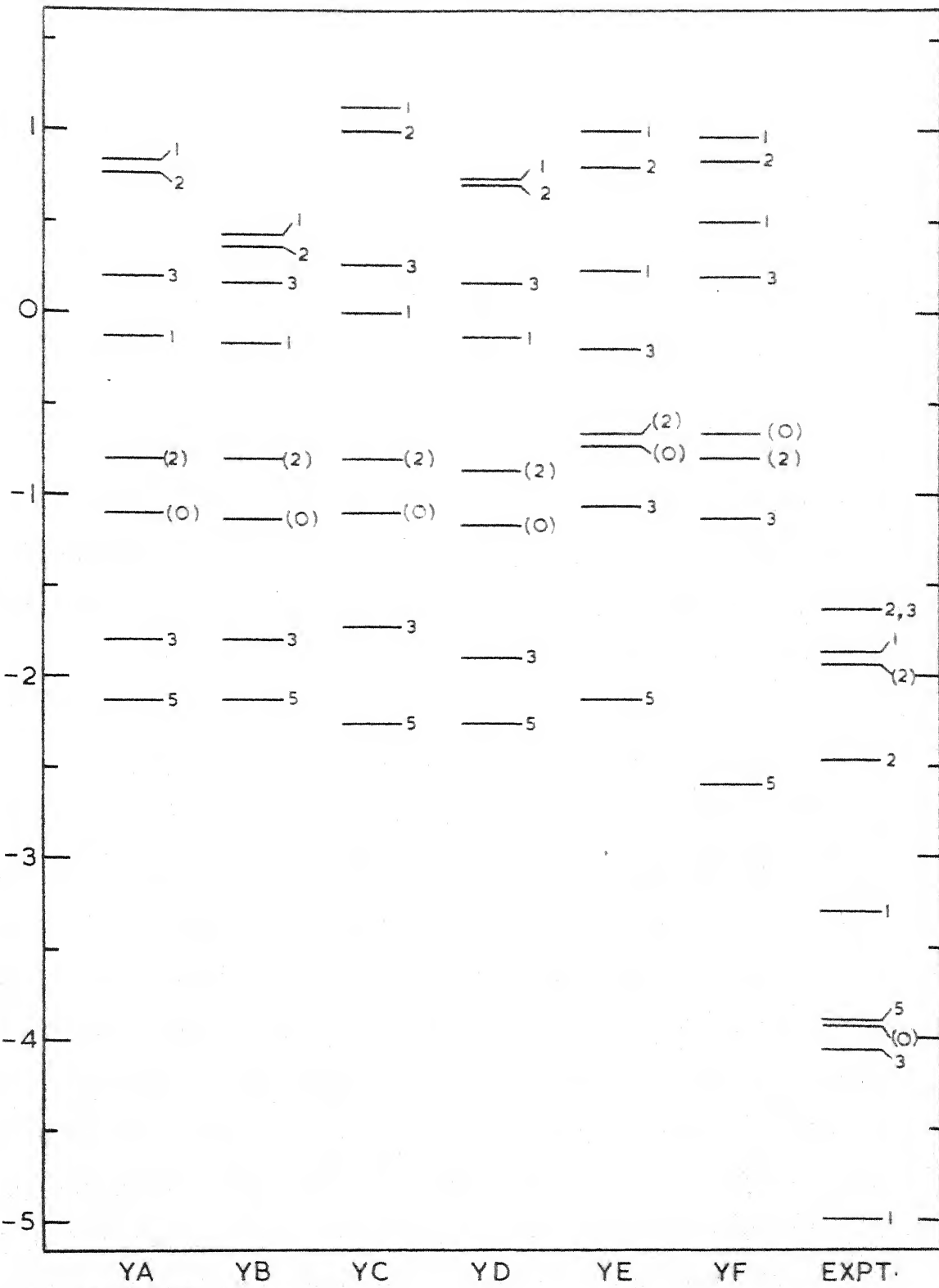


FIG. V.2 Positive parity states of ^{18}F obtained with effective Yale interaction and HF wave functions. Levels with $T = 1$ are specified with bracketed spin. All other levels have $T = 0$.

corrections, and using HF and experimental single particle energies respectively (see Tables IV.11(b) and IV.5). Cases YC and YD refer to calculations done using uncorrected (without coulomb and centre-of-mass corrections) HF wave functions for $^{18}_0$ and with HF and experimental single particle energies respectively (see Tables IV.13(a) and IV.5). Cases YE and YF refer to calculations done using experimental single particle energies, and wave functions obtained from HF calculations with coulomb and centre-of-mass corrections for the nuclei $^{16}_0$ and $^{18}_0$ respectively (see Tables IV. 11(a) and IV.13(a)). All calculations with effective Yale interaction have been carried out for $b = 2.09F$ since for this value of b ($=\sqrt{\hbar/m_A\omega}$) we could obtain minimum total energy for $^{16}_0$ in self-consistent HF calculations (see Figure IV.1). For consistency, calculations for Sussex interaction have been done for $b = 2.0F$. The experimental single particle energy difference between $1d_{5/2}$ and $2s_{1/2}$ state was taken to be 0.87 MeV, as obtained from experimental levels of $^{17}_0$. This is not justified for $^{18}_F$ for which an average of the neutron and proton single particle energies for $2s_{1/2}$ states should be taken. However, the discrepancy would be small. The experimental levels for $^{18}_0$ and $^{18}_F$, shown in Figures V.1 and V.2, have been taken from references (Hea 64) and (Poi 65) respectively. The absolute ground state energies are determined as follows. Using the binding energy data of Koenig et. al. (Kog 62), the ground state energies of valence nucleons are taken to be

$$-B.E.(^{18}O) - B.E.(^{16}O) + 2 B.E.(^{17}O) = -3.90 \text{ MeV for } ^{18}O$$

and

$$-B.E.(^{18}F) - B.E.(^{16}O) + B.E.(^{17}O) + B.E.(^{17}F) = -5.00 \text{ MeV}$$

for ^{18}F .

As seen from the figures, except for the $4^+ (\mathcal{T}=1)$ states the calculated levels are in very poor agreement with experimental results in all the cases. In particular, the observed ground state of ^{18}F is a 1^+ state whereas in all our calculations we get 5^+ state as lowest state and first 1^+ state lies much higher. However, the fact that very similar results are obtained in various cases supports our assumption that HF field, if constrained to remain spherically symmetric, would not be very different for ^{16}O , ^{17}O and ^{18}O . Results obtained with effective Yale interaction using pure oscillator wave functions and experimental single particle energies are shown in Figures (V.3 - V.4) for $\mathcal{T}=1$ and $\mathcal{T}=0$ states respectively. In these figures, HO1 and HO2 refer to calculations done with harmonic oscillator (HO) wave functions in configuration space consisting of $(1d_{5/2} 2s_{1/2})$ and $(1d_{5/2} 2s_{1/2} 1d_{3/2})$ states respectively. The importance of including the $1d_{3/2}$ configuration is obvious from the figures. It lowers the $\mathcal{T}=1$ levels, thereby improving the agreement with experiments and also the first 1^+ level in ^{18}F is pushed below the lowest 5^+ state. In Figures (V.3 - V.4), we also compare the calculated $\mathcal{T}=1$ and $\mathcal{T}=0$ levels obtained with HF wave functions in case YB with the results of Kuo and Brown (referred to as KB), and Clement and Baranger (referred to as

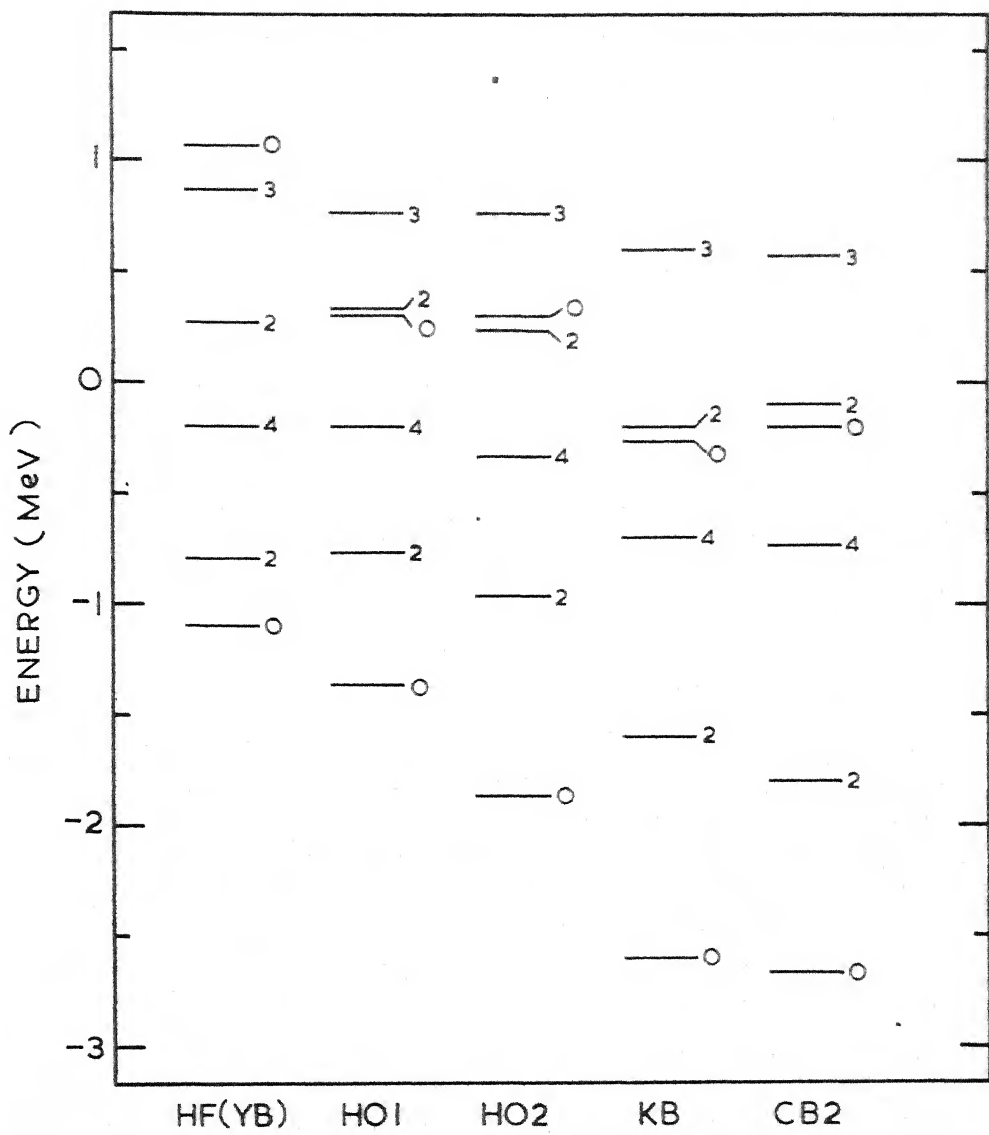


FIG. V.3 Comparison of calculated HF and HO positive parity ($\tau = 1$) levels of $^{18}_0$ for effective Yale interaction with the results of Kuo and Brown (KB), and Clement and Baranger (results with second-order Born correction are referred to as CB2).

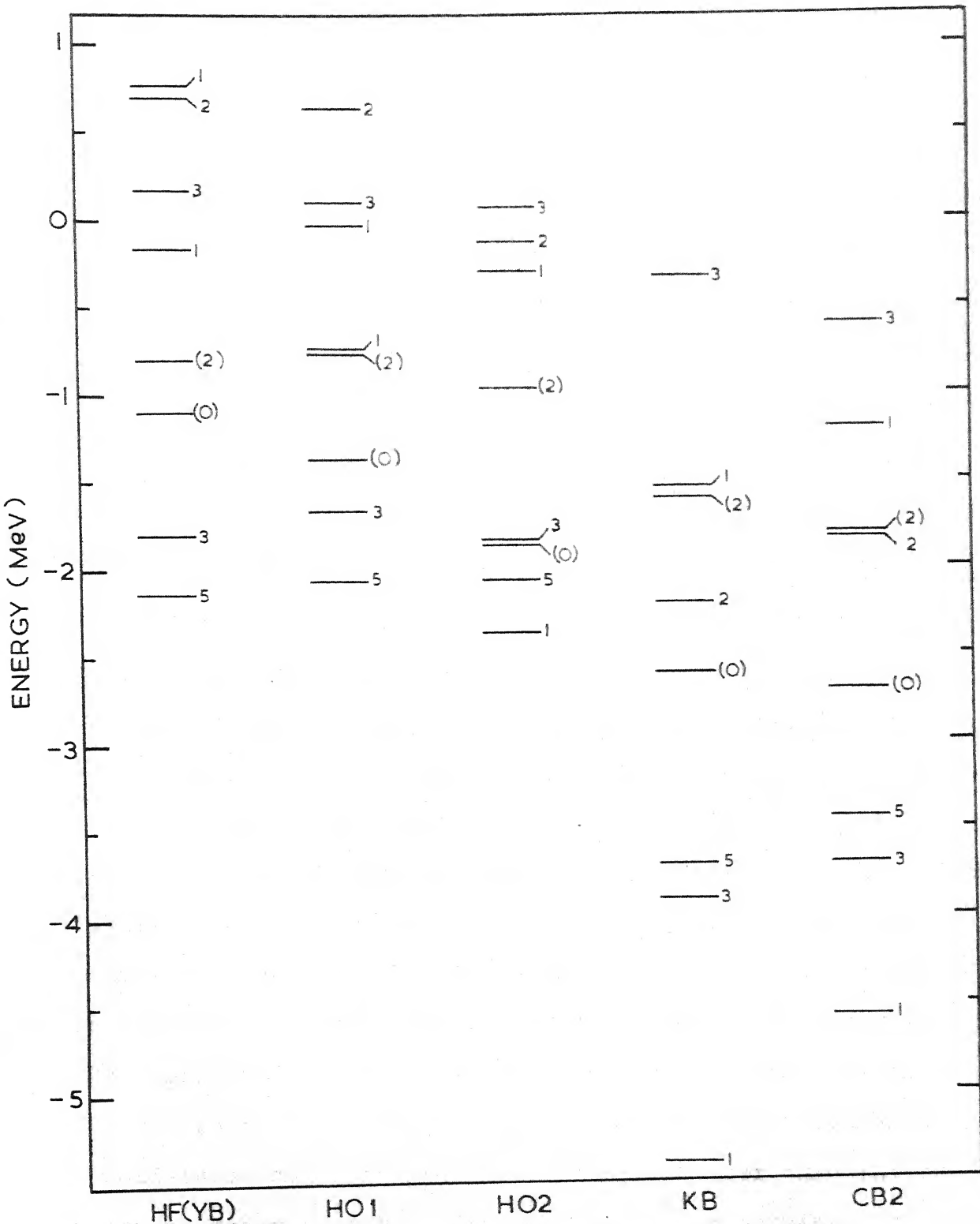


FIG. V. 4 Comparison of calculated HF and HO positive parity levels of ^{18}F for effective Yale interaction with the results of Kuo and Brown (KB), and Clement and Baranger (CB2). Levels with bracketed spin have $\tau = 1$. All other levels have $\tau = 0$.

CB2 when second-order Born term is included). Both these calculations were done in a configuration space consisting of ($1d_{5/2}$ $2s_{1/2}$ $1d_{3/2}$) harmonic oscillator states and using experimental single particle energies. KB and CB2 levels shown here include the contribution of second-order Born term but not the core-polarization effects. On comparing the HF spectrum obtained in case YB and the HOI spectrum (see Figures V.3 - V.4) we find that, other parameters being held fixed, HF and HO wave functions do not give very different results.

In Tables V.1 and V.2, we present the calculated two-body HO and HF matrix elements in the s-d shell obtained in various cases. Results of several other calculations are also given for comparison. Federman (Fen 65) and Arima (Ara 68) $\mathcal{T}=1$ matrix elements have been obtained from best fit to experimental levels of ^{18}O . Arima $\mathcal{T}=0$ matrix elements are obtained from best fit to experimental levels of ^{18}O , ^{18}F and ^{18}Ne . The values obtained in two different cases, first when all but the 1.7MeV , 1^+ state in ^{18}F were included from the fit and second when this state was also included are referred to as A1 and A2 in Table V.2. It can be seen that no impressive agreement of the calculated HF matrix elements exists with any one of these calculations. In particular, the $J=0^+$ HF matrix elements are considerably smaller than the results of other calculations. However, Federman-Talmi (FT) and Arima have obtained positive values for $J=3^+$ and 4^+ ($\mathcal{T}=1$) matrix elements. In our calculations, $J=3^+$ ($\mathcal{T}=1$) HF matrix element is always positive although much smaller in magnitude.

Table V.1

$\mathcal{T} = 1$, Two-body matrix elements in the s-d shell.
All numbers are in MeV.

Configuration J	Present Work (Yale)			HO	KB (IJ)	CB2 (Tabakin)	FT	Arime
	YA	YC	YE					
$\frac{5}{2}\frac{5}{2}$	0	-0.85	-0.87	-0.62	-0.58	-1.17	-1.47	-3.24
$\frac{5}{2}\frac{3}{2}$	2	-0.58	-0.62	-0.57	-0.69	-0.57	-1.02	-1.59
$\frac{5}{2}\frac{1}{2}$	4	-0.21	-0.23	-0.21	-0.25	-0.21	-0.39	$\angle 1$ MeV 0.03 0.02
$\frac{5}{2}\frac{1}{2}$	2	-0.45	-0.46	-0.34	-0.35	-0.43	-0.52	$\angle 1$ MeV -0.48 -0.69
$\frac{5}{2}\frac{1}{2}$	0	-0.72	-0.73	-0.43	-0.39	-0.56	-0.76	-0.77 -0.93
$\frac{5}{2}\frac{1}{2}$	2	-0.82	-0.85	-0.56	-0.75	-1.04	-1.27	-0.76 -0.81
$\frac{1}{2}\frac{1}{2}$	3	0.005	0.0005	0.02	0.03	-0.09	$\angle 1$ MeV 0.72 1.00	
$\frac{1}{2}\frac{1}{2}$	$\frac{1}{2}$	0	-0.96	-1.02	-0.65	-0.67	-1.64	-2.23 -2.30 -1.97 -2.07

Table V.2

$\mathcal{T} = 0$, Two-body matrix elements in the s-d shell.
All numbers are in Mev.

Configuration JJ'	Present Work (Yale)					KB	GB 2	(Tabakin)	Al	A2	Arima
	YA	YC	YE	YF	EO						
$\frac{5}{2} \frac{5}{2}$	$\frac{5}{2} \frac{5}{2}$	1	0.12	0.19	0.37	0.88	-0.22	-0.53	1 MeV	0.01	-4.33
3	-0.50	-0.52	-0.42	-0.44	-0.59	-0.93			0.58	-1.06	
5	-2.13	-2.29	-2.12	-2.60	-2.09	-3.64	-3.46	-4.26	-3.65		
$\frac{5}{2} \frac{5}{2}$	$\frac{5}{2} \frac{1}{2}$	3	-0.94	-0.97	-0.64	-0.67	-0.86	-1.41	-1.29	-3.53	-3.64
5	$\frac{5}{2} \frac{1}{2}$	1	-0.42	-0.41	-0.28	-0.24	-0.29	-0.45	-4.27	-0.89	
$\frac{5}{2} \frac{1}{2}$	$\frac{5}{2} \frac{1}{2}$	2	-0.16	-0.14	-0.08	-0.04	-0.22		-3.70	-2.87	
3	-2.02	-2.11	-1.34	-1.34	-1.83	-3.36	-3.43	-2.60	-2.13		
$\frac{1}{2} \frac{1}{2}$	$\frac{1}{2} \frac{1}{2}$	1	-1.25	-1.32	-0.93	-0.95	-2.32	-3.94	-3.44	-3.67	-4.56

The results obtained with Sussex interaction are shown in Figures (V.5 - V.6) for ^{18}O and ^{18}F respectively along with the experimental levels. In these figures, SA and SB refer to calculations done using uncorrected HF wave functions for ^{16}O (see Table IV.27(b)), and HF single particle (see Table IV.24) and experimental single particle energies respectively. H01 and H02 are the results obtained with pure oscillator wave functions in a smaller ($1\text{d}_{5/2} 2\text{s}_{1/2}$) and larger ($1\text{d}_{5/2} 2\text{s}_{1/2} 1\text{d}_{3/2}$) configuration space respectively. Clement and Baranger results obtained with bare Tabakin interaction without second-order corrections (referred to as CB1) are also given for comparison. In Table V.3, calculated two-body HF matrix elements for Sussex interaction in the s-d shell have been compared with Clement and Baranger results for Tabakin interaction (CB1).

The calculated energy levels of ^{10}Be for effective Yale interaction are shown in Figure V.7 along with the experimental data. In this figure, XA and XB refer to calculations done using HF wave functions for ^{10}Be (see Table IV.12), and HF single particle (see Table IV.5) and experimental single particle energies respectively. XC is the result of calculation using HF wave functions of ^8Be (see Table IV.9) and experimental single particle energies. Again, H01 and H02 are the results of calculations using oscillator wave functions with experimental single particle energies in configuration space consisting of ($1\text{p}_{3/2} 1\text{p}_{1/2}$) and ($1\text{p}_{3/2} 1\text{p}_{1/2} 1\text{d}_{5/2}$) states respectively. The experimental energy separation between $1\text{p}_{3/2}$ and $1\text{p}_{1/2}$ states was taken

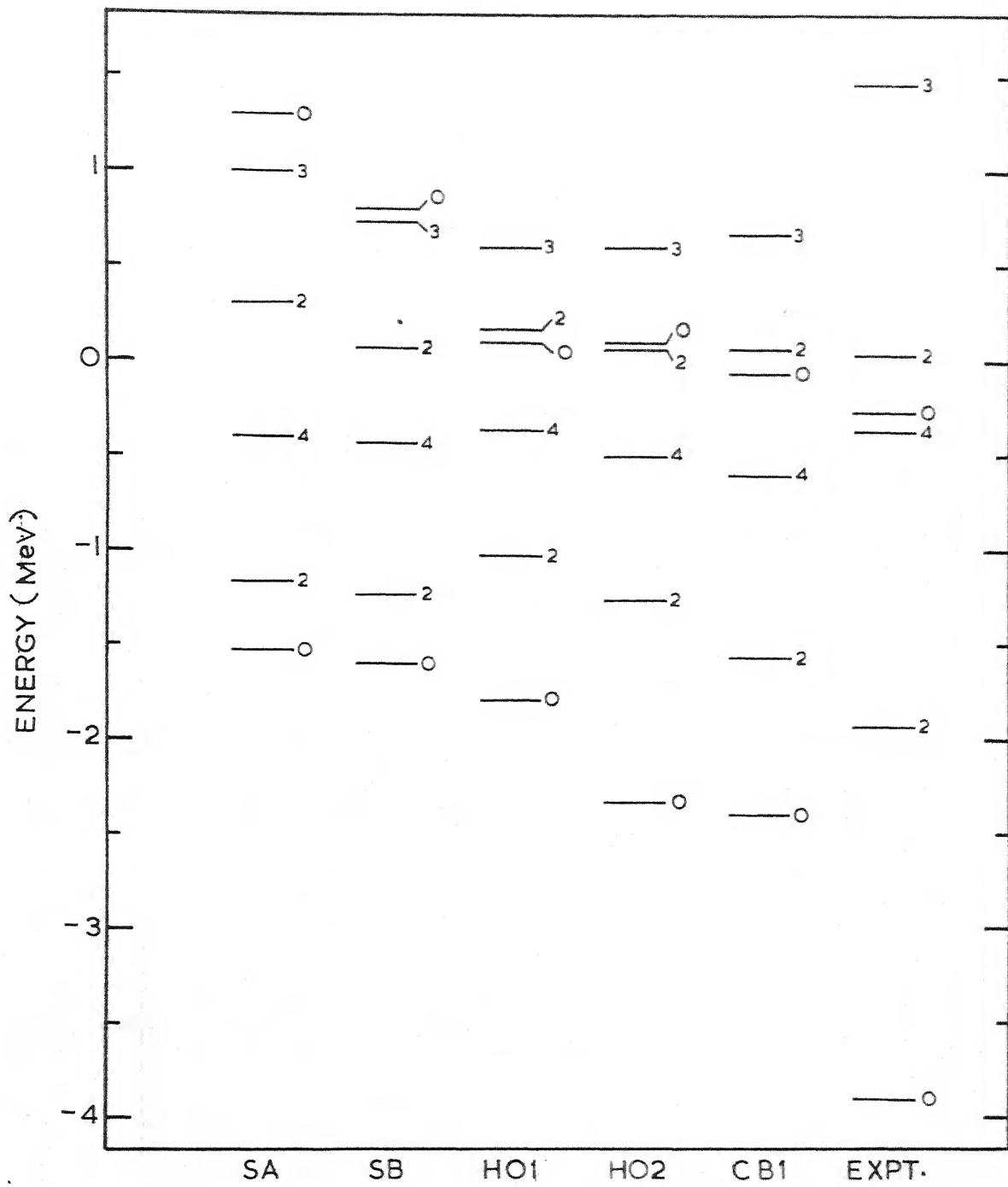


FIG. V.5 Comparison of calculated HF and HO positive parity levels of ^{18}O for Sussex interaction with the results of Clement and Baranger (results without second-order Born correction are referred to as CB1), and experiments. The results of Clement and Baranger (CB1) and experiments.

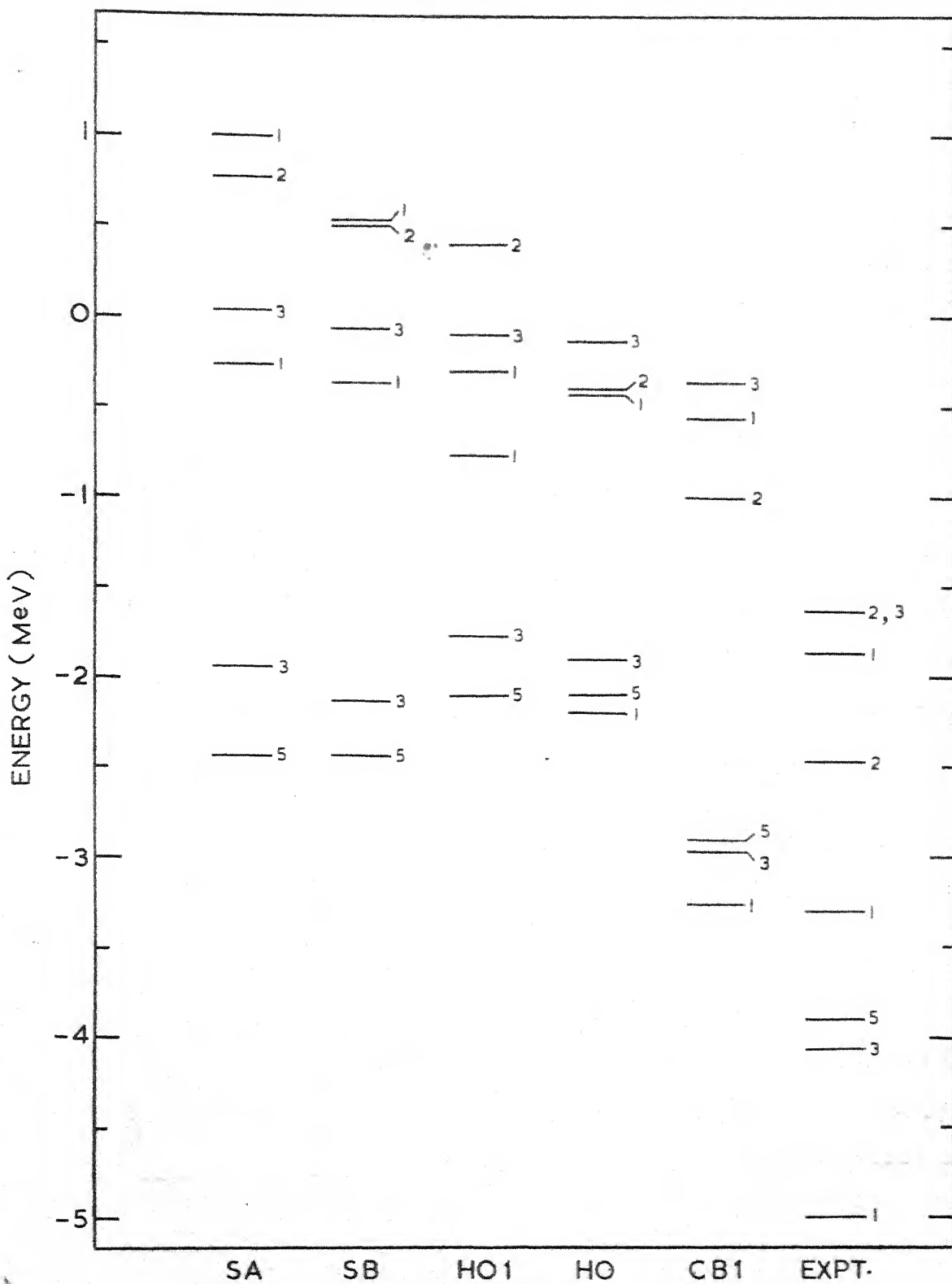


FIG. V.6 Comparison of calculated HF and HO positive parity ($\tau = 0$) levels of ^{18}F for Sussex interaction with the results of Clement and Baranger (CB1), and experiments.

Table V.5

Two-body matrix elements in s-d shell.
All numbers are in MeV.

Configuration				J	T	Present Work (Sussex)		CBI (Tabakin)
						HF	HO	
$\frac{5}{2}^-$	$\frac{5}{2}^-$	$\frac{5}{2}^-$	$\frac{5}{2}^-$	0	1	-1.22	-1.53	-1.00
				2	1	-0.91	-0.80	
				4	1	-0.42	-0.36	
$\frac{5}{2}^-$	$\frac{5}{2}^-$	$\frac{5}{2}^-$	$\frac{1}{2}^+$	2	1	-0.55	-0.49	
$\frac{5}{2}^-$	$\frac{5}{2}^-$	$\frac{1}{2}^+$	$\frac{1}{2}^+$	0	1	-0.37	-0.66	
$\frac{5}{2}^-$	$\frac{1}{2}^+$	$\frac{5}{2}^-$	$\frac{1}{2}^+$	2	1	-1.11	-0.95	-1.06
				3	1	-0.14	-0.25	
$\frac{1}{2}^+$	$\frac{1}{2}^+$	$\frac{1}{2}^+$	$\frac{1}{2}^+$	0	1	-1.33	-1.92	-2.17
$\frac{5}{2}^-$	$\frac{5}{2}^-$	$\frac{5}{2}^-$	$\frac{5}{2}^-$	1	0	-0.12	-0.50	-2.89
				3	0	-0.72	-0.75	
				5	0	-2.45	-2.12	
$\frac{5}{2}^-$	$\frac{5}{2}^-$	$\frac{5}{2}^-$	$\frac{1}{2}^+$	3	0	-0.96	-0.80	-1.10
$\frac{5}{2}^-$	$\frac{5}{2}^-$	$\frac{1}{2}^+$	$\frac{1}{2}^+$	1	0	-0.39	-0.23	
$\frac{5}{2}^-$	$\frac{1}{2}^+$	$\frac{5}{2}^-$	$\frac{1}{2}^+$	2	0	-0.38	-0.47	-2.91
				3	0	-2.35	-1.98	
$\frac{1}{2}^+$	$\frac{1}{2}^+$	$\frac{1}{2}^+$	$\frac{1}{2}^+$	1	0	-1.46	-2.31	-2.71

to be 6MeV. All calculations have been done for $b=2.09F$. We find that the calculated difference between the ground state and first 2^+ state is much less compared to experimental separation. However, the calculated energy separation between the first and the second 2^+ states is 5.89 MeV in case XB compared to experimental separation of 5.9 MeV.

In all our calculations we find that calculated HF spectra are compressed compared to experimental levels. The poor agreement with the experimental results may be due to the nature of the nucleon-nucleon interactions used in our calculations. As seen in Chapter IV, both these interactions give 3-4MeV less binding when used in spherical HF calculations. However, spin-orbit splittings in various nuclei have been satisfactorily reproduced with both these interactions (Shn 67b: Elt 67). Thus, it appears that the spin-orbit part of these interactions is reasonable but the central part is weak. In yet another entirely different approach, Gunye has calculated (Gue 68b, 69) the low-lying states of various odd and even mass light nuclei by projecting out good angular momentum states from an intrinsic deformed HF state. He has carried out the calculations for 2s-1d shell nuclei (Gue 68b) with effective Yale interaction, and for 1p shell nuclei (Gue 69) with both effective Yale and Sussex interactions. In all the cases the projected HF spectra for even mass nuclei are found to be compressed compared to the experimental levels. For example, in the case of ^{18}O , the calculated separation between the ground state

and first 2^+ state is 0.51 MeV compared to the experimental value of 1.93 MeV. The effect of increasing 3S_1 state matrix elements arbitrarily by over 30 percent so as to reproduce the experimental binding energies of various nuclei is to spread out the projected spectra. Since the results obtained by projection method are close to shell model results (Reh 58), the compressed spectrum obtained in the present shell model calculations in HF basis seems to be consistent with the findings of Gunye.

It should be emphasized that the poor agreement of our results with the experimental data does not imply the shortcomings in the HF basis since we have not made any attempt to calculate the important second-order corrections in both the interactions arising from core excitations (besides the Born term for Sussex interaction). To the best of our knowledge, no attempt till now has been made to use self-consistent single particle energies and wave functions obtained with realistic potentials in the shell model calculations. Kuo and Brown (Kuo 66) have calculated single particle energies in ^{17}O with their realistic potential and obtained qualitative agreement with observed energies, but they did not use calculated single particle energies in obtaining the spectra of $A=18$ nuclei. Our calculation is a first step towards a more complete shell model calculation in the HF basis. In fact, it has been shown that low-lying states of ^{18}O are abundant in deformed components (Bron 66; End 65) and the assumption of two nucleons outside

a closed ^{16}O core is not very good. The transition rate from second 0^+ to first 2^+ state is also very large and suggests that these states should be mainly composed of deformed components. However, Kuo and Brown (Kuo 66) have satisfactorily reproduced the energy levels of these states by using simple two particle model with p-h corrections. It is expected that such core excitation corrections will spread apart the calculated $\mathcal{T}=1$ HF spectrum by depressing the lower states and raising the higher levels and thus, the agreement with the experiment would improve. Studies of Kuo and Brown, and Clement and Baranger show that in the harmonic oscillator basis most important of these corrections are 3p-1h corrections arising from excitation energies of $2\hbar\omega$. Contributions of higher levels, which involve excitation energies $>2\hbar\omega$, are relatively unimportant. However, this may not be true in HF basis. Bassichis et. al. (Bas 69) have made explicit calculations for the second-order energies and probabilities of 2p-2h components in the ground state of ^4He and ^{16}O using perturbation theory in HF basis. They find that the relative phases (signs of expansion coefficients) of the HF wave functions of unoccupied states play an important role in deciding the importance of a particular level. It is quite likely that excitations to some of the high-lying levels may be more important than to low-lying levels contrary to the predictions of simple shell-model picture in harmonic oscillator representation. However, no conclusive remarks can be made about the magnitude of such

corrections in HF basis unless explicit calculations are made.

In another calculation carried out for $^{18}_0$ the residual interaction between the last two neutrons in $^{18}_0$ was taken to be of the form $(a + b\vec{\sigma}_1 \cdot \vec{\sigma}_2) \exp(-r^2/r_0^2)$. Two-body matrix elements in the s-d shell were calculated in a basis of HF wave functions and we tried to determine the parameters of the potential which would give a good fit to the experimental energy levels of $^{18}_0$. But no set of parameters could satisfactorily reproduce the experimental levels of $^{18}_0$. Thus, it appears that a simple residual interaction of the form described above is not suitable for a HF basis.

APPENDIX A

The local potential, used in our calculations of single particle energies, is of the following form.

$$V_{\ell j} = - V_N f(r) - \left(\frac{\hbar}{m_e c}\right)^2 \frac{V_{SO}}{a_{SO}} (\vec{\ell} \cdot \vec{\sigma})_j g(r) + Z_A Z_\mu e^2 h(r) + \frac{\hbar^2 \ell(\ell+1)}{2\mu \sigma^2}, \quad (A.1)$$

where

$$f(r) = \left\{ 1 + \exp\left(\frac{r-R_N}{a_N}\right) \right\}^{-1},$$

$$g(r) = \frac{\exp\left(\frac{r-R_{SO}}{a_{SO}}\right) \left\{ 1 + \exp\left(\frac{r-R_{SO}}{a_{SO}}\right) \right\}^{-2}}{r},$$

$$h(r) = \begin{cases} \frac{1}{r} & \text{for } r \geq R_C \\ \frac{1}{2R_C} (3 - \frac{r^2}{R_C^2}) & \text{for } r < R_C, \end{cases} \quad (A.2)$$

V_N = Central nuclear potential,

V_{SO} = Spin-orbit nuclear potential,

$$(\vec{\ell} \cdot \vec{\sigma})_j = \ell_j \quad \text{for } j = \ell + \frac{1}{2} \\ = -(\ell + 1) \quad \text{for } j = \ell - \frac{1}{2} \quad (A.3)$$

(xiiri)

r_x , a_x are the radius and diffuseness parameters of the x^{th} part of the potential and $R_x = r_x A^{1/3}$.

A , Z_A are the core mass and its charge,

μ , Z_μ are the particle reduced mass and its charge.

The radial wave functions $u_{nlj}^L(r)$ are the solutions of the following Schrödinger equation,

$$-\frac{\hbar^2}{2\mu} \frac{d^2}{dr^2} u_{nlj}^L(r) + [V_{lj}(r) - E_{nlj}] u_{nlj}^L(r) = 0 \quad (\text{A.4})$$

The binding energies of the single particle levels are fed in and the strength parameters V_N and V_{SO} are obtained by the method of successive iterations till the values converge.

The wave functions $u_{nlj}^L(r)$ are normalized to unity.

A separable form of the local potential is given by,

$$V(\vec{r})\Psi(\vec{r}) = \int V\left(\frac{\vec{r}+\vec{r}'}{2}\right) H(|\vec{r}-\vec{r}'|)\Psi(\vec{r}') d\vec{r}'. \quad (\text{A.5})$$

$H(|\vec{r}-\vec{r}'|)$ is given the Gaussian form, normalized to unity,

$$H(|\vec{r}-\vec{r}'|) = \pi^{-3/2} a_{nl}^{-3} \exp\left\{-\left(\frac{|\vec{r}-\vec{r}'|}{a_{nl}}\right)^2\right\}, \quad (\text{A.6})$$

where a_{nl} is the non-locality range parameter. An approximate relationship between the wave function u_{nlj}^{NL} , calculated in a potential of the form, given in equation A.5, and the local wave function u_{nlj}^L is given by,

$$u_{nlj}^{NL}(r) = \exp(-a_{nl}^2 V'_j(r)/8) u_{nlj}^L(r), \text{ where}$$

$$V'_j(r) = \frac{2\mu}{\hbar^2} \left[V_N f(r) + \left(\frac{\hbar^2}{m\pi c}\right)^2 \frac{V_{SO}}{a_{SO}} (\vec{l} \cdot \vec{\sigma}) g(r) - Z_A Z_\mu e^2 h(r) \right] \quad (\text{A.7})$$

APPENDIX B

It has been mentioned before that the two-body coulomb and centre-of-mass matrix elements used in the HF calculations with effective Yale interaction were calculated with a maximum relative $\ell=2$ (see Section IV.1). This has caused some error in our calculations since higher ℓ values are also quite important for both of these matrix elements. The new coulomb and centre-of-mass matrix elements in the configuration space consisting of $s_{1/2}$, $p_{3/2}$ and $p_{1/2}$ oscillator states of $n = 1, 2$ and 3 major shells were calculated with maximum relative $\ell=10$. The revised HF results obtained by using these new matrix elements are shown in Table B.1 for the nuclei ^4He , ^8Be , ^{12}C and ^{16}O . On comparing with the older results (see Table IV.1) we find that the effect of truncation at $\ell=2$ on most of the static properties of closed shell nuclei is small. However, the wave functions are affected, mainly in the tail region.

Table B.1

Results of revised HF calculations with effective Yale interaction for various nuclei

	$^4_{\text{He}}\text{2}$	$^8_{\text{Be}}\text{4}$	$^{12}_{\text{C}}\text{6}$	$^{16}_{\text{O}}\text{8}$
$b(F)$	1.76	2.09	2.09	2.09
Single particle energies (MeV)	neutron	proton	neutron	proton
$1s_{1/2}$	-23.03	-22.29	-22.10	-20.71
$1p_{3/2}$	5.48	6.32	-1.22	0.16
$1p_{1/2}$	7.10	7.87	0.65	2.03
$B.b./A$ (MeV)	-3.77	-0.037	-0.037	-1.238
Matter r.m.s. radius (F)	1.775	3.005	2.667	2.519
Orange r.m.s. radius (F)	1.778	3.050	2.686	2.531

APPENDIX C

It is assumed that Sussex interaction V can be broken up into central, spin-orbit and tensor parts which are tensors of rank zero, one and two respectively in the scalar product $(S^{(k)} \cdot v^{(k)})$. Here $S^{(k)}$ refers to the spin variables and $v^{(k)}$ to the orbital motion. Thus, we can write,

$$\begin{aligned}
 V &= \sum_{k=0}^2 (S^{(k)} \cdot v^{(k)}) \\
 &= \sum_{k=0}^2 V(k) \\
 &= V(0) + V(1) + V(2) \tag{C.1}
 \end{aligned}$$

and the matrix elements of $V(k)$ are

$$\begin{aligned}
 \langle n' s \ell' J | V(k) | n s \ell J \rangle &= \langle n' s \ell' J | S^{(k)} \cdot v^{(k)} | n s \ell J \rangle \\
 &= (-1)^{J+S+\ell} \begin{Bmatrix} s & \ell' & J \\ \ell & s & k \end{Bmatrix} \langle s || S^{(k)} || s \rangle \times \\
 &\quad \times \langle n' \ell' || v^{(k)} || n \ell \rangle. \tag{C.2}
 \end{aligned}$$

Summing over k on both the sides we obtain,

$$\begin{aligned}
 \langle n' s \ell' J | V | n s \ell J \rangle &= \sum_k (-1)^{J+S+\ell} \begin{Bmatrix} s & \ell' & J \\ \ell & s & k \end{Bmatrix} \langle s || S^{(k)} || s \rangle \times \\
 &\quad \times \langle n' \ell' || v^{(k)} || n \ell \rangle. \tag{C.3}
 \end{aligned}$$

Multiplying both the sides by $(-1)^{J+S+\ell'} [J][k'] \begin{Bmatrix} s & \ell' & J \\ \ell & s & k \end{Bmatrix}$

and summing over J we get

$$\begin{aligned}
 & \sum_J (-1)^{J+S+\ell'} [J][k'] \begin{Bmatrix} s & \ell' & J \\ \ell & s & k \end{Bmatrix} \langle n' s \ell' J | V | n s \ell J \rangle \\
 &= \sum_{k' \neq k} [J][k] \begin{Bmatrix} s & \ell' & J \\ \ell & s & k \end{Bmatrix} \begin{Bmatrix} s & \ell' & J \\ \ell & s & k' \end{Bmatrix} \times \\
 & \quad \times \langle s \parallel s^{(k)} \parallel s \rangle \langle n' \ell' \parallel v^{(k')} \parallel n \ell \rangle \\
 &= \sum_k \delta_{kk'} \langle s \parallel s^{(k)} \parallel s \rangle \langle n' \ell' \parallel v^{(k)} \parallel n \ell \rangle \\
 &= \langle s \parallel s^{(k')} \parallel s \rangle \langle n' \ell' \parallel v^{(k')} \parallel n \ell \rangle. \quad (C.4)
 \end{aligned}$$

Thus, in equation (C.4) the uncoupled matrix elements of any particular component are expressed as a sum of matrix elements of the total potential V in different channels. The coupled matrix elements of $V(k)$ are obtained by substituting equation (C.4) in equation (C.2).

The off-diagonal matrix elements of the Sussex interaction V , with radial quantum numbers differing by more than one, have been calculated using the following expression, given by Elliott et. al. (Elt 68a),

$$\begin{aligned}
\langle n' | V | n \rangle = & \left\{ 2(n' - n - 1) \langle n' - 1 | V | n \rangle + \sqrt{(n+1)(n+l+\frac{3}{2})} \langle n' - 1 | V | n+1 \rangle \right. \\
& + \sqrt{n(n+l+\frac{1}{2})} \langle n' - 1 | V | n-1 \rangle - \sqrt{(n'-1)(n'-\frac{1}{2}+l)} \times \\
& \left. \times \langle n'-2 | V | n \rangle + \langle n'-1 | [r^2, V] / 2b^2 | n \rangle \right\} \sqrt{n'(n'+l+\frac{1}{2})} . \\
& \quad \quad \quad (C.5)
\end{aligned}$$

The relation (C.5) connects the matrix elements with $n' - n = 2$ to those with $n' - n \leq 1$ and is true for the matrix elements of any general interaction V in an oscillator basis. It is assumed that interaction V is momentum independent so that commutator $[r^2, V]$ vanishes.

REFERENCES

(Abl 66) - Y. Abgrall and G. Monsonego, Nucl. Phys. 75 (1966) 632.

(Ami 64) - U. Amaldi, Jr., G. Campos Venuti, G. Cortellessa, C. Fronterotta, A. Reale, F. Salvadori and P. Hillman, Phys. Rev. Letts. 13 (1964) 341.

(Ani 68) - I. Angeli, J. Csikai and Hunyadi, Phys. Letts. 29B (1968) 36.

(Ara 68) - A. Arima, S. Cohen, R.D. Lawson and M.H. Macfarlane, Nucl. Phys. A108 (1968) 94.

(Bar 63) - H. Baranger, Cargese Lectures in Theoretical Physics (W.A. Benjamin, Inc. New York) 1963.

(Bas 65) - W.H. Bassichis and G. Ripka, Phys. Lett. 15 (1965) 320.

(Bas 67) - W.H. Bassichis, A.K. Kerman and J.P. Svenne, Phys. Rev. 160 (1967) 746.

(Bas 69) - W.H. Bassichis and H.R. Strayer, Phys. Rev. Letts. 23 (1969) 30.

(Bee 57) - H.A. Bethe and J. Goldstone, Proc. Roy. Soc. (London) A238 (1957) 551.

(Bee 63) - H.A. Bethe, B.H. Brandow and A.G. Petscheck, Phys. Rev. 129 (1963) 225.

(Brk 67) - D.H. Brink and E. Bosker, Nucl. Phys. A91 (1967) 1.

(Brl 65) - C. Bressel, A. Kerman and E. Lomon, Bull. Am. Phys. Soc. 10 (1965) 584: C. Bressel, Ph.D. Thesis, M.I.T. (1965).

(Brn 67) - R.A. Bryan and B.L. Scott, Phys. Rev. 164 (1967) 1215: R.A. Bryan and B.L. Scott, Phys. Rev. B135 (1964) 434.

(Bron 64) - G.E. Brown, Lectures on theory of nuclear matter (Universitetes Institut for Teoretisk Fysik and Nordita, Copenhagen, 1964).

(Bron 66) - G.E. Brown and A.M. Green, Nucl. Phys. 75 (1966) 401.

(Bron 67) - G.E. Brown, Unified theory of nuclear models (North-Holland Publishing Company - Amsterdam) second edition 1967.

(Brr 55) - K.A. Brueckner and C.A. Levinson, Phys. Rev. 97 (1955) 1344; K.A. Brueckner, Phys. Rev. 100 (1955) 36.

(Brr 58) - K.A. Brueckner, J.L. Gammel and H. Weitzer, Phys. Rev. 110 (1958) 431.

(Brr 61) - K.A. Brueckner, A.M. Lockett and M. Rotenberg, Phys. Rev. 121 (1961) 255.

(Brr 62) - K.A. Brueckner and K.S. Masterson, Phys. Rev. 128 (1962) 2267.

(Brt 62) - G. Breit, M.H. Hull, K.E. Lassila, K.D. Pyatt and H.M. Ruppel, Phys. Rev. 128 (1962) 826.

(Bry 60) - T.A. Brody and M. Moshinsky, Tables of Transformation Brackets (Universidad Nacional Autonoma de Mexico, Mexico) 1960.

(Clt 68) - C. Clement and E. Baranger, Nucl. Phys. A108 (1968) 27.

(Con 63a) - B.L. Cohen, Phys. Rev. 130 (1963) 227.

(Con 63b) - B.L. Cohen, Rev. Mod. Phys. 35 (1963) 332.

(Dam 64) - T. Dahlblom, K.G. Fögel, B. Quist and A. Torn, Nucl. Phys. 56 (1964) 177.

(Das 66) - K.T.R. Davies, S.J. Krieger and M. Baranger, Nucl. Phys. 84 (1966) 545.

(Das 69) - K.T.R. Davies, M. Baranger, R.M. Tarbutton and T.T.S. Kuo, Phys. Rev. 177 (1969) 1519.

(Dey-Preprint) - J.Dey, J.P. Elliott, A.D. Jackson, H.A. Mavromatis, E.A. Sanderson and B. Singh: to be published.

(Edn 59) - R.J. Eden, V.J. Emery and S. Sampather, Proc. Roy. Soc. (London) A253 (1959) 177; R.J. Eden, V.J. Emery and S. Sampather, *ibid* A253 (1959) 186.

(Eds 57) - A.R. Edmonds, *Angular Momentum in Quantum Mechanics* (Princeton Univ. Press, 1957).

(Eln 67) - L.R.B. Elton and A. Swift, *Nucl. Phys.* A94 (1967) 52.

(Elt 57) - J.P. Elliott and B.H. Flowers, *Proc. Roy. Soc. (London)* A242 (1957) 57.

(Elt 67) - J.P. Elliott, H.A. Mavromatis and E.A. Sanderson, *Phys. Letts.* 24B (1967) 358.

(Elt 68a) - J.P. Elliott, A.D. Jackson, H.A. Mavromatis, E.A. Sanderson and B. Singh, *Nucl. Phys.* A121 (1968) 241.

(Elt 68b) - J.P. Elliott and A.D. Jackson, *Nucl. Phys.* A121 (1968) 279.

(Eng 65) - T. Engeland, *Nucl. Phys.* 72 (1965) 68.

(Feh 64) - H. Feshbach and E. L. Lomon, *Ann. Phys. (N.Y.)* 29 (1964) 19.

(Fen 65) - P. Federman and I. Talmi, *Phys. Lett.* 19 (1965) 490.

(Gos 58) - L.C. Gomes, J.D. Walecka and V.F. Weisskopf, *Ann. Phys.* 3 (1958) 241.

(Grg 68) - H. Von. Grünberg, *Zeitschrift für Physik* 215 (1968) 359.

(Grn 62) - A.M. Green, *Nucl. Phys.* 33 (1962) 218.

(Grn 67) -- A.M. Green and T. Sawada, *Nuel. Phys.* B2 (1967) 267.

(Gue 68a) - M.R. Gunye, *Nucl. Phys.* A118 (1968) 174.

(Gue 68b) - M.R. Gunye, *Nucl. Phys.* A120 (1968) 691.

(Gue 69) - M.R. Gunye, *Nucl. Phys.* A132 (1969) 225.

(Haa 62) - T. Hamada and I.D. Johnston, *Nucl. Phys.* 34 (1962) 383.

(Hea 64) - P. Hewka, R. Middleton and J. Wiza, *Phys. Letts.* 10 (1964) 93.

(Hor 67) - H.R. Collard, L.R.B. Ellon, R. Hofstadter, Landolt - Börnstein, *Numerical data and functional relationships in Science and Technology New Series* (Springer-Verlag 1967).

(Hun 57) - L. Hulthen and M. Sugawara, Encyclopedia of Physics, Vol. XXXIX, Springer-Verlag, Berlin-Göttingen-Heidelberg, 1957.

(Jan 69) - A.D. Jackson and J.P. Elliott, Nucl. Phys. A125 (1969) 276.

(Jaw 51) - R. Jastrow, Phys. Rev. 81 (1951) 165.

(Kaa-Preprint) - S. Kahana, H.C. Lee and C.K. Scott Brookhaven National Laboratory, Upton, New York BNL 13198.

(Kao 65) - A. Kallio, Phys. Letts. 18 (1965) 51.

(Ken 64) - A.K. Kerman and A.M. Lockett, Comptes Rendus du Congres International de Physique Nucleaire, Vol. II (1964).

(Ken 65) - I. Kelson, Phys. Letts. 16 (1965) 143.

(Ken 66) - A. Kerman, J.P. Svenne and F. Villars, Phys. Rev. 147 (1966) 710.

(Kög 62) - L.A. König, J.H.E. Mattauch and A.H. Wapstra, Nucl. Phys. 31 (1962) 18.

(Kon 67) - D.S. Koltun, Phys. Rev. Letts. 19 (1967) 910.

(Kör 65) - H.S. Köhler, Phys. Rev. 138 (1965) B831.

(Kör 66) - H.S. Köher and R.J. McCarthy, Nucl. Phys. 36 (1966) 611.

(Kör 67) - H.S. Köhler and R.J. McCarthy, Nucl. Phys. A106 (1967) 313.

(Krr 66) - S.J. Krieger, K.T.R. Davies and M. Baranger, Phys. Letts. 22 (1966) 607.

(Krr-Preprint) - S.J. Krieger, to be published in Phys. Rev.

(Kuo 65) - T.T.S. Kuo and G.E. Brown, Phys. Letts. 18 (1965) 54.

(Kuo 66) - T.T.S. Kuo and G.E. Brown, Nucl. Phys. 85 (1966) 40.

(Kuo 67) - T.T.S. Kuo, Nucl. Phys. A103 (1967) 71.

(Laa 62) - K.E. Lassila, M.H. Hull, Jr., and H.M. Ruppel, F.A. McDonald and G. Breit, Phys. Rev. 126 (1962) 881.

(Len 64) - C.A. Levinson, Lectures on Hartree-Fock Theory and its Applications to Nuclei (T.I.F.R.) Bombay, 1964.

(Ler 60) - J.S. Levinger, M. Razavy, O. Rojo and N. Webre, Phys. Rev. 119 (1960) 230.

(Lon 68) - E.L. Lomon and H. Feshbach, Ann. Phys. (N.Y.) 48 (1968) 94;
E.L. Lomon and H. Feshbach, Ann. Phys. (N.Y.) 29 (1964) 19.

(Lyh 67) - R.P. Lynch and T.T.S. Kuo, Nucl. Phys. 495 (1967) 561.

(Mah 65) - J.H.E. Mattauch, W. Thiele and A.H. Wapstra, Nucl. Phys. 67 (1965) 1.

(Man 63) - K.S. Masterson and A.H. Lockett, Phys. Rev. 129 (1963) 776.

(Mar 66) - A.D. Mackellar, Ph.D. Thesis, Texas, A and M University, 1966 (Oak Ridge National Laboratory Report ORNL-TM-1374).

(Marr 68) - H.H. MacGregor, R.H. Arndt and R.M. Wright, Phys. Rev. 169 (1968) 1128 and references cited there.

(Mas 49) - W. Magnus and F. Oberhettinger, Functions of Mathematical Physics, (Chelsea Publ. Co., New York) 1949.

(Mas 69) - H.A. Mavromatis, E.A. Sanderson and A.D. Jackson, Nucl. Phys. 124 (1969) 1.

(Moe 53) - P.M. Morse and H. Feshbach, Methods of Theoretical Physics (McGraw-Hill, New York, 1953).

(Moi 60) - S.A. Moszkowski and B.L. Scott, Ann. Phys. (N.Y.) 11 (1960) 65.

(Mun 65) - R. Muthukrishnan and M. Baranger, Phys. Letts. 18 (1965) 160.

(Ner 68) - C.W. Nestor Jr., K.T.R. Davies, S.J. Krieger and M. Baranger, Nucl. Phys. 113 (1968) 14.

(Net 63) - R.K. Nesbat, Rev. Mod. Phys. 35 (1963) 352.

(Nos 67) - H.P. Noyes, P. Signell, N.R. Yoder and R.M. Wright, Stanford Linear Accelerator Centre Report SLACPUB-269 (1967).

(Pal 66) - H.K. Pal, J.P. Svenne and A.K. Kerman, International Nuclear Physics Conference, Gattlinberg, 1966.

(Pal 67) - H.K. Pal and A.P. Stamp, Phys. Rev. 158 (1967) 924.

(Poi 65) - A.R. Polletti and E.K. Warburton, Phys. Rev. 137 (1965) B595.

(Ray 63) - H. Razavy, Phys. Rev. 130 (1963) 1091.

(Red 68) - R.V. Reid, Ph.D. Thesis, Cornell University (1968).

(Reh 58) - H. Redlich, Phys. Rev. 110 (1958) 468.

(Ria 68) - G. Ripka, Advances in Nucl. Phys, Vol. 1 (Plenum Press, 1968) 183.

(Riu 65) - M. Riou, Rev. Mod. Phys. 37 (1965) 375.

(Shn 66) - Carl Shakin and Y.R. Waghmare, Phys. Rev. Letts. 16 (1966) 403.

(Shn 67a) - C.M. Shakin, Y.R. Waghmare and M.H. Hull, Jr., Phys. Rev. 161 (1967) 1006.

(Shn 67b) - C.M. Shakin, Y.R. Waghmare, M. Tomaselli, and M.H. Hull, Jr., Phys. Rev. Vol. 161 (1967) 1015.

(Sil 65) - P. Signell, Phys. Rev. 139 (1965) B315 and references cited there.

(Slr 60) - John C. Slater, Quantum theory of Atomic Structure Vol. I and II (McGraw-Hill Book Company, Inc.) 1960.

(Sve 65) - J.P. Svenne, Ph.D. Thesis M.I.T., 1965.

(Tan 64) - F. Tabakin, Ann. of Phys. 30 (1964) 51.

(Tan 68) - R.M. Tarbutton and K.T.R. Davies, Nucl. Phys. A120 (1968) 1.

(Tyn 66) - H. Tyren, S. Kullander, O. Sundberg, R. Ramachandran, P. Isaacson, Nucl. Phys. 79 (1966) 321.

(Ulh 58) - Ulrich Meyer Berkhou, Ann. Phys. 8 (1958) 119.

(Vae 68) - I.Sh. Vashakidze, T.R. Dzhalaganyan and Dzh. V. Neboniya, Sov. Journal Nucl. Phys. 7 (1968) 611.

(Van 67) - D. Vautherin and M. Vénéroni, Phys. Letts. 25B (1967) 175.

(Vis 63) - F. Villars in Proceedings of the International School of Physics, Enrico Fermi Course 23, 1961 Academic Press Inc., New York (1963).

(Wae 64) - Y.R. Waghmare, Phys. Rev. 134 (1964) B118.

(Wog 67) - C.W. Wong, Nucl. Phys. A104 (1967) 417.

(Wog 68) - C.W. Wong, Nucl. Phys. A108 (1968) 481.

(Yai 54) - Y. Yamaguchi and Y. Yamaguchi, Phys. Rev. 95 (1954) 1628.